DEVELOPMENT OF SENSING PLATFORMS USING BULK OPTODE TECHNIQUE FOR
DETECTION OF SILVER AND MERCURY IONS

Mr. Manoon Phichi

จุฬาลงกรณ์มหาวิทยาลัย
CHULALONGKORN UNIVERSITY

A Dissertation Submitted in Partial Fulfillment of the Requirements
for the Degree of Doctor of Philosophy in Chemistry
Department of Chemistry
FACULTY OF SCIENCE
Chulalongkorn University
Academic Year 2019
Copyright of Chulalongkorn University

การพัฒนาแพลตฟอร์มการรับรู้โดยใช้เทคนิคบัลค์ออปโทดสำหรับการตรวจวัด
ไอออนเงินและปรอท

นายมนูญ พิชิ

วิทยานิพนธ์นี้เป็นส่วนหนึ่งของการศึกษาตามหลักสูตรปริญญาวิทยาศาสตรดุษฎีบัณฑิต
สาขาวิชาเคมี ภาควิชาเคมี
คณะวิทยาศาสตร์ จุฬาลงกรณ์มหาวิทยาลัย
ปีการศึกษา 2562
ลิขสิทธิ์ของจุฬาลงกรณ์มหาวิทยาลัย

Thesis Title                    DEVELOPMENT OF SENSING PLATFORMS USING BULK OP TODE TECHNIQUE FORDETECTION OF SILVER AND MERC URY IONS

By                               Mr. Manoon Phichi

Field of Study              Chemistry

Thesis Advisor            Associate Professor WANLAPA AEUNGMAITREPIROM, Ph.D.

Thesis Co Advisor       Associate Professor APICHAT IMYIM, Ph.D.

Accepted by the FACULTY OF SCIENCE, Chulalongkorn University in Partial Fulfillment of the Requirement for the Doctor of Philosophy

........................................................... Dean of the FACULTY OF SCIENCE

(Professor POLKIT SANGVANICH, Ph.D.)

DISSERTATION COMMITTEE

........................................................... Chairman

(Associate Professor VUDHICHAI PARASUK, Ph.D.)

........................................................... Thesis Advisor

(Associate Professor WANLAPA AEUNGMAITREPIROM, Ph.D.)

........................................................... Thesis Co-Advisor

(Associate Professor APICHAT IMYIM, Ph.D.)

........................................................... Examiner

(Professor THAWATCHAI TUNTULANI, Ph.D.)

........................................................... Examiner

(Associate Professor PAKORN VARANUSUPAKUL, Ph.D.)

........................................................... External Examiner

(Assistant Professor CHOMCHAI SUKSAI, Ph.D.)

มนูญ พิชิ : การพัฒนาแพลตฟอร์มการรับรู้โดยใช้เทคนิคบัลค์ออปโทดสำหรับการตรวจวัดไอออน
เงินและปรอท. (
DEVELOPMENT OF SENSING PLATFORMS USING BULK OPTODE TECHNIQUE FORD
ETECTION OF SILVER AND MERCURY IONS) อ.ที่ปรึกษาหลัก : รศ. ดร.วัลภา เอื้องไมตรี
ภิรมย์, อ.ที่ปรึกษาร่วม : รศ. ดร.อภิชาติ อิ่มยิ้ม

งานวิจัยนี้ได้อธิบายอุปกรณ์การวิเคราะห์ชนิดใหม่สำหรับตรวจวัดไอออนเงินและปรอทโดย
ใช้เทคนิคบัลค์ออปโทด โดยออปโทดประกอบด้วย 25,27-ได(เบนโซไทอะโซลิล)-26,28-ไฮดรอกซีคา
ลิกซ์[4]เอรีน (CU1) เป็นไอโอโนฟอร์ชนิดเลือกไอออน โครโมไอโอโนฟอร์ XIV เป็นไลโปฟิลิกพีเอช
อินดิเคเตอร์ และ KTpCIPB เป็นไอออนเอกซ์เชนจ์เจอร์ ถูกเตรียมขึ้นและใช้เป็นสารรับรู้ในอุปกรณ์
การวิเคราะห์ที่พัฒนาขึ้น สารรับรู้นี้ตอบสนองต่อไอออนเงินและปรอท ด้วยการเปลี่ยนแปลงสีจากน้ำ
เงินเป็นเหลือง ในงานวิจัยนี้อุปกรณ์การวิเคราะห์ฐานกระดาษร่วมกับการตรวจวัดเชิงสีได้ถูกสร้างขึ้น
ด้วยวิธีการอย่างง่าย โดยการหยดสารละลายค็อกเทลลงบนกระดาษกรองและวิธีการตรวจวัดอย่างง่าย
ทำโดยการจุ่มอุปกรณ์ตรวจวัดลงในสารละลายตัวอย่าง ในแพลตฟอร์มนี้การตรวจวัดคู่กันของไอออน
เงินและปรอทในสารละลายผสมสามารถทำได้โดยการเติมอีดีทีเอและโซเดียมคลอไรด์เพื่อเป็นมาสกิ้ง
เอเจนท์ ตามลำดับ นอกจากนี้เพื่อพัฒนาอุปกรณ์รับรู้แบบไร้เครื่องมืออย่างแท้จริงโดยปราศจากการใช้
เครื่องมืออิเล็กทรอนิกส์ใด ๆ การตรวจวัดแบบวัดระยะทางได้ถูกเสนอขึ้นโดยการใช้อุปกรณ์การ
วิเคราะห์ฐานเชือก ในอุปกรณ์ชนิดนี้ออปโทดนาโนสเฟียร์ขนาดเส้นผ่านศูนย์กลาง 110 นาโนเมตรได้
ถูกเตรียมขึ้นและถูกนำไปผสมลงบนพื้นผิวของเชือกชนิดพอลิเอสเตอร์โดยวิธีการอย่างง่ายด้วยการปิ
เปตต์ และใช้วิธีการตรวจวัดอย่างง่าย ทำโดยหยดสารละลายตัวอย่างซ้ำๆ ลงบนเชือก ในแพลตฟอร์มนี้
ใช้สำหรับการตรวจวัดไอออนปรอท โดยระยะทางของการเปลี่ยนแปลงสีจะสัมพันธ์กับความเข้มข้น
ของไอออนปรอทในสารละลายตัวอย่าง ดังนั้นวิธีการตรวจวัดทำได้อย่างง่ายโดยวัดระยะทางของการ
เปลี่ยนแปลงสีตามความยาวเชือกด้วยไม้บรรทัด ในขั้นสุดท้ายอุปกรณ์ที่นำเสนอได้นำไปประยุกต์ใช้
ในการหาปริมาณไอออนเงินและปรอทในตัวอย่างจริงและได้ผลการทดลองที่สอดคล้องกันกับผลการ
ทดลองที่ได้จากเทคนิค ICP-OES

| สาขาวิชา | เคมี | ลายมือชื่อนิสิต ................................................ |
|---|---|---|
| ปีการศึกษา | 2562 | ลายมือชื่อ อ.ที่ปรึกษาหลัก ............................. |
| | | ลายมือชื่อ อ.ที่ปรึกษาร่วม ............................. |

# # 5772106823 : MAJOR CHEMISTRY

KEYWORD: Bulk optode, Paper-based analytical device, Thread-based analytical device, Silver ion, Mercury ion

Manoon Phichi :
DEVELOPMENT OF SENSING PLATFORMS USING BULK OPTODE TECHNIQUE FORDETECTION OF SILVER AND MERCURY IONS. Advisor: Assoc. Prof. WANLAPA AEUNGMAITREPIROM, Ph.D. Co-advisor: Assoc. Prof. APICHAT IMYIM, Ph.D.

This research described new analytical devices for $Ag^+$ and $Hg^{2+}$ detection using bulk optode technique. The optode containing 25,27-di(benzothiazolyl)-26,28-hydroxycalix[4]arene (CU1) as an ion-selective ionophore, chromoionophore XIV as a lipophilic pH indicator, and KT$p$ClPB as an ion-exchanger was prepared and used as a sensing agent in the proposed devices. The optode sensors responded to $Ag^+$ and $Hg^{2+}$ by changing the color from blue to yellow. The colorimetric-based detection was carried out by using the proposed paper-based analytical device. A simple fabrication method was performed by simply dropping the cocktail onto the filter paper, and the detection method was easily performed by immersing the paper strip into the sample solutions. In this platform, the dual detection of $Ag^+$ and $Hg^{2+}$ in their mixed solutions was achieved by adding EDTA and NaCl as masking agents, respectively. Additionally, to demonstrate a truly instrument-free optode sensor without the need of any electronic equipment, the distance-based detection was proposed by using the thread-based analytical device. The optode nanosphere with 110 nm in diameters was successfully prepared and incorporated onto the surface of polyester thread by a simple manual pipetting, and the detection method was easily performed by repeatedly dropped sample solutions onto the thread. In this platform, the $Hg^{2+}$ detection on thread-based device was exhibited. The distances of the color change correlated to the $Hg^{2+}$ concentrations in sample solutions, so the detection method was easily performed by measuring the length of the color change along the thread with a ruler. Finally, the proposed devices were successfully applied to determine the amount of $Ag^+$ and $Hg^{2+}$ in real samples, and the results were in agreement with the values obtained from ICP-OES.

| | | | |
|---|---|---|---|
| Field of Study: | Chemistry | Student's Signature | ............................... |
| Academic Year: | 2019 | Advisor's Signature | .............................. |
| | | Co-advisor's Signature | ......................... |

# ACKNOWLEDGEMENTS

Manoon  Phichi

# TABLE OF CONTENTS

จุฬาลงกรณ์มหาวิทยาลัย
CHULALONGKORN UNIVERSITY

# LIST OF TABLES

**Page**

# LIST OF FIGURES

# LIST OF ABBREVIATIONS

| | |
|---|---|
| AgNPs | Silver nanoparticles |
| C | Chromoionophore (deprotonated form) |
| $CH^+$ | Chromoionophore (protonated form) |
| cm | Centimeter |
| $cm^2$ | Square centimeter |
| **CU1** | 25,27-di(benzothiazolyl)-26,28-hydroxycalix[4]arene |
| DLS | Dynamic light scattering |
| DOS | Bis(2-ethylhexyl) sebacate |
| DSLR | Digital single-lens reflex |
| EDTA | Ethylenediaminetetraacetic acid |
| h | Hour |
| HT18C6 | Hexathia-18-crown-6 |
| ICP-OES | Inductively coupled plasma optical emission spectrometry |
| ISEs | Ion-selective electrodes |
| ISOs | Ion-selective optodes |
| kg | Kilogram |
| KT$p$ClPB | Potassium tetrakis(4-chlorophenyl)borate |
| L | Ionophore |
| LED | Light-emitting diode |
| LOD | Limit of detection |
| M | Molar |
| $M^{n+}$ | Metal ion |
| mg | Milligram |
| mL | Milliliter |

| | |
|---|---|
| mm | Millimeter |
| mM | Millimolar |
| MΩ.cm | Megaohm-centimeter |
| nM | Nanomolar |
| nm | Nanometer |
| NPOE | *ortho*-Nitrophenyl octyl ether |
| PADs | Paper-based analytical devices |
| PAN | 1-(2-Pyridylazo)-2-naphthol |
| ppb | Part per Billion |
| ppm | Part per million |
| PVC | Polyvinylchloride |
| rpm | Revolutions per minute |
| $R^-$ | Ion-exchanger |
| RSD | Relative standard deviation |
| THF | Tetrehydrofuran |
| $\mathit{\Delta E}$ | The color difference |
| μL | Microliter |
| μM | Micromolar |

# CHAPTER I

# INTRODUCTION

## 1.1 Statement of the problem

Heavy metals are one of environmental pollutions that are a serious problem in many countries [1-3]. The natural phenomenon such as volcanic eruption or human activities such as mining, oil drilling, and agricultural activities can discharge heavy metals to environment [4-6]. Since the heavy metal ions can dissolve in water, various water sources are easily contaminated by heavy metals. Mercury (Hg) and silver (Ag) are the high toxic heavy metals which have been assigned to the highest toxicity class of heavy metal pollutants [7, 8]. $Hg^{2+}$ is one of common forms of mercury that can accumulate in food chain and human's body [9, 10]. The accumulation of Hg can damage to brain, kidneys, nervous, and endocrine system in humans [11, 12]. Ag is a heavy metal used in diverse industries since its effective antibacterial properties are noticeable [13]. However, the accumulation of $Ag^+$ in human's body can cause permanent skin damage by forming insoluble sediments and accumulation in the skin layer, eyes, or around nerves [8].

Since the contamination of $Ag^+$ and $Hg^{2+}$ in environment can harm to living organism and human health, the determination of $Ag^+$ and $Hg^{2+}$ using various techniques were frequently explored and published. However, the conventional methods for detection of $Ag^+$ and $Hg^{2+}$ such as cold-vapor atomic absorption spectroscopy (CVAAS) [14, 15], inductively coupled plasma mass spectrometry (ICP-MS) [16], inductively coupled plasma atomic emission spectrometry (ICP-AES) [17], electrochemical method [18], and cold-vapor atomic fluorescence spectrometry [19] suffer laborious and high cost operations because the sophisticate instrument and

specialist are required. For this reason, the determination of $Ag^+$ and $Hg^{2+}$ using the conventional techniques is not suitable for on-site analysis. Hence, research about the detection of $Ag^+$ and $Hg^{2+}$ using a simple technique is interesting.

Ion-selective optode (ISOs) or bulk optode is one of colorimetric detection methods that is attracted for metal ion detection. The conventional optodes are normally consisted of lipophilic sensing components including ion-selective ionophore, chromoionophore, and ion-exchanger embedded in the hydrophobic polymer films [20]. The ion-selective sensing behavior is based on the ion-exchange process of target ion ($M^{n+}$) and hydrogen ion ($H^+$) between water surrounding and hydrophobic sensing phase consisting of ionophore (L), chromoionophore (C), and ion-exchanger ($R^-$). Ionophore can extract $M^{n+}$ from water to the hydrophobic sensing phase while $H^+$ from chromoionophore ($CH^+$) is released to water to maintain the electroneutrality. This extraction process leads to the change of optical properties of the optode. Because a fast response, extensive response range, simple preparation, high sensitivity, high selectivity, and easy detection by naked eye are the benefits of ISOs, various ISOs systems have been studied and developed for heavy metal detection.

Many researches involving ISOs have fabricated the optode sensor in a platform of planar thin film and have detected the change of optical signal with conventional spectrophotometer [21-27]. However, these methods often cannot be used as a truly instrument-free for on-site analysis since they still required sophisticated scientific instruments for signal detection. In this research, we were interested in the development of new ISOs platforms to use as a truly instrument-free device without requirements of a conventional sophisticated scientific instrument for using as a portable device for $Ag^+$ and $Hg^{2+}$ detection.

In this work, we were interested in an ion-selective ionophore of 25,27-di(benzothiazolyl)-26,28-hydroxycalix[4]arene or **CU1**. This compound was first designed, synthesized, and characterized by Ngeontae *et al.* in 2008 [28]. In their

work, **CU1** was successfully incorporated to an ion-selective electrodes (ISEs) platform for $Ag^+$ detection. In addition, **CU1** was also successfully incorporated to the conventional planar film optode by Wattanayon in 2013 [29]. From these previous works, **CU1** showed a highly selective binding with $Ag^+$ in ISEs and ISOs (planar film) platforms. For this reason, **CU1** was chosen to use as an ion-selective ionophore for new ISOs platforms in our research.

## 1.2 Research objective

The aim of this research was to develop ion selective optodes (ISOs) sensing platforms including paper-based analytical device and thread-based analytical device as an instrument-free and portable devices for detection of $Ag^+$ and $Hg^{2+}$ in real aqueous samples.

## 1.3 Scope of research

The cocktail solutions including three sensing components consisting of **CU1** as an ion-selective ionophore, KT$p$ClPB as an ion-exchanger, and chromoionophore as a lipophilic pH indicator were prepared, and the cocktail solutions were employed to fabricate the proposed device in different platforms. The paper-based analytical device was firstly fabricated by manual pipetting the cocktail solution to the filter paper. In this platform, four types of commercial lipophilic pH indicator including chromoionophore I, VII, VIII, XIV were investigated, and the cocktail composition were optimized to obtain good selectivity and sensitivity. Next, the cocktail solutions were employed to prepare the ion-selective optode nanosphere by solvent-displacement method, and the optode nanosphere suspension was applied to fabricate the thread-based analytical device. The determination of $Ag^+$ and $Hg^{2+}$ by using the fabricated devices was examined. The parameters affected to the optode response

including effect of pH, response time, selectivity, repeatability, working range were studied. Finally, the fabricated devices were applied to determine $Ag^+$ and $Hg^{2+}$ concentrations in real aqueous samples with spiked method, and the determination of $Ag^+$ and $Hg^{2+}$ in samples by using ICP-OES was also performed for the comparisons.

## 1.4 Benefits of the research

We have expected to obtain new ion-selective optode platforms that could be used as a simple and portable device for determination of $Ag^+$ and $Hg^{2+}$ in real aqueous samples with a satisfactory experimental result.

จุฬาลงกรณ์มหาวิทยาลัย
CHULALONGKORN UNIVERSITY

# CHAPTER II

# THEORY AND LITERATURE REVIEWS

## 2.1 Ion-selective optodes (ISOs)

### 2.1.1 Components of ISOs

Optode sensing phase is a hydrophobic plasticized phase of the polymeric membrane. The plasticized phase is composed of a hydrophobic polymer, a plasticizer, and three main sensing reagents including a complexing agent (ionophore), a lipophilic ionic salt (ion-exchanger), and a lipophilic pH indicator (chromoionophore). All composition of optode affect to the response of sensor in terms of selectivity and sensitivity. Therefore, type and quantity of all components are important for the optode preparation. The role of each component is explained as listed below.

― *Polymer*

Some properties of the polymer matrices used in plasticized phase of optode are mechanical stability, chemically inert, and elasticity. Normally, the polymeric phase in optode sensor is often prepared with poly(vinyl chloride) (PVC) which provides the appropriate properties as described earlier.

― *Plasticizer*

The role of plasticizer used in plasticized phase of optode is a membrane solvent for homogeneous incorporating the others sensing components in hydrophobic sensing phase. The properties of plasticizer used in optode should have hydrophobicity, low vapor pressure, and high ability for dissolving all optode sensing

constituents in the plasticized phase. There are various types of plasticizer used to prepare optode with a different lipophilicity characteristic; however, bis(2-ethylhexyl) sebacate (DOS, apolar) and *ortho*-nitrophenyl octyl ether (*o*-NPOE, polar) are often used to prepare the membrane optode. The structure of DOS and *o*-NPOE are shown in **Figure 2.1**.



**Figure 2.1** Chemical structures of some plasticizers.

— *Ionophore (ion-selective ionophore)*

Ionophore or ion-selective ionophore is the most important component of the ISOs since it provides the selectivity of the optode sensor. The roles of ionophore are the lipophilic complexing agent which can selectively bind with only the target ion and extract the target ion from aqueous sample phase to organic sensing phase by forming strong, selective, and reversible complex with target ion in the hydrophobic sensing phase. To prevent the leaching of ionophore from hydrophobic sensing phase to aqueous solution, the hydrophobic groups should be contained in its chemical structure. Some examples of commercial ionophores used in various previous researches are shown in **Figure 2.2.**

**Figure 2.2** Chemical structures of some ionophores.

─ *Chromoionophore (proton-selective ionophore)*

Chromoionophore is a lipophilic pH indicator which can change the optical property when its structure changes from protonated form to deprotonated form or vice versa. Protonated form and deprotonated form of chromoionophore show different colors and absorption wavelengths. When the target cation is extracted from aqueous sample to sensing phase, the abundances of positive charge from target in the optode sensing matrix cause the leaching out of proton from sensing phase by forming a deprotonated form of chromoionophore. Hence, with the presence of chromoionphore in sensing phase, the changes of optical property of optode sensor resulted from the target cation could be obtained. Some examples of commercial chromoionophores are shown in **Figure 2.3.**

Chromoionophore I

Chromoionophore VII

Chromoionophore VIII

Chromoionophore XIV
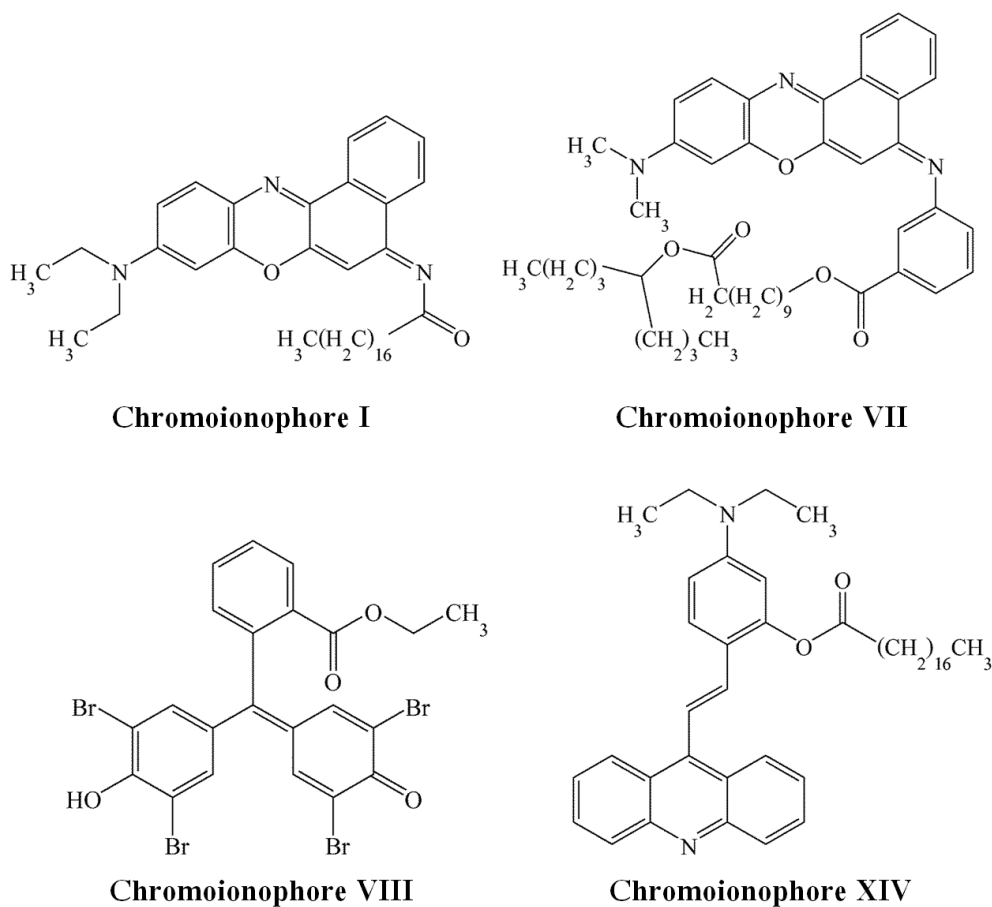
**Figure 2.3** Chemical structures of some chromoionophores.

– *Ion-exchanger*

Ion-exchanger or ionic additive is a lipophilic ionic salt which is added to maintain the charge balance in the sensing phase and to prevent the co-extraction of counter ion from aqueous solution. Some ion-exchangers used to prepare the cation-selective optode are shown in **Figure 2.4**.
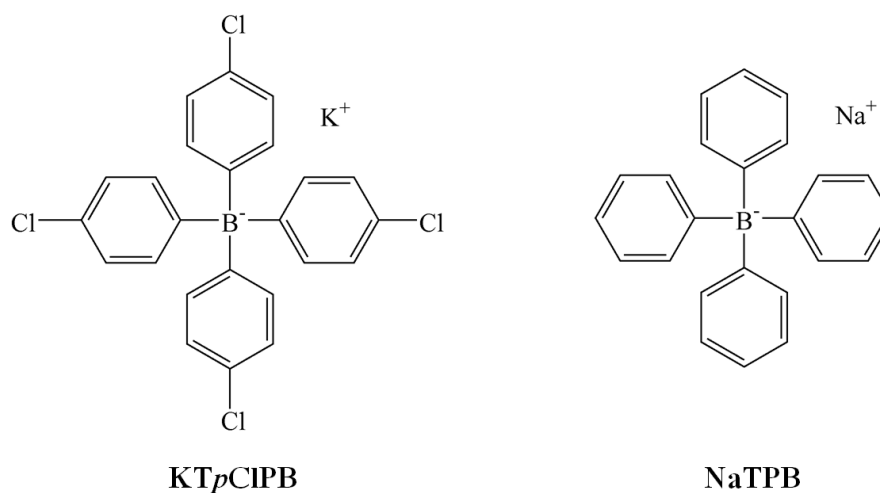
**Figure 2.4** Chemical structures of some ion-exchanger.

### 2.1.2 The response mechanism of ISOs [20, 30]

The ion-selective optode behavior is based on the ion-exchange process of target ion ($M^{n+}$) and hydrogen ion ($H^+$) between water sample surrounding (aqueous phase) and hydrophobic sensing phase (organic phase) consisting of ionophore (L), chromoionophore (C), and ion-exchanger ($R^-$). Ionophore extracts $M^{n+}$ from water to the hydrophobic sensing phase by formation of a coordinated compound while $H^+$ from chromoionophore ($CH^+$) is simultaneously released to water to maintain the electroneutrality. Hence, the color of sensing phase changed from the color of protonated chromoionophore ($CH^+$) to deprotonated chromoionophore (C). The exchange process can be described in **Figure 2.5** and **Equation (2.1)**.
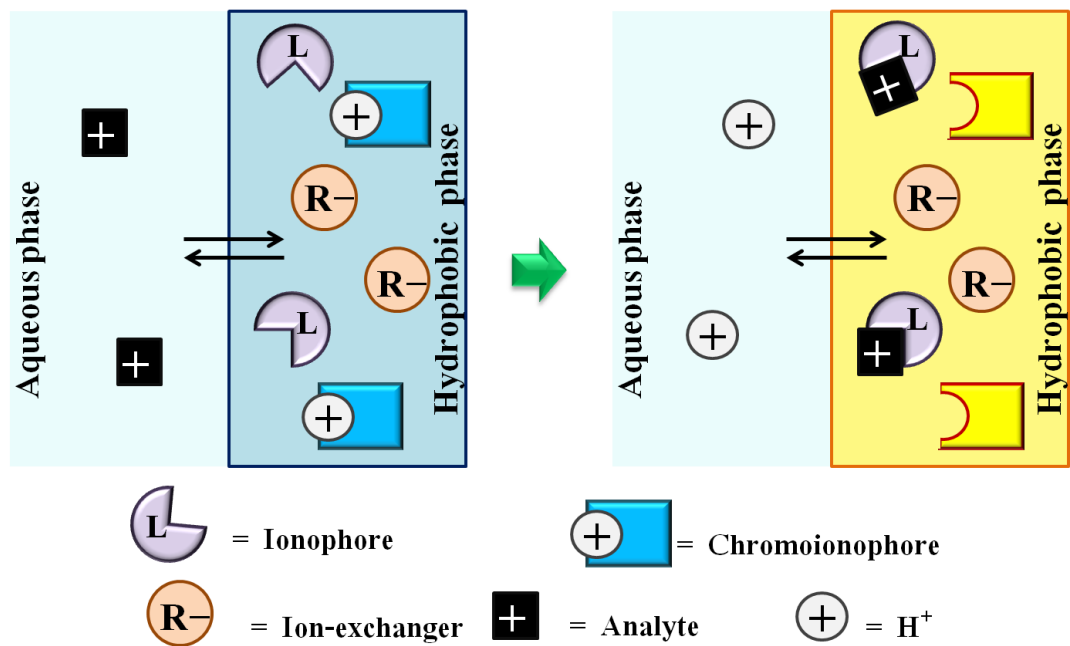
**Figure 2.5** Response mechanism of ion selective optode.

$$M_{(aq)}^{n+} + zL_{(org)} + nCH_{(org)}^{+} + R_{(org)}^{-} \rightleftharpoons ML_{Z(org)}^{n+} + nC_{(org)} + nH_{(aq)}^{+} + R_{(org)}^{-} \quad (2.1)$$
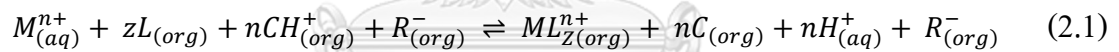
where z is the metal ion-ionophore complex ratio. According to the ion-exchange equilibrium from **Equation (2.1)**, the ion-exchange constant ($K_{Exch}^{M}$) can be calculated as **Equation (2.2)**.

$$K_{Exch}^{M} = \frac{[ML_Z^{n+}][H^+]^n[C]^n}{[M^{n+}][CH^+]^n[L]^z} \quad (2.2)$$

From **Equation (2.2)**, the response function for $M^{n+}$ can be derived into **Equation (2.3)**,

$$[M^{n+}] = \frac{1}{K_{Exch}^M} \left(\frac{\alpha}{1-\alpha}[H^+]\right)^n \left[\frac{R_{tot}^- - (1-\alpha)C_{tot}}{n(L_{tot} - \frac{z}{n}\{R_{tot}^- - (1-\alpha)C_{tot}\})^z}\right] \qquad (2.3)$$

where 1-$\alpha$ is the degree of protonation of the chromoionophore, and $R_{tot}^-$, $L_{tot}$ and $C_{tot}$ are the total concentration of ion-exchanger, ionophore and chromoionophore in the hydrophobic phase, respectively. The degree of deprotonation of chromoionophore ($\alpha$) can be acquired by experimental data according to **Equation (2.4).**

$$\alpha = \frac{[C]}{[C_{tot}]} = \frac{A_{prot} - A}{A_{prot} - A_{deprot}} \qquad (2.4)$$

where A, $A_{prot}$, and $A_{deprot}$ are the absorbance of chromoionophore in equilibrium, chromoionophore in fully protonated form ($\alpha = 0$), and chromoionophore in fully deprotonated form ($\alpha = 1$), respectively, and C is the concentration of deprotonated form of chromoionophore. To obtain $A_{prot}$ and $A_{deprot}$, the optode sensors are immersed in the acid and base solutions, respectively (normally using 1 M $HNO_3$ and 1 M NaOH), and the optode sensors are immersed into the sample solutions containing target ion ($M^{n+}$) to obtain A.

To acquire the response curve for $M^{n+}$ detection, the degree of protonation of chromoionophore is ploted as a function of logarithm of the concentration of $M^{n+}$ while other terms are kept constant. The sigmoidal curve from calculation which is fitted to the experimental data by varying $K_{Exch}^M$ can be obtained as shown in **Figure 2.6.**
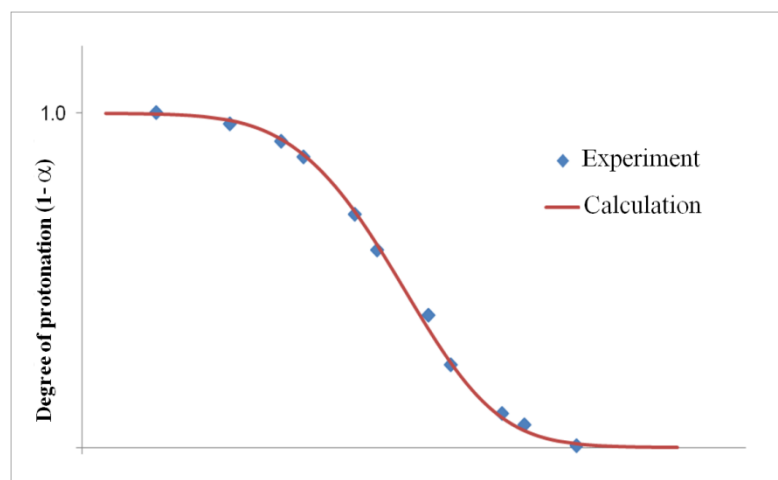
**Figure 2.6** Sigmoidal response curve of the ISOs.

## 2.2 Paper-based analytical device

### 2.2.1 Characteristics of paper-based analytical device

Paper-based analytical devices (PADs) are one of microfluidic platforms which was first introduced by Whitesides group in 2007 [31]. PADs have the same some characteristics with the conventional microfluidic devices. The excellent characteristics of cellulose paper are flexibility, high surface and pores which can transport the liquids via capillary forces within the cellulose fiber network, so the external pumping for the liquid flows is not required. Since there are many advantages of PADs such as a portable, light weight, stability, ease of maintaining, easy to use, low cost device, and environmental friendliness [32], PADs have been attended for chemical sensor applications [33, 34]. Moreover, because of these advantages, PADs are suitable for using as portable devices for environmental analysis and clinical diagnostics in developing countries where scientific instruments and well trained users are insufficient. Some PADs for analytical applications are summarized in **Table 2.1.**

**Table 2.1** Summary of some paper-based analytical device reported in recent years.

| Applications | Details | Ref. |
|---|---|---|
| Clinical diagnostics | Detection of *Pseudomonas aeruginosa* (PA) in human saliva and tap water using electrochemical detection on paper | [35] |
| Clinical diagnostics | Simultaneous detections of orthophosphate and calcium ions in human serum for hyperphosphatemia diagnostics using paper-based device with LED-based fluorescence detectors | [36] |
| Clinical diagnostics | Detection of two steroids including dexamethasone and prednisolone in herbal medicine samples using electrochemical detection on paper | [37] |
| Environmental analysis | Detection of total ammonia in freshwaters for evaluation of water quality using acid-base indicator screening on paper and colorimetric-based detection | [38] |
| Environmental analysis | Simultaneous detections of glycerol, magnesium, and calcium in biodiesel samples using liquid-liquid microextraction coulple with colorimetric-based detection on paper | [39] |

## 2.2.2 Paper-based analytical devices for $Ag^+$ and $Hg^{2+}$ detection

Since a portable, low cost, and handy device is desired for on-site analysis, the paper-based analytical devices are one of alternative methods for $Ag^+$ and $Hg^{2+}$ detection. Various paper-based devices incorporating with colorimetric detection method have been published. There are many researches incorporated paper-based devices with colorimetric sensing agent such as silver nanoparticles (AgNPs), silver nanoplate (AgNPLs), gold nanoparticles (AuNPs), platinum nanoparticles (PtNPs), curcumin nanoparticles (CURNs), HOTT chelating agent, and ZIF-8/GO nanosheets. Some recent paper-based analytical devices for $Ag^+$ or $Hg^{2+}$ determination are summarized in **Table 2.2**.

15
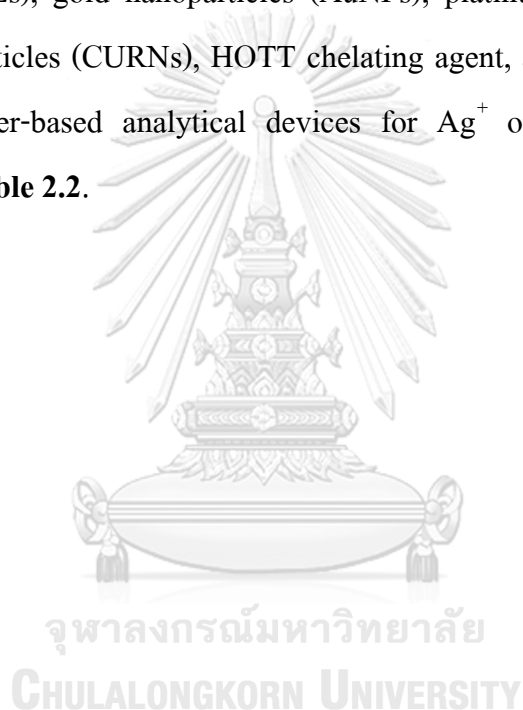
**Table 2.2** Determination of $Ag^+$ ang $Hg^{2+}$ by paper-based analytical devices

| Reagents | Analytes | Fabrication methods | Detection limit | Response time | Ref. |
|---|---|---|---|---|---|
| Curcumin nanoparticles (CURNs) | $Hg^{2+}$ | Wax dipping | 0.17 ppm (without preconcentration) 0.003 ppm (50 times preconcentration) | 15 min | [40] |
| Silver nanoplate (AgNPLs) | $Hg^{2+}$ | Screen printing | 0.12 ppm (without preconcentration) 2 ppb (70 times preconcentration) | Almost immediately (5 h for preconcentration) | [41] |
| Silver nanoparticles (AgNPs) | $Hg^{2+}$ | AKD inkjet printing | 0.001 ppm | – | [42] |
| Gold nanoparticles (AuNPs) | $Hg^{2+}$ | Solid-ink printing | 50 nM | 40 min | [43] |
| Platinum nanoparticles (PtNPs) | $Hg^{2+}$ | Printing + plastic module | 0.01 µM | 5 min | [44] |

**Table 2.2** (cont.) Determination of $Ag^+$ ang $Hg^{2+}$ by paper-based analytical devices.

| Reagents | Analytes | Fabrication methods | Detection limit | Response time | Ref. |
|---|---|---|---|---|---|
| Nanoparticle Autocatalytic | $Ag^+$ | Immersing in reagent | 30 μM (without UV light) | 90 min | [45] |
| sensor | | | 6 μM (under UV light) | | |
| | $Cu^{2+}$ | Immersing in reagent | 60 μM (without UV light) | 90 min | |
| | | | 30 μM (under UV light) | | |
| The indicators containing | $Hg^{2+}$ | Printing the indicator | 0.19 μM | 10 min | [46] |
| formulations (18 spot) | $Ag^+$ | Printing the indicator | 1.69 μM | 10 min | |
| | $Cu^{2+}$ | Printing the indicator | 1.40 μM | 10 min | |
| Chelating (HOTT) | $Ag^+$ | Hand drawing | 0.1 μM | – | [47] |
| ZIF-8/GO nanosheets | $Ag^+$ | Immersing in reagent | 0.1 μM | – | [48] |

**2.3 Thread-based analytical device**

**2.3.1 Characteristics of thread-based analytical device**

Threads are one of alternative materials that is utilized for fabrication of microfluidic devices. Thread-based microfluidic device was first fabricated by Li, Tian, and Shen in 2010 [49]. The major advantage of thread-based device is unnecessary patterning of hydrophobic barrier since the liquid can be transported along the thread via capillary force without requirement of external pumping and a barrier. Moreover, thread provides more alternative types of materials than paper such as rayon, nylon, cotton, polyester, wool, natural silk, and etc. The different materials can provide the difference of wicking property and transportation rate of liquid sample or reagent along the threads. Thread-based analytical devices were therefore fabricated for many applications such as food analysis, clinical diagnostics and environmental analysis. Some recent applications of thread-based analytical devices are summarized in **Table 2.3.**

จุฬาลงกรณ์มหาวิทยาลัย

CHULALONGKORN UNIVERSITY

**Table 2.3** Summary of some thread-based analytical device reported in recent years.

| Applications | Details | Ref. |
|---|---|---|
| Food analysis | Determination of total phenolic and antioxidant in green tea samples using cotton thread couple with paper-based platforms and colorimetric-based detection | [50] |
| Food analysis | Detections of ascorbic acid in aqueous sample and orthodiphenols in olive and sunflower oil samples using cotton thread combined with paper-based electrochemical detector at the end of thread | [51] |
| Clinical diagnostics | Detections of protein and nucleic acid in human serum for diagnosing genetic disease in human using thread-based device and colorimetric-based detection | [52] |
| Clinical diagnostics | Detection of human ferritin in human serum for lung cancer diagnosis using immunoassay on thread-based device and electrochemical detection | [53] |
| Environmental analysis | Detection of phenol in tap and drinking water using thread-based device combined with electrochemical biosensor | [54] |

**2.3.2 Thread-based analytical device for heavy metal detection**

Thread-based analytical devices provide several advantages which are suitable to develop a portable and low-cost device for analytical applications. Some recent applications of thread-based analytical devices for detection of some metal ions are summarized in **Table 2.4.** However, to the best of our knowledge, the applications of thread-based analytical devices for $Ag^+$ and $Hg^{2+}$ detection have never been reported.

**Table 2.4** Summary of some thread-based analytical device reported in recent years.

| Analytes | Reagents | Detection methods | Ref. |
|---|---|---|---|
| $Cu^+$ | Oxidized tetramethylbenzidine | Colorimetric-based detection | [55] |
| Al | Chrome azurol S and cetyltrimethylammonium bromide | Distance-based detection | [56] |
| $Cu^{2+}$, $Zn^{2+}$ | Zincon | Thermal lens detection | [57] |
| $Ni^{2+}$ | Dimethylglyoxime | Distance-based detection | [58] |
| $K^+$ | Dibenzo-18-crown-6-ether | Colorimetric-based detection | [59] |
| $Mg^{2+}$ | Eriochrome black T | Distance-based detection | [60] |
| $K^+$ | Potassium ionophore I | Potentiometric detections | [61] |
| $Na^+$ | Sodium ionophores X | Potentiometric detections | [61] |
| $Ca^{2+}$ | Calcium ionophore II | Potentiometric detections | [61] |

## 2.4 ISOs Platforms for metal ions detection

### 2.4.1 The conventional planar films optode

Various previous researches have been reported the ISOs sensors for metals ion detections using the conventional planar film optodes. To fabricate the classic planar film optode, the cocktail solution is firstly prepared by dissolving the following materials: ionophore, ion-exchanger, chromoionophore, hydrophobic polymer, and plasticizer in an appropriate solvent. The cocktail solutions are then spread on the supporting transparent material (normally used a glass slide). The detection methods are performed by using the conventional scientific instruments such as UV-Visible or fluorescent spectrophotometers. To measure the optical signal from optode planar

films, the films are directly placed in the optical path of spectrophotometer or in a flow‑through cell for the flow‑through system analysis. Some ISOs with a classic thin film are summarized in **Table 2.5**, and the chemical structures of some reagents in **Table 2.5** are shown in **Figure 2.7**.

**Table 2.5** Determination of metal ions by conventional planar films ISOs systems.

| Analyte | Ionophore | Chromoionphore or fluorophore | Detection system | Detection mode | LOD (M) | Ref. |
|---|---|---|---|---|---|---|
| $Pb^{2+}$ | Lead ionophore IV | Chromoionophore I | Flow-through | Absorbance | $8.97 \times 10^{-9}$ | [21] |
| $Pb^{2+}$ | ETH5435 | Chromoionophore VII | Flow-through | Absorbance | $3.2 \times 10^{-12}$ | [22] |
| $Pb^{2+}$ | Diphenylcarbazone | - | Flow-through | Absorbance | $5.6 \times 10^{-8}$ | [23] |
| $Pb^{2+}$ | Lead ionophore IV | Chromoionophore VII | Batch | Fluorescence | - | [24] |
| $Hg^{2+}$ | HT18C6 | Chromoionophore V | Batch | Absorbance | $2.0 \times 10^{-7}$ | [25] |
| $Hg^{2+}$ | PAN | - | Flow-through | Reflectance | $5.5 \times 10^{-7}$ | [26] |
| $Li^{+}$ | Litium ionophore VIII | Chromoionophore XIV | Flow-through | Reflectance | $1.4 \times 10^{-4}$ | [27] |
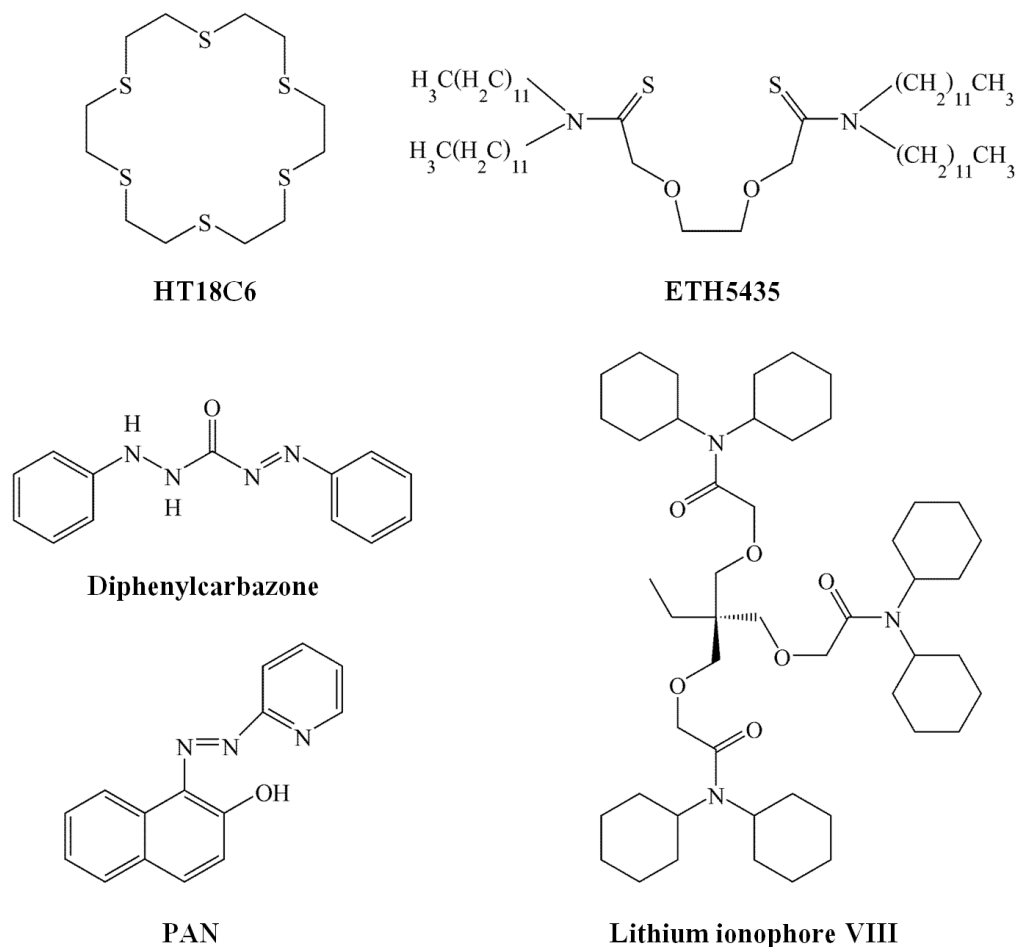
**Figure 2.7** Chemical structures of ionophores for metal ion detection in previous works.

### 2.4.2 Development of ISOs in other platforms

The ISOs on conventional planar film offer some disadvantages such as long response time, the need of sophisticate scientific instruments, and the use of large amount of cocktail solution to prepare the sensing films. Many researches developed the ISOs in various other platforms such as surface of microspheres [62], polymer swelling [63], and emulsion forming micelles [64]. However, these platforms still required a huge instrument which often cannot be applied for on-site analysis. Since

the paper-based and thread-based analytical devices provide many advantages as previous descript, recently, the sensing process by means of ISOs has incorporated with paper-based or thread-based analytical devices. The fabrication and detection methods of some paper-based or thread-based platforms using ISOs as a colorimetric sensing agent proposed in previous works are summarized as below.

In 2015, Wang, Qin, and Meyerhoff [65] first fabricated the paper-based analytical device by using ISOs as a colorimetric sensing agent. In their work, the solution of sensing components including sodium ionophore VI, chromoionophore I, and KTFPB were introduced to a piece of Whatman filter paper (Grade 5). After the evaporation of solvent, the paper-based devices were placed in 96 well plates. In detection method, a sample solution or one of standard solution was gently added to a well which was contained a paper-based sensor. The pictures of paper-based sensor were then taken with a smart phone (in dark room and using flash light from smart phone as light source) and then analyzed the color numerical data (hue-based color) with ImageJ. The paper-based optode sensor showed a highly selective with $Na^+$ over other common cations ($K^+$, $Ca^{2+}$, $Mg^{2+}$, and $Li^+$) by changing the color of paper from blue to purplish as shown in **Figure 2.8**. With their proposed device, $Na^+$ concentration could be detected with the dynamic range from $10^{-4}$ to $10^{-1}$ M.
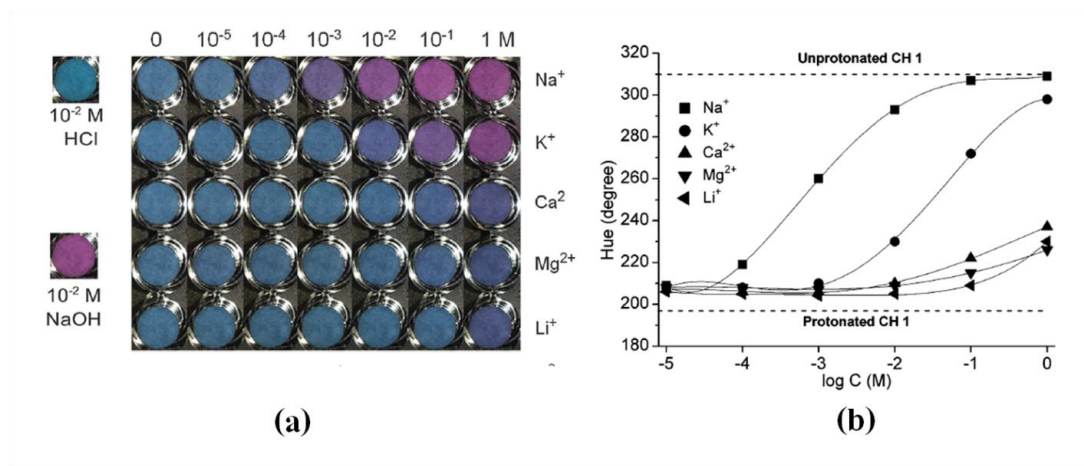
**Figure 2.8** Picture of paper‑based device proposed by Wang and co‑workers upon adding various concentrations of different metal ions (a), and the hue‑based response curve of each metal ion (b) [65].

The colorimetric detection by ISOs systems on the thread‑based analytical device was first introduced by Erenas, Orbe‑Payá, and Capitan‑Valley in 2016 [59]. In their work, the optode sensing components including dibenzo18‑crown‑6‑ether, chromoionophore I, KT$p$ClPB, PVC, and NPOE were dissolved in THF and added to the cotton thread in proposed thread‑based device as shown in **Figure 2.9**. After the evaporation of solvent, a sample solution or one of standard solution was dropped onto one tail‑end of thread (sampling zone) to allow the liquid flow into the detection zone contained the ISOs sensing agent. The pictures of device were then taken with a digital camera and then analyzed the color numerical data (hue‑based color) with ImageJ. The thread‑based optode sensor showed a highly selective with $K^+$ over other common cations ($Na^+$, $Ca^{2+}$, and $Mg^{2+}$) by changing the color of paper from blue to magenta. With their proposed device, $K^+$ concentration could be detected with the dynamic range from $2.4\times10^{-5}$ to 0.95 M.
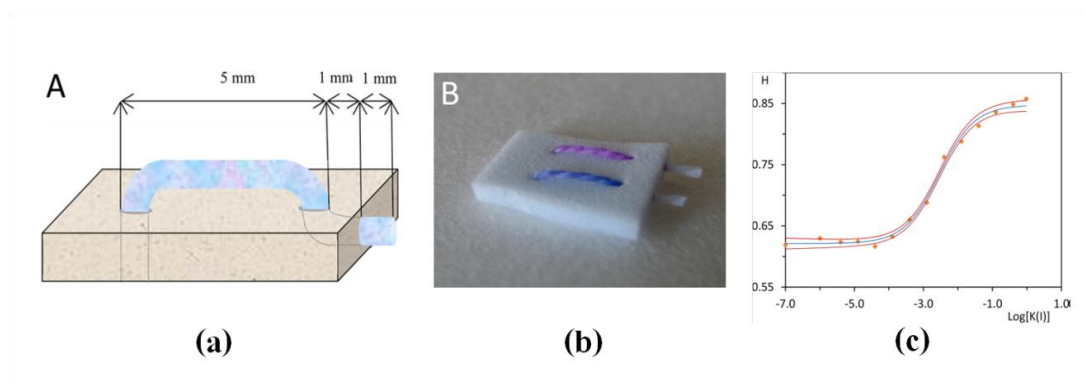
**Figure 2.9** The design of thread-based analytical device proposed by Erenas and co-workers (a), a real picture of thread-based device (b), and the hue-based response curve of $K^+$(c) [59].

In 2018, Gerold, Bakker, and Henry [66] fabricated the paper-based analytical device by using ISOs as a colorimetric sensing agent. In their work, ISOs was first synthesized into the platform of optode nanosphere. The cocktail solution of sensing components including potassium ionophore I, chromoionophore I, NaTFPB, and Pluronic F-127 in THF as a solvent was injected into $H_2O$ using a micropipette. After the evaporation of THF, the suspension of optode nanosphere with 178 nm in diameter was formed (characterized by dynamic light scattering). In detection method, the optode nanosphere was pipette onto the wax printed paper-based device, and a sample solution or one of standard solution was gently added to the same position of optode nanosphere. The pictures of paper-based sensor were then taken with a digital camera and then analyzed the color numerical data with ImageJ. The paper-based optode sensor showed a highly selective with $K^+$ over other common cations ($Na^+$, $Li^+$, and $Mg^{2+}$) by changing the color of paper from blue to reddish-purple as shown in **Figure 2.10**. With their proposed device, $K^+$ concentration could be detected with the dynamic range from 0.1 to 5 mM.
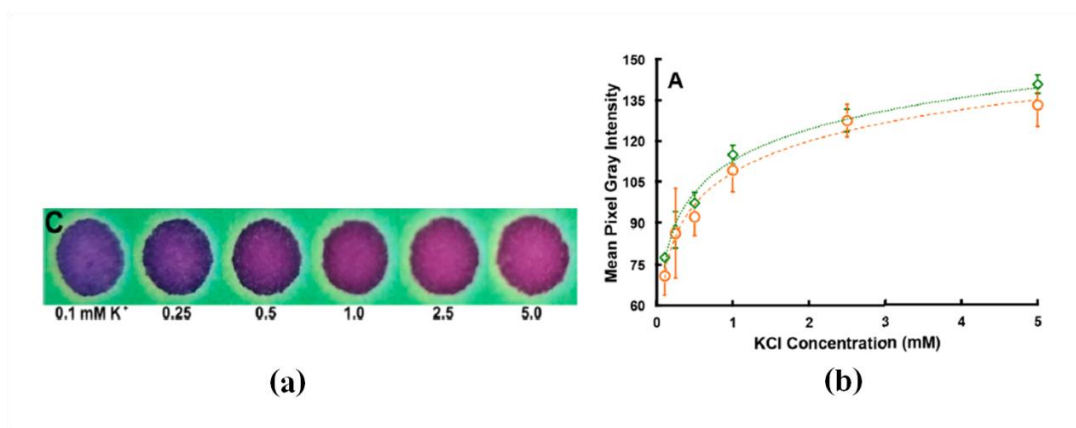
**Figure 2.10** Picture of paper-based device proposed by Gerold and co-workers upon adding various concentration of $K^+$ (a), and the response curve of $K^+$ (b) [66].

In 2018 Shibata and co-workers [67] developed the colorimetric $Na^+$ analysis using ISOs system in paper-based platform. The optode sensing components including sodium ionophore IV, chromoionophore I, KT$p$ClPB, PVC, and DOS were dissolved in cyclohexanone, and the cocktail solution was deposited onto the detection area of the proposed device as shown in **Figure 2.11** by printing technique. The $Na^+$ detection method was performed by dropping a sample or one of standard solution onto the inlet area of proposed device. The picture of the bottom side of device was taken with a scanner and then analyzed the color numerical data with ImageJ. The paper-based optode sensor showed a highly selective with $Na^+$ over other common cations ($K^+$, $Li^+$, $Ca^{2+}$, and $Mg^{2+}$) by changing the color of paper from blue to red. With their proposed device, $Na^+$ concentration could be detected with the dynamic range from $10^{-5}$ to 1 M.
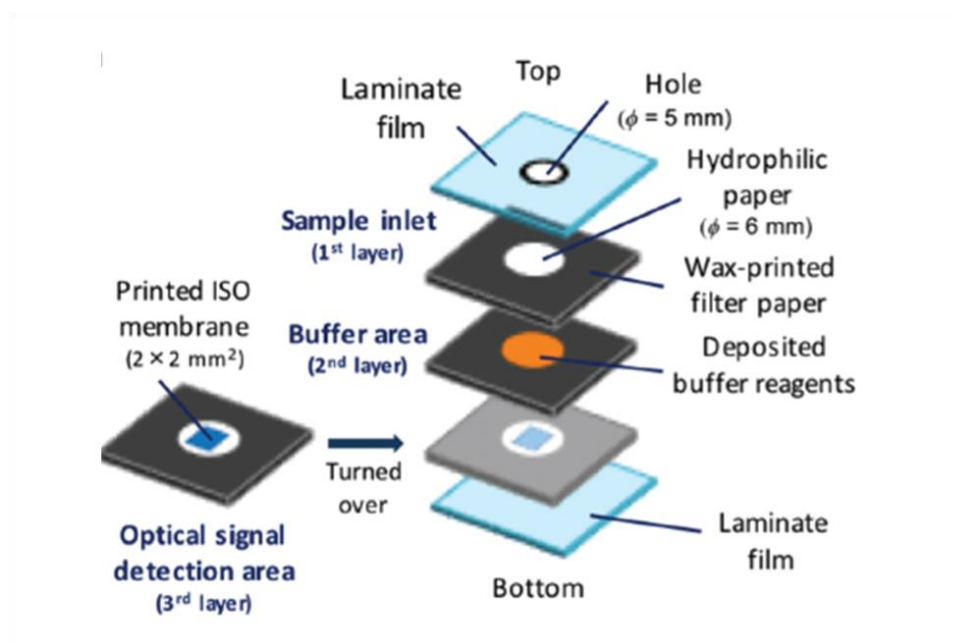
**Figure 2.11** The design of paper-based analytical device for Na$^+$ detection proposed by Shibata and co-workers [67].

In 2019, a paper-based analytical device using the ISOs systems was incorporated with distance-based detection for Ca$^{2+}$ analysis by Shibata, Hiruta, and Citterio [68]. In their work, ISOs was first synthesized into the platform of optode nanosphere. The cocktail solution of sensing components including calcium ionophore IV, chromoionophore I, NaTFPB, and Pluronic F-127 in THF as a solvent was injected into H$_2$O on a vortex mixure with a spinning speed of 1000 rpm. After removal of THF by ejection with N$_2$, the suspension of optode nanosphere with approximately 200 nm in diameter was formed (characterized by dynamic light scattering). The proposed paper-based device was fabricated by wax printing technique with a pattern as shown in **Figure 2.12.** The optode nanosphere suspensions were inkjet-printed onto along the channel of the device. To perform Ca$^{2+}$ analysis with distance-based assay method, a sample or one of standard solution was applied to the inlet area of proposed device. The device was then incubated to allow the liquid flow along the detection channel.

After that, the lengths of the color change were measured by the naked-eye visual readout. The paper-based optode sensor showed a highly selective with $Ca^{2+}$ over other common cations ($Na^+$, $K^+$, $Li^+$, and $Mg^{2+}$) and some heavy metals cations ($Zn^{2+}$, $Cu^{2+}$, $Ni^{2+}$, $Hg^{2+}$, and $Al^{3+}$). With their proposed device, $Ca^{2+}$ concentration could be detected with the dynamic range from 0.05 to 5 mM. Their research showed that the incorporating of paper-based ISOs device with distance-based analysis could eliminate the requirement of digital camera which make them more facile than colorimetric detection method.

The chemical structures of some reagents in **Section 2.4.2** are shown in **Figure 2.13**
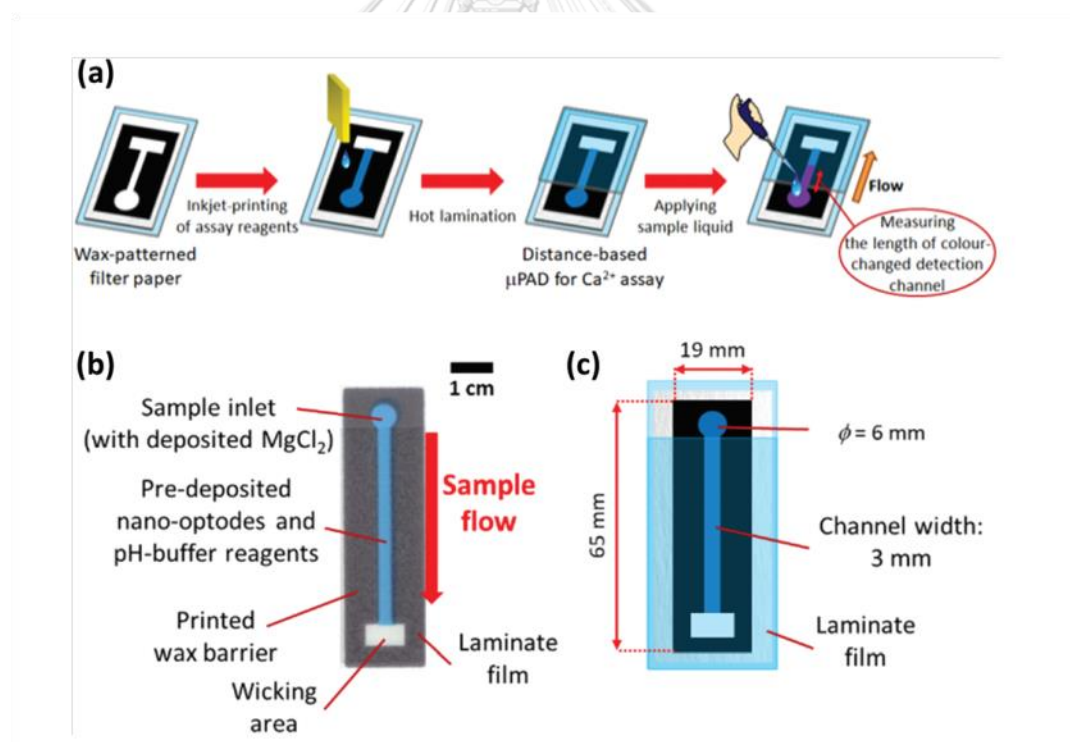


**Figure 2.12** The design of paper-based analytical device and the detection procedures for $Ca^{2+}$ detection proposed by Shibata and co-workers [68].
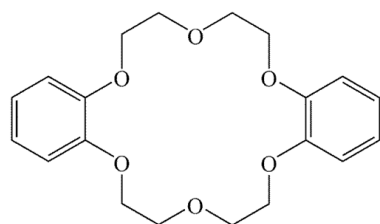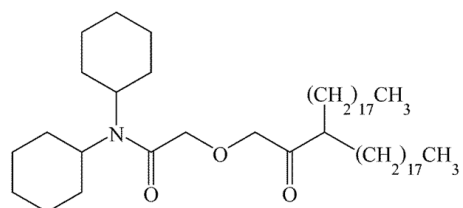
**Dibenzo-18-crown-6-ether**                **Calcium ionophore IV**
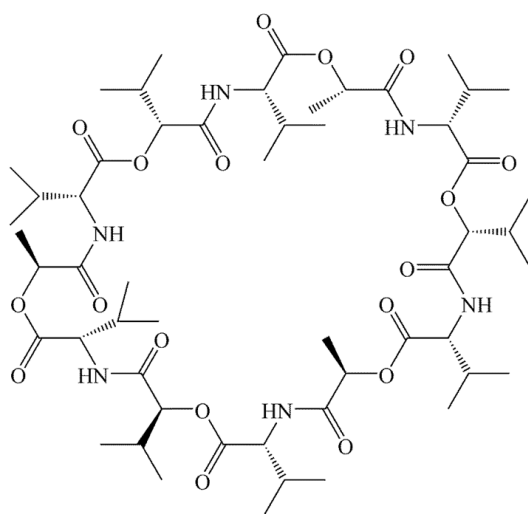


**Potassium ionophore I (valinomycin)**

**Figure 2.13** Chemical structures of some reagents in Section 2.4.2

จุฬาลงกรณ์มหาวิทยาลัย

CHULALONGKORN UNIVERSITY

# CHAPTER III

# EXPERIMENTAL

## 3.1 Reagents and materials

All reagents were used without future purification. List of all reagents used in this research is shown in **Table 3.1**

**Table 3.1** List of all reagents using in this research

| Reagents | Manufacturers | Grade |
|---|---|---|
| 25,27-Di(benzothiazolyl)-26,28-hydroxycalix[4]arene (**CU1**) | Supramolecular Chemistry Research Unit (SCRU) | - |
| High molecular weight polyvinyl chloride (PVC) | Sigma-Aldrich | Selectophore® |
| Bis(2-ethylhexyl) sebacate (DOS) | Sigma-Aldrich | Selectophore® |
| Potassium tetrakis(4-chlorophenyl)borate (KT$p$ClPB) | Sigma-Aldrich | Selectophore® |
| 9-(Diethylamino)-5-(octadecanoylimino) -5H-benzo[a]phenoxazine (chromoionophore I) | Sigma-Aldrich | Selectophore® |

**Table 3.1** (cont.) List of all reagents using in this research

| Reagents | Manufacturers | Grade |
|---|---|---|
| 9-Dimethylamino-5-4-(15-butyl-1,13-dioxo-2,14-dioxanonadecyl) phenyliminobenzoaphenoxazine (chromoionophore VII) | Sigma-Aldrich | Selectophore® |
| 3',3'',5',5''-Tetrabromophenolph-thaleinethyl ester (chromoionophore VIII) | Sigma-Aldrich | Selectophore® |
| 2-[2-(9-Acridinyl)vinyl]-5-(diethylamino)phenyl stearate (chromoionophore XIV) | Sigma-Aldrich | Selectophore® |
| Tetrahydrofuran (THF) | Sigma-Aldrich | Selectophore® |
| Sodium nitrate | Fluka | AR Grade |
| Magnesium nitrate | Merck | AR Grade |
| Potassium nitrate | Merck | AR Grade |
| Calcium nitrate tetrahydrate | Ajax Finechem | AR Grade |
| Chromium(III) nitrate nonahydrate | Fisher Scientific | AR Grade |
| Iron(III) nitrate | Merck | AR Grade |
| Cobalt(II) nitrate hexahydrate | Fisher Scientific | AR Grade |
| Nickel(II) nitrate hexahydrate | Carlo Erba | AR Grade |

**Table 3.1** (cont.) List of all reagents using in this research

| Reagents | Manufacturers | Grade |
|---|---|---|
| Copper(II) nitrate trihydrate | Merck | AR Grade |
| Zinc(II) nitrate | Merck | AR Grade |
| Cadmium(II) nitrate tetrahydrate | Carlo Erba | AR Grade |
| Lead(II) nitrate | Honey well | AR Grade |
| Sodium chloride | Fisher Scientific | AR Grade |
| Sodium acetate anhydrous | Carlo Erba | AR Grade |
| Sodium tetraborate | Merck | AR Grade |
| Sodium carbonate anhydrous | J.T.Baker | AR Grade |
| Glacial acetic acid | Merck | AR Grade |
| Citric acid monohydrous | Carlo Erba | AR Grade |
| Tri-sodium citrate dehydrate | Fisher Scientific | AR Grade |
| Boric acid | Merck | AR Grade |

All aqueous solutions were prepared in ultrapure water which was obtained from water purification system (Millipore) with a resistivity of 18.2 M$\Omega$ .cm. Filter paper including Whatman No.1 (Grade 1, 180 μm in thickness) and No.42 (Grade 42, 200 μm in thickness) were acquired from GE Healthcare UK limited (Buckinghamshire, U.K.). 100% Polyester sewing thread was purchased from local community store in Bangkok, Thailand.

### 3.2 Apparatus

The cocktail solution was shaken using a vortex mixer to homogenize the mixer. All pictures were taken with a DSLR camera (Nikon D5200), and a cube light box with a stable LED light source was used to control the ambient light. The

absorption spectra of the optode nanosphere were acquired from Hewlett‑Packard 8453 UV‑Visible spectrophotometer, Germany. The particle size distribution profile of the optode nanosphere was evaluated by dynamic light scattering (DLS), Zetasizer Nano ZSP, Malvern, UK. The pH values of solutions were measured using a benchtop pH meter, Mettler Toledo FE20 FiveEasy$^{TM}$ Plus, Switzerland. The concentrations of $Ag^+$ and $Hg^{2+}$ in samples were analyzed by inductively coupled plasma optical emission spectrometer, Thermo Scientific, model iCAP 6500 series.

## 3.3 Ion selective optode in a platform of paper‑based analytical device

### 3.3.1 Paper‑based device preparation

To prepare the cocktail solutions, **CU1**, KT$p$ClPB, chromoionophore XIV, PVC, and DOS were weighed in an empty 12 mL glass bottle according to the weight shown in **Table 3.2** (total weight of 90 mg). Then, 2 mL of THF was added using a micropipette, and the mixer solution was shaken in a vortex mixer to homogenize mixer. After that, the filter paper was cut into a piece of $1 \times 5$ cm$^2$, and the 4 µL of the prepared cocktail solution was dropped onto a piece of filter paper. To repeat the detection, 3×4 µL of cocktail solution were dropped onto the different positions in the same filter paper. After THF was evaporated (around 5 min at ambient temperature), three circles of blue color with $8.4 \pm 0.5$ mm on the filter paper were observed. These blue circles were used as the detection zone for colorimetric detection.

**Table 3.2** Cocktail compositions for paper-based device preparation.

| Chemicals | % Chromoionophore XIV (% mol relative to KT$p$ClPB) | | | | | |
|---|---|---|---|---|---|---|
| | 25% | | 50% | | 75% | |
| | Amount (mmol kg$^{-1}$) | Weight (mg) | Amount (mmol kg$^{-1}$) | Weight (mg) | Amount (mmol kg$^{-1}$) | Weight (mg) |
| **CU1** | 10.94 | 0.71 | 10.94 | 0.71 | 10.94 | 0.71 |
| KT$p$ClPB | 7.47 | 0.33 | 7.47 | 0.33 | 7.47 | 0.33 |
| Chromoionophore XIV | 1.87 | 0.11 | 3.74 | 0.21 | 5.60 | 0.32 |
| PVC | - | 29.61 | - | 29.58 | - | 29.55 |
| DOS | - | 59.24 | - | 59.16 | - | 59.09 |

### 3.3.2 Colorimetric Ag$^+$ and Hg$^{2+}$ quantitative detection using paper-based device

The working solutions were prepared by adding 3 mL of sample or standard solution, 500 µL of 0.1 M acetic-acetate buffer, and 250 µL of 0.1 M masking agent (NaCl or EDTA) into a 5 mL volumetric flask. The final volume was then filled by milli-Q water. After that, a prepared paper-based device was immersed into the working solution. After 10 or 15 min for Ag$^+$ or Hg$^{2+}$ detection, respectively, a picture of paper-based device was taken by placing the paper strip on a plastic sheet, and the photography was performed in a cube light box with a stable LED light source to obtain the same ambient light of all pictures. Moreover, to obtain the same light exposure of all pictures, DSLR camera was used in M mode. Three main parameters of DSLR camera including ISO (gain), F (aperture), and shutter speed were kept constant of ISO200, F5.6, and 1/640 s, respectively. The fabrication and detection method of paper-based device are illustrated in **Figure 3.1**
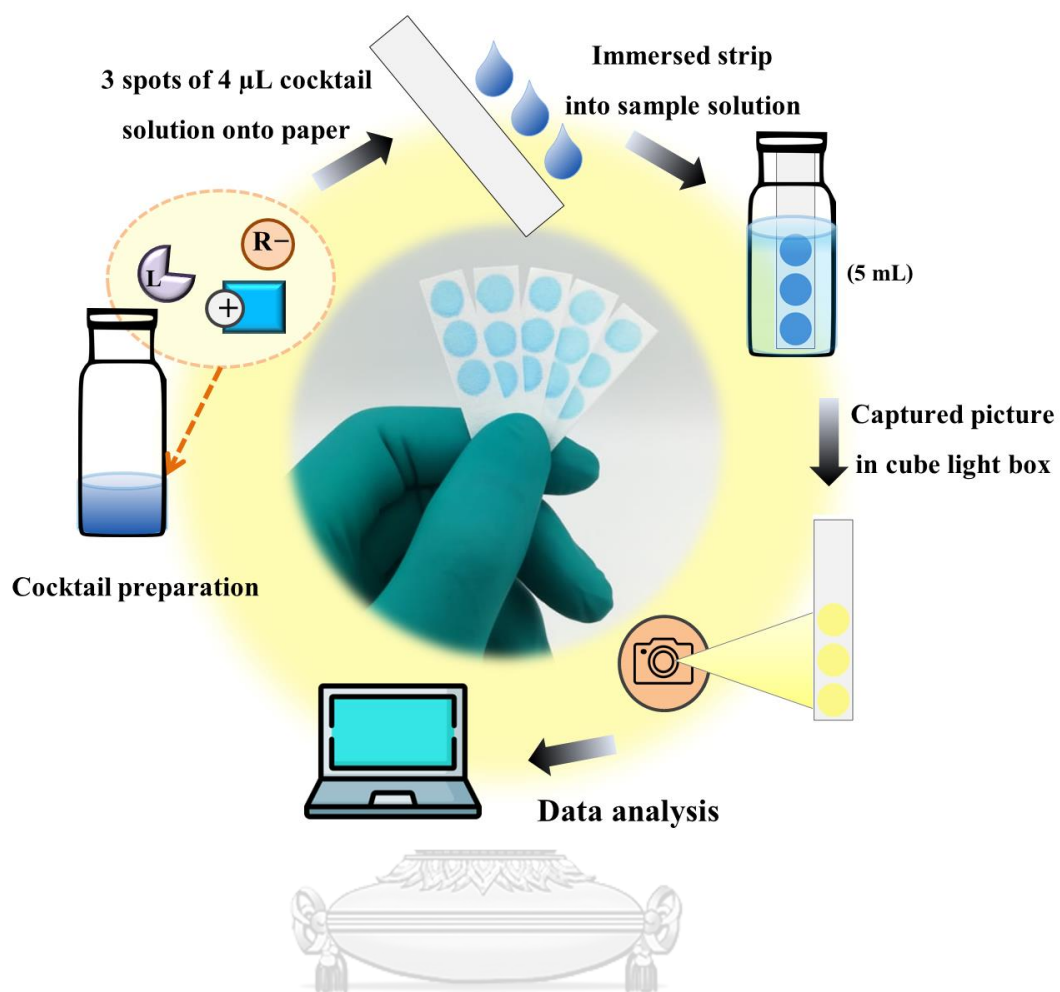
**Figure 3.1** Schematic illustration of the preparation and detection method of the proposed paper-based device.

### 3.3.3 Image analysis

The pictures acquisitions were further analyzed by ImageJ software to earn the RGB (Red-Green-Blue) color intensity values of detection zone. The RGB color intensity can be transferred into various numerical color data such as HSV (HSB), CMY, CIE $L^*a^*b^*$ color space, and etc [69, 70]. In this work, CIE $L^*a^*b^*$ color space was obtained by using free online site (http://colorizer.org/). The values of $L^*a^*b^*$ were further calculated into $\Delta E$ by using **Equation (3.1)**, when $\Delta L^*, \Delta a^*, and \Delta b^*$ are the difference of $L^*$ (lightness from black to white), $a^*$ (green to red), and $b^*$ (blue to yellow) between the color of strip after immersing in buffer and standard or sample solutions. Finally, the acquired $\Delta E$ was used to plot a calibration response according to **Equation (3.2)**.

$$\Delta E = \sqrt{(\Delta L^*)^2 + (\Delta a^*)^2 + (\Delta b^*)^2} \tag{3.1}$$

$$\Delta E = \frac{A_1 - A_2}{1 + e^{(\log[M^{n+}] - x_0)/dx}} + A_2 \tag{3.2}$$

## 3.4 Ion selective optode in a platform of thread-based analytical device

### 3.4.1 Ion selective optode nanosphere preparation

The optode nanosphere preparation method was adapted according to previous report [66] as follows: 0.84 mg of **CU1**, 0.40 mg of KT*p*ClPB, 0.38 mg of Chromoionophore XIV, 2.4 mg of DOS, and 2.0 mg of pluronic p123 were dissolved in 1.20 mL of THF, and the mixture was shaken by a vortex mixer. Then, 1.0 mL of prepared solution was gradually dropped into 3.0 mL of milli-Q water with a spinning speed of 300 rpm. After that, THF was removed by blowing the solution with $N_2$ gas until 60% weight of solution remaining. The prepared optode nanosphere was stored in

a refrigerator for further use. The fabrication scheme of optode nanosphere is illustrated in **Figure 3.2**
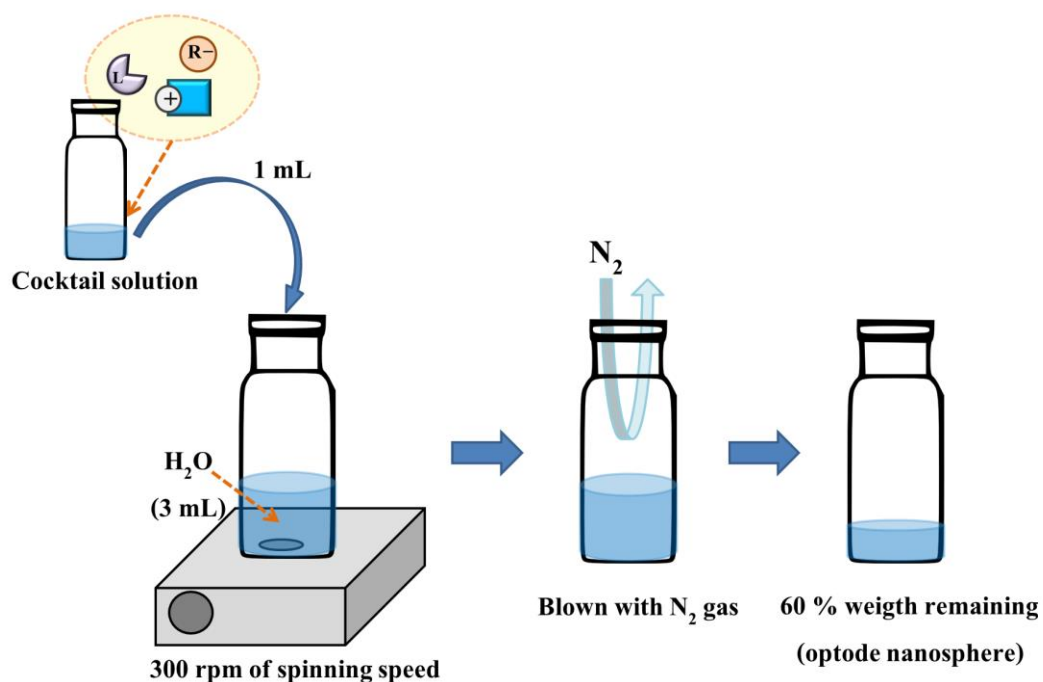


**Figure 3.2** Schematic illustration of the preparation of optode nanosphere.

## 3.4.2 Study of ISOs nanosphere characteristic by UV-Visible spectrophotometry

To study the property of the optode nanosphere acquisition, four parameters including effect of pH, $Ag^+$ concentrations, $Hg^{2+}$ concentrations, and selectivity of the optode nanosphere were investigated. The absorptions of the optode nanosphere in the aqueous solution with different conditions were measured. For the pH effect, citric–citrate (pH 3.0), acetic–acetate (pH 4.0 – 6.0), and boric–borate (pH 7.0 – 10.0) buffer solutions were prepared in the concentrations of 0.01 M with different pH values consisting of pH 3.0 to 10.0. Various concentrations of $Ag^+$ or $Hg^{2+}$ in acetic-acetate

buffer solution at pH 5.0 were also studied. Moreover, other metal ions including $Na^+$, $K^+$, $Mg^{2+}$, $Ca^{2+}$, $Cr^{3+}$, $Fe^{3+}$, $Co^{2+}$, $Ni^{2+}$, $Cu^{2+}$, $Zn^{2+}$, $Cd^{2+}$, and $Pb^{2+}$ were prepared in the concentration of 1 mM with acetic-acetate buffer at pH 5.0. The absorption spectra were recorded using UV-Visible spectrophotometer by adding 50 µL of the optode nanosphere dispersion to 2 mL of each solution.

### 3.4.3 Thread-based device preparation

The 100% polyester thread was purchased from a local community store, Bangkok, Thailand. To remove undesirable impurities and natural waxes presented on the thread surface, thread was boiled in 10 mg $mL^{-1}$ $Na_2CO_3$ solution for 5 min and washed several times with DI water until pH of washing water was approximately neutral. The thread was allowed to dry at room temperature and kept in plastic zip bag for further use. To fabricate thread-based device, threads were cut into approximate 7 cm in length. For marking the positions of the optode nanosphere or the sample solution drop zone, threads were tied knots in the middle. A plastic sheet was cut into $10.0 \times 20.0$ $cm^2$ with $5.0 \times 15.0$ $cm^2$ vacancy as shown in **Figure 3.3.** Then, threads were stretched on the plastic sheet and attached them with adhesive tape on the end.

**plastic sheet**

thread

knot

adhesive tape

5 cm

adhesive tape
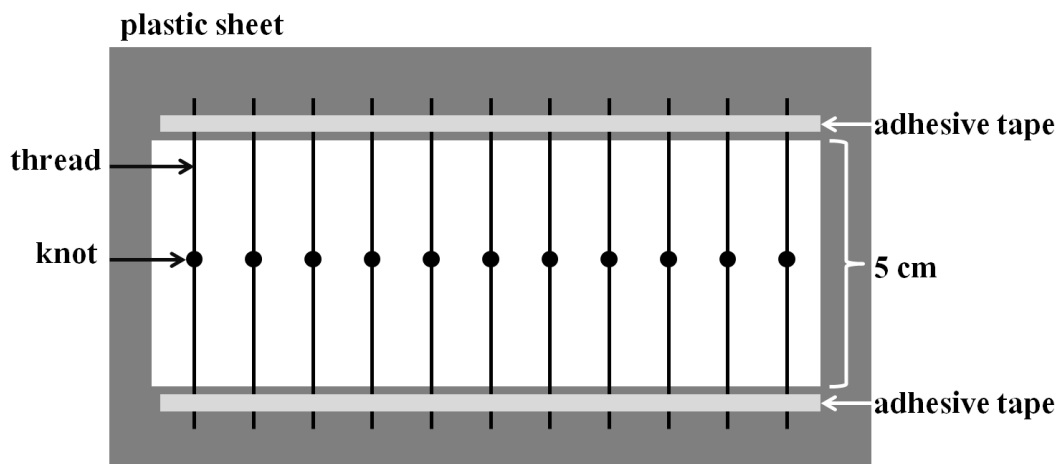
**Figure 3.3** Schematic illustration of the proposed thread-based device.

### 3.4.4 Distance-based $Ag^+$ and $Hg^{2+}$ quantification

3 mL of sample solution or one of the standard aqueous solutions and 500 μL of 0.1 M acetic-acetate buffer were mixed in a 5 mL of volumetric flask, and milli-Q water was filled to final volume. 3 μL of the optode nanosphere was dropped onto a knot in the middle of thread using micropipette and then allowed to dry in ambient temperature. To increase the amount of sensing particles attached on the thread surface, 3 μL of optode nanosphere suspension was repeatedly dropped onto the same knot 3 times. To determine $Hg^{2+}$ or $Ag^+$ concentrations by using the length measurement method, 3 μL of the prepared sample solutions were repeatedly dropped onto the knots of thread. After repeatedly dropping the sample solution onto the same knot 15 times (total volume = 45 μL), the distance of the color change was then measured by using a ruler to determine $Ag^+$ or $Hg^{2+}$ concentrations. The detection merthod by the proposed thread-based analytical device is illustrated in **Figure 3.4**
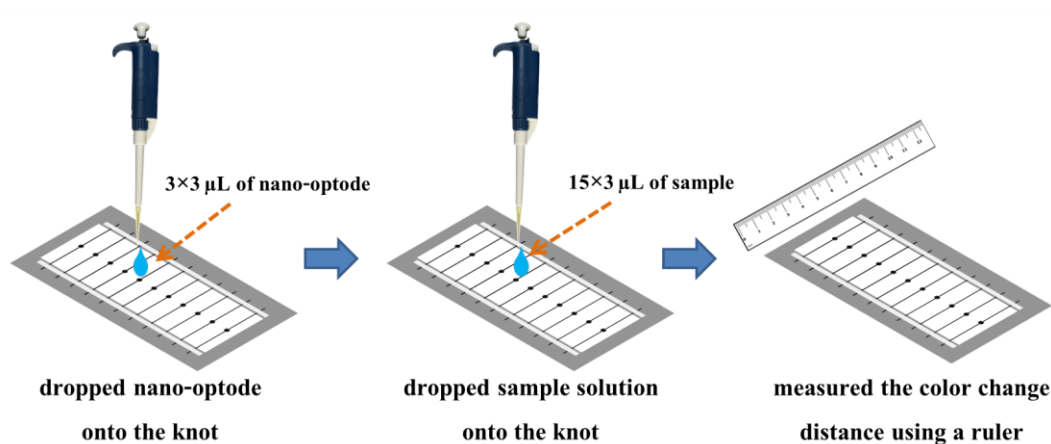
**Figure 3.4** Schematic illustration of the detection method by the proposed thread-based device.

## 3.5 Real sample analysis

To apply the proposed optode devices for quantitative determination of $Ag^+$ and $Hg^{2+}$ in real samples, the determination of target ions in various aqueous sample solutions were performed. Real water samples were collected from diverse local sources in Thailand including the water from commercial bottled water, tap water, pond water, and agricultural wastewater. These water samples were filtered through filter paper No.1 and stored in plastic bottles. The pHs of solutions were first adjusted to working pH (pH ~ 5) using 1 M $HNO_3$ before used. To identify the accuracy of the proposed method, the determinations of $Ag^+$ and $Hg^{2+}$ in real water samples were performed using spiked technique. Then, the experiment was performed with the same method as described in **Section 3.3.2** for paper-based device and **Section 3.4.4** for thread-based device. Moreover, the proposed paper-based devices were also applied to determine the total silver in a cleaning product sample containing silver nanoparticles (AgNPs). The ingredient list in cleaning product sample as shown below;

ingredient in 100 mL of product including

|    |    |    |
|----|----|----|
| ─ pure silver (99.99%) | 10 mg |
| ─ polyvinylpyrrolidone (PVP) | 120 mg |
| ─ ethyl alcohol | 10 mL |
| ─ water | 90 mL. |

To determine the amount of $Ag^+$ in sample with the proposed device, AgNPs in sample were first oxidized to silver ion using oxidizing agent. The cleaning product sample was diluted 18 folds in a volumetric flask (50 mL) with milli-Q water. 30% $H_2O_2$ was added to the solution and stirred for 2 h. To identify the accuracy of the proposed method, spiking technique was performed. The experiment was then performed with the same method as described in **Section 3.3.2**. Finally, the amounts of $Ag^+$ and $Hg^{2+}$ in real samples were also determined with ICP-OES.

จุฬาลงกรณ์มหาวิทยาลัย

CHULALONGKORN UNIVERSITY

# CHAPTER IV

# RESULTS AND DISCUSSION

## 4.1 Characteristic of CU1 to selectivity of ISOs

**CU1** is a derivative of calix[4]arene which has two benzothiazole groups in its structure as shown in **Figure 4.1**. Two sulfur atoms in its structure cause the inclination of **CU1** to bind with some soft cations. As reported in previous research [28], **CU1** showed a highly selective binding with $Ag^+$ in an ion-selective electrodes (ISEs) platform. However, it was found that the $Ag^+$ detection using ISEs suffered the interfering from $Hg^{2+}$ because of the same mercaptophilic property and the similar ionic radius. For this reason, the use of **CU1** as an ion-selective ionophore in our proposed platforms showed the capability of the proposed ISOs for dual detection of both $Ag^+$ and $Hg^{2+}$.
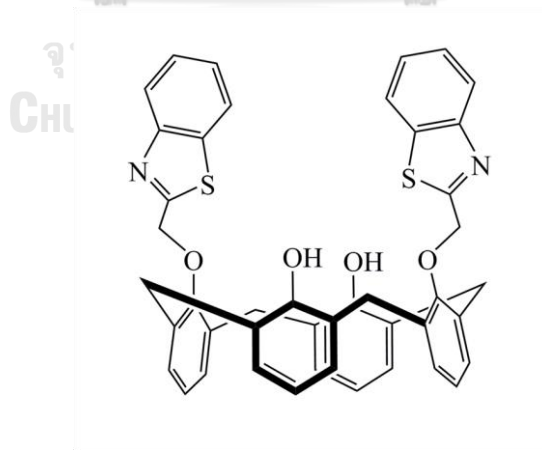


**Figure 4.1** Chemical structure of **CU1**.

**4.2 Study of types of chromoionophore**

The concentrations of target ions were observed by the color change of chromoionophore. Hence, four types of commercial lipophilic pH indicator including chromoionophore I, VII, VIII, XIV (the chemical structures shown in **Figure 2.3**) were investigated. The proposed paper-based devices were prepared according to the procedure in **Section 3.3.1** by using the different types of chromoionophore. The criterions to select type of chromoionophore were the chromoionophore which provided high $\Delta E$ and also high selectivity for $Ag^+$ and $Hg^{2+}$ detection using the prepared paper-based device. To investigate these, the prepared paper-based devices were immersed in different metal ion solutions (1 mM) and different pHs of buffer solutions (10 mM). Affter 15 min, the pictures of the paper-based devices were taken and $\Delta E$ was further calculated.

The pictures and $\Delta E$ of the paper-based device prepared using chromoionophore I are shown in **Figure 4.2a**. The most clearly color change of the paper-based device from blue to purple in the presence of $Ag^+$ and $Hg^{2+}$ at pH 8.0 was observed. However, the color change was not obviously observed by the naked eye.

The pictures and $\Delta E$ of the paper-based device prepared using chromoionophore VII are shown in **Figure 4.2b**. The most clearly color change of the paper-based device from purple to red in the presence of $Ag^+$ and $Hg^{2+}$ at pH 5.0, 6.0, and 8.0 was observed. However, the color change was not obviously observed by the naked eye.

The pictures and $\Delta E$ of the paper-based device prepared using chromoionophore VIII are shown in **Figure 4.2c**. The most clearly color change of the paper-based device from yellow to blue in the presence of $Ag^+$ and $Hg^{2+}$ at pH 8.0 was observed. However, the paper-based device suffers low selective property.

The pictures and $\Delta E$ of the paper-based device prepared using

chromoionophore XIV are shown in **Figure 4.2d**. The most clearly color change of the paper-based device from blue to yellow in the presence of $Ag^+$ and $Hg^{2+}$ at pH 5.0 was observed. The color change of the device was obviously observed by the naked eye, and high selective property with only $Ag^+$ and $Hg^{2+}$ at this pH was acquired. Therefore, chromoionophore XIV was chosen for further studies.
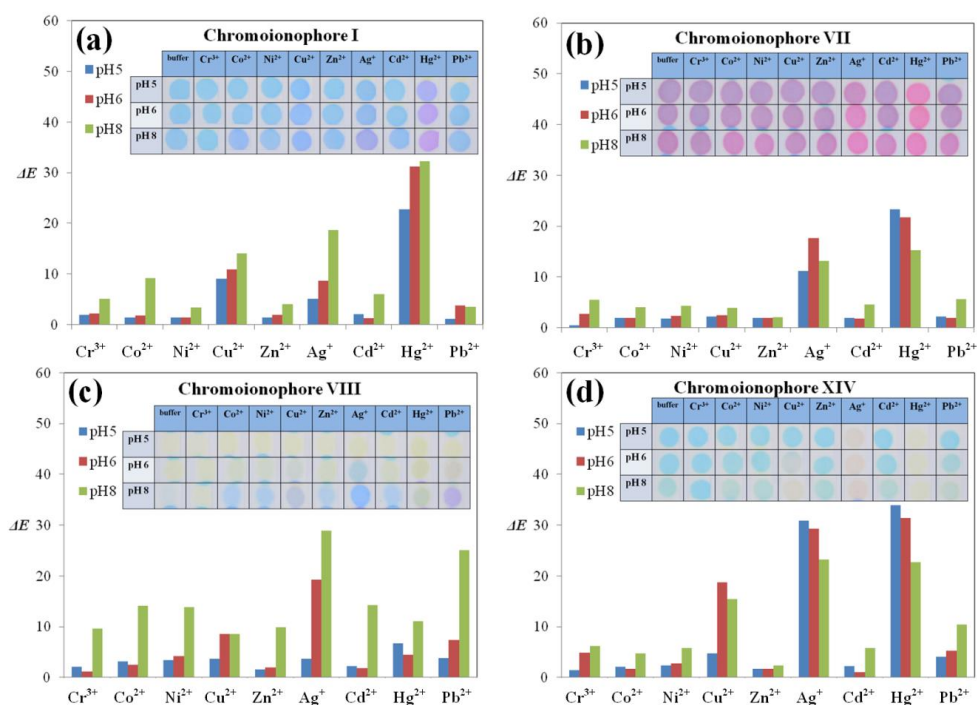


**Figure 4.2** $\Delta E$ and pictures of the paper-based device using chromoionophore I (a), VII (b), VIII (c), and XIV (d) (75% relative to mole of KTpClPB)

## 4.3 Ion selective optode in a platform of paper-based analytical device

### 4.3.1. Response behavior of ISOs on paper-based analytical device

The hydrophobic plasticized-based PVC containing **CU1** as an ionophore, KTpClPB as an ion-exchenger, and chromoionophore XIV as a lipophilic pH indicator was introduced to the cellulose filter paper by dropping the cocktail solution directly

using a micropipette. After the evaporation of THF, the plasticized-based sensing component was coated on surface or trapped in pores of filter paper. Since the properties of cellulose paper were hydrophilic and high surface to volume ratio, high contact surface between the sensing component and aqueous sample solution was acquired. We assumed that the optode mechanism was an identical mechanism with the conventional planar film optode. According to **Equation (2.1),** the sensing mechanism was based on the cation-exchange process of target ion ($Ag^+$ or $Hg^{2+}$) and hydrogen ion ($H^+$) between water surrounding and hydrophobic plasticized-based PVC consisting of **CU1** (L), chromoionophore XIV (C), and KT$p$ClPB ($R^-$). **CU1** extracted $Ag^+$ or $Hg^{2+}$ from water to hydrophobic plasticized-based PVC while $H^+$ from chromoionophore XIV ($CH^+$) was released to water to maintain the electroneutrality. Hence, the color of the hydrophobic plasticized-based PVC on cellulose filter paper was changed from blue ($CH^+$) to yellow (C).

The best fit for experimental data with the theoretical line from **Equation (2.3)** is shown in **Figure 4.3**. The solid lines were the calculation lines and the circle spots were the experimental data. The results showed that the correlation coefficients ($R^2$) were 0.9865 and 0.9567 for $Ag^+$ and $Hg^{2+}$, respectively. However, the fitting $\Delta E$ directly to the Boltzman equation (**Equation (3.2)**) showed better correlations with $R^2$ more than 0.99 (see **Figure 4.12** in **Section 4.3.8**). Moreover, the fitting experimental data with optode response function in **Equation (2.3)** was necessary to use the signals from fully protonated form and fully deprotonated form of chromoionophore. Therefore, to simplify the experiment by avoidance the measuring signals of fully protonated form and fully deprotonated form of chromoionophore and achieve the better correlation, $\Delta E$ were used directly in a calibration response according to **Equation (3.2)** [59, 65, 69-71].
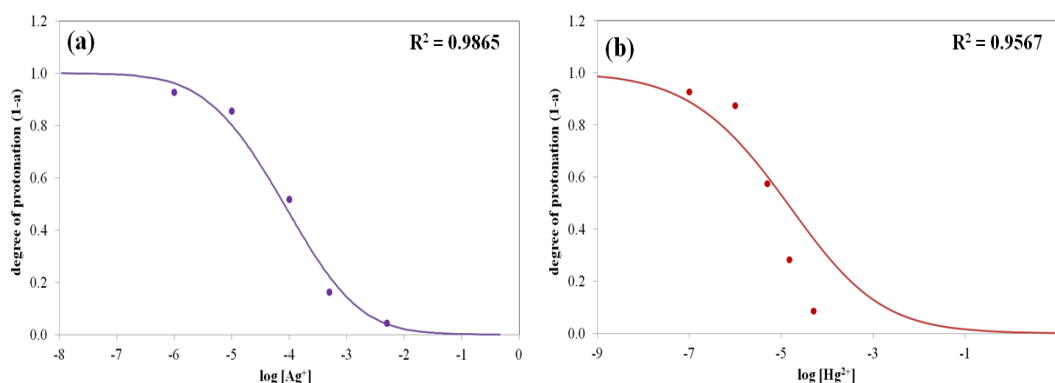
**Figure 4.3** Sigmoidal response curves of the paper-based optode for Ag$^+$ (a) and Hg$^{2+}$ (b).

### 4.3.2 Effect of filter paper types

Three different concentrations of analytes were used to show the effect of paper types on the color difference ($\Delta E$). Filter paper No.42 provided higher $\Delta E$ values than filter paper No.1 at all Ag$^+$ and Hg$^{2+}$ concentrations as shown in **Figure 4.4**. The different responses may be due to the different pore sizes of cellulose paper (2.5 µm and 11 µm for No.42 and No.1, respectively). A higher surface-to-volume ratio (smaller pores) results in stronger colorimetric signals since a larger amount of plasticized PVC phase was located at the surface of cellulose fibers. Hence, the filter paper No.42 was chosen for further experiments.
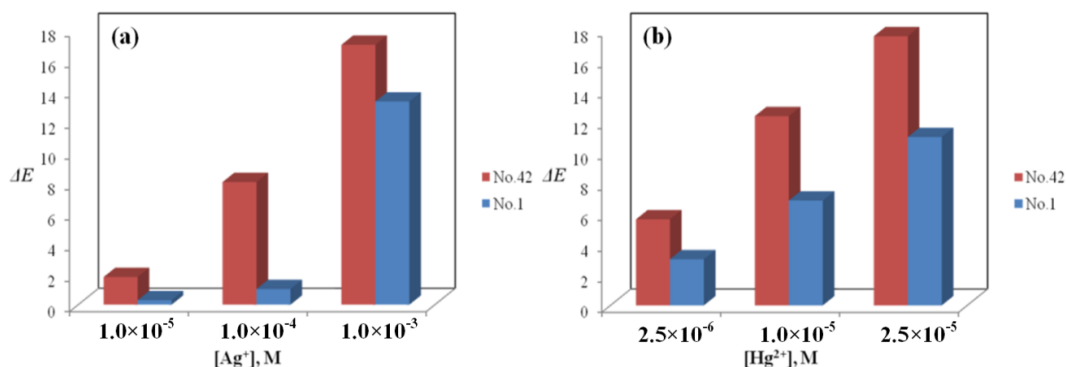
**Figure 4.4** Effect of paper types on the response of sensor in acetic-acetate buffer pH 5.0 with the immersing time of 10 min for $Ag^+$(a) and $Hg^{2+}$ (b) at different concentrations.

### 4.3.3 Cocktail composition

The amounts of all components in the hydrophobic plastized-based sensing polymer were leading to responses of paper-based optode device. 90 mg of all sensing components including **CU1** (L), KT$p$ClPB (R$^-$), chromoionophore XIV (C), PVC, and DOS were dissolved in 2 mL of THF. The weight of PVC and DOS was kept constant at a ratio of 1:2 (PVC:DOS). The amount of L, R$^-$, and C was kept in the order of L > R$^-$ > C to obtain the good sensitivity according to previous report [21]. In this work, 10.94 mmol kg$^{-1}$ of **CU1** and 7.47 mmol kg$^{-1}$ of KT$p$ClPB in the cocktail solution were fixed following a condition in ISEs from previous work [28]. To optimize the concentration of chromoionophore XIV, 25% (1.87 mmol kg$^{-1}$), 50% (3.74 mmol kg$^{-1}$), and 75% (5.60 mmol kg$^{-1}$) of chromoionophore XIV (percentage relative to amount of KT$p$ClPB) were studied. The response curves fitted with **Equation (3.2)** of three different amounts of chromoionophore XIV are shown in **Figure 4.5.** The results clearly showed that the increase of the percentage of chromoiophore in the sensing

phase led to the higher $\Delta E$ of the paper-based device. The highest $\Delta E$ was found when 75% of chromoionophore XIV in the cocktail solution was prepared. Hence, 75% of chromoionophore XIV was selected for the cocktail preparation.
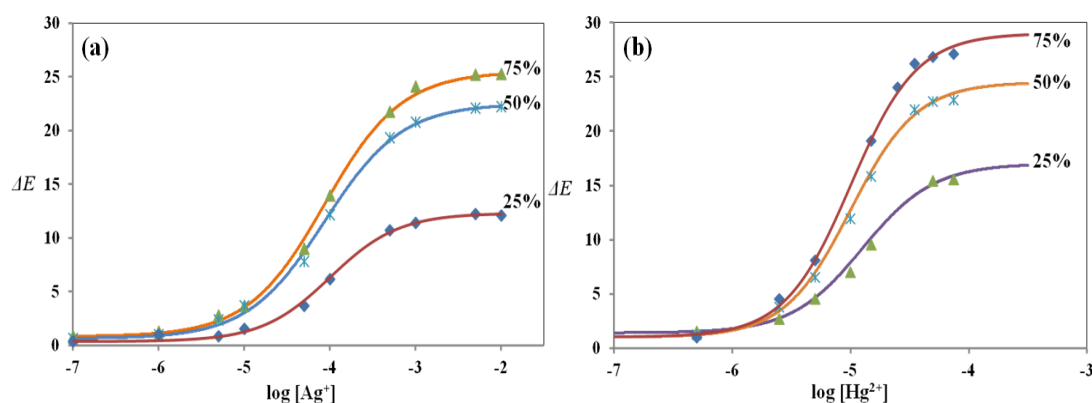


**Figure 4.5** Sigmoidal response curves of the paper-based device with different amounts of chromoionophore XIV for $Ag^+$ (a) and $Hg^{2+}$ (b) in 0.01 M acetic-acetate buffer at pH 5.0 with the immersing time of 10 min.

### 4.3.4 Effect of pH

Because the optode sensing process is implicated with the exchange equilibrium of matal ions ($M^{n+}$) and proton ($H^+$) between two phases, pH of solution can affect some of the parameters such as LOD, working range, and selectivity of optode. Hence, the effect of pH of the working solution was studied. The response curves fitted with **Equation (3.2)** of three different pH values including pH 4.0, 5.0, and 6.0 were obtained as shown in **Figure 4.6**. The results showed that both of $Ag^+$ and $Hg^{2+}$ response curves shifted to a lower concentration range when pH increased from 4.0 to 6.0, so the maximum response (highest $\Delta E$) could be obtained when the pH of solution was 6.0. However, at pH 6.0, some metal ions such as $Cu^{2+}$, $Pb^{2+}$, and $Cr^{3+}$ could interfere $Ag^+$ and $Hg^{2+}$ detections as shown in term of the selectivity coefficient

according to **Table 4.1** (see in **Section 4.3.6**). The interference of some metal ions at higher pH may be due to the non-selective binding between deprotonated hydroxyl group (phenolate group) of **CU1** and some borderline or hard metal ions such as $Cu^{2+}$ and $Pb^{2+}$. For this reason, the recognition of **CU1** with these interfering metal ions was increased. Hence, the working solution was prepared in the buffer solution pH 5.0 for further experiment to achieve a low limit of detection and better selectivity.
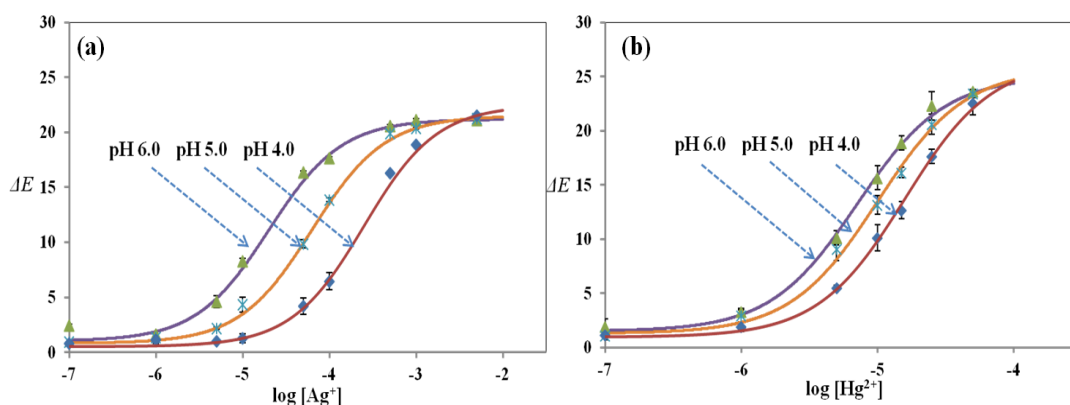


**Figure 4.6** Effect of pH on the sigmoidal response curves of sensor for $Ag^+$ (a) and $Hg^{2+}$ (b) in 0.01 M acetic-acetate buffer at pH 4.0 – 6.0 with the immersing time of 10 min.
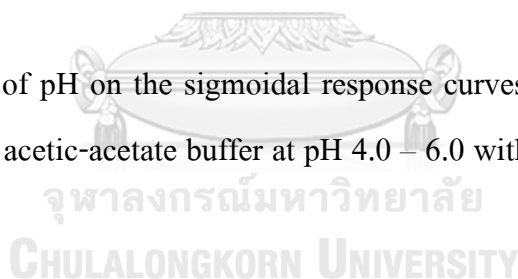
### 4.3.5 Response time

The $Ag^+$ and $Hg^{2+}$ determinations were performed by immersing the paper-based device into the working solutions, so the immersion time of the determination method was evaluated. To study this parameter, 0.1 μM – 1 mM of $Ag^+$ and 0.1 μM – 50 μM of $Hg^{2+}$ were prepared, and the paper strips were immersed into these solutions. The pictures of the paper strip were taken with various fixed times from 0 to 40 min. The color changes ($\Delta E$) of the detection zone were plotted as a function of time as shown in **Figure 4.7**. For $Ag^+$ detection (**Figure 4.7a**), to acquire a steady response, the

strips had to be immersed into the solution at least 10 min. In the case of $Hg^{2+}$ detection, the strips had to be immersed into the 50 µM solution around 10-20 min to obtain a steady response (**Figure 4.7b**). However, $\varDelta E$ continuously increased even the time up to 40 min for the strip immersed in highly diluted $Hg^{2+}$ concentration from 1 to 25 µM. The long response times in highly diluted solutions were due to the slow mass transport of ions from the bulk of solution to reach a required absolute amount of them in sensing phase [22, 25]. To perform the detection method in a shortest time, the fixed-time method was chosen for further experiments. For this reason, 10 min and 15 min of immersion time were fixed for $Ag^+$ and $Hg^{2+}$, respectively.
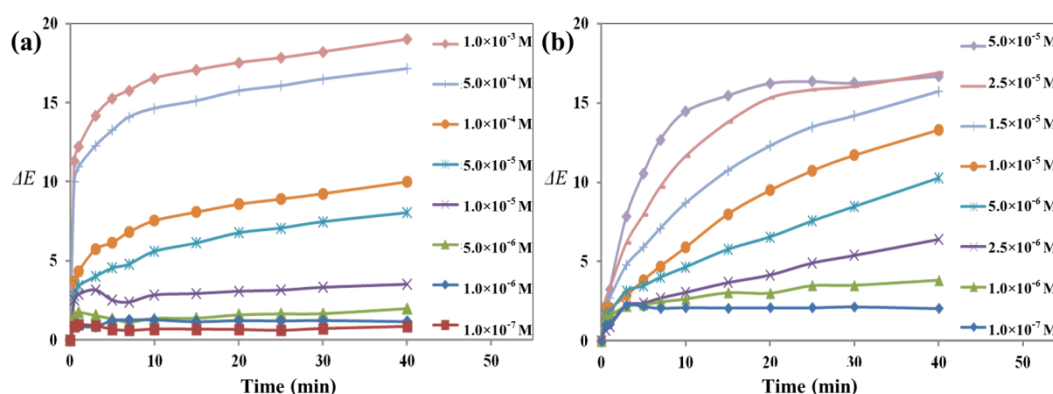


**Figure 4.7** Response times of the paper-based optode device in the presence of various concentrations of $Ag^+$ (a) and $Hg^{2+}$ (b) in 0.01 M acetic-acetate buffer at pH 5.0 with 5 mM EDTA and 5 mM NaCl as a masking agent for $Ag^+$ and $Hg^{2+}$ detections, respectively.

### 4.3.6 Selectivity of paper-based optode device

The selectivity of the paper-based optode device was studied using separate solution method (SSM) [72]. Various concentrations of metal ions including $Na^+$, $K^+$, $Ag^+$, $Mg^{2+}$, $Ca^{2+}$, $Co^{2+}$, $Ni^{2+}$, $Cu^{2+}$, $Zn^{2+}$, $Cd^{2+}$, $Hg^{2+}$, $Pb^{2+}$, $Cr^{3+}$, and $Fe^{3+}$ were separately prepared. The detection methods of each metal ions using proposed paper-based device

were performed according to the procedure in **Section 3.3.2** without adding masking agents. The response curves of the paper-based device for different metal ions are demonstrated in **Figure 4.8.** The paper strips were also immersed in 1 M $HNO_3$ and 1 M NaOH to acquire fully protonated form and fully deprotonated form, respectively. To assess the selectivity of the paper-based optode sensor, the logarithm of selectivity coefficients were calculated by measuring the horizontal interval between half deprotonation points of $Hg^{2+}$ and each metal ions response curves [65]. According to results in **Figure 4.8** and the logarithm of the selectivity coefficients in **Table 4.1**, the paper-based optode device showed a highly selective with $Ag^+$ and $Hg^{2+}$ over the other metal ions. Since the same mercaptophilic property and the similar ionic radius were found in $Ag^+$ and $Hg^{2+}$ [73], the optode showed highly selective with $Ag^+$ and $Hg^{2+}$ in the buffer solution pH 5.0 with the logarithm of the selectivity coefficients were $-0.7$ over $Ag^+$, $-4.2$ over $Fe^{3+}$, and less than $-5.0$ over others cations.
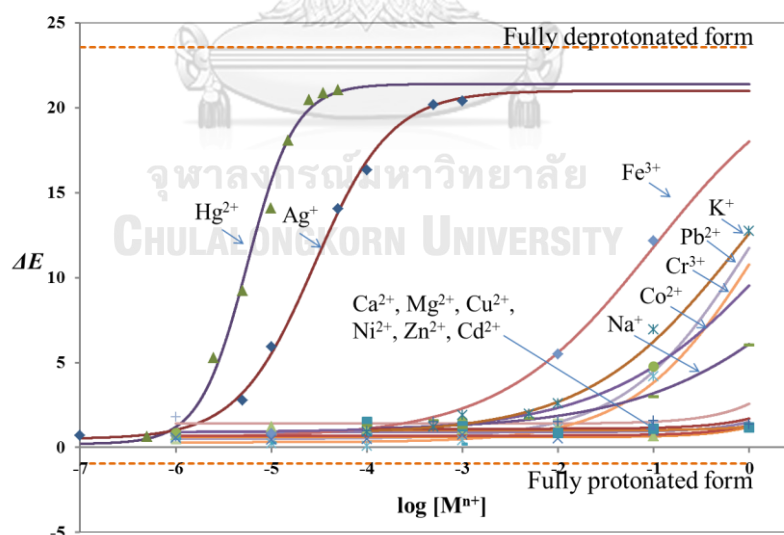


**Figure 4.8** Response curves of the paper-based optode device toward different metal ions in 0.01 M acetic-acetate buffer at pH 5.0 with the immersion time of 10 min.

**Table 4.1** Logarithm of the selectivity coefficients at pH 5.0 and 6.0 of the paper strip based $Hg^{2+}$ selective optode.

| log of selectivity coefficient | | |
|---|---|---|
| **Metal ions** | **pH 6.0** | **pH 5.0** |
| $Hg^{2+}$ | 0.0 | 0.0 |
| $Ag^+$ | $-0.5$ | $-0.7$ |
| $Cu^{2+}$ | $-2.2$ | $<-5.0$ |
| $Pb^{2+}$ | $-3.8$ | $<-5.0$ |
| $Cr^{3+}$ | $-3.9$ | $<-5.0$ |
| $Fe^{3+}$ | $-4.3$ | $-4.2$ |
| $K^+$ | $-4.4$ | $<-5.0$ |
| $Co^{2+}$ | $-4.6$ | $<-5.0$ |
| $Na^+$ | $<-5.0$ | $<-5.0$ |
| $Mg^{2+}$ | $<-5.0$ | $<-5.0$ |
| $Ca^{2+}$ | $<-5.0$ | $<-5.0$ |
| $Ni^{2+}$ | $<-5.0$ | $<-5.0$ |
| $Zn^{2+}$ | $<-5.0$ | $<-5.0$ |
| $Cd^{2+}$ | $<-5.0$ | $<-5.0$ |

### 4.3.7 Determination of $Ag^+$ and $Hg^{2+}$ in mixing solution

From selectivity study according to **Section 4.3.6**, the proposed paper-based optode device showed a highly selective with both $Ag^+$ and $Hg^{2+}$ by changing the color from blue to yellow as seen in the **Figure 4.9a**. To achieve the dual determination in mixing solution, some masking agents were required. For $Ag^+$ detection, EDTA was used to eliminate $Hg^{2+}$ by forming $Hg^{2+}$-EDTA complex [74]. On the other hand, for $Hg^{2+}$ detection, $Cl^-$ was used to eliminate $Ag^+$ by precipitation of AgCl(s). To examine this assumption, separated $Ag^+$ and $Hg^{2+}$ solutions were prepared in the presence of 5 mM of these masking agents. The response curves of $Ag^+$ and $Hg^{2+}$ in the presence of 5 mM EDTA and 5 mM NaCl are shown in **Figure 4.10a** and **Figure 4.10b,** respectively. The results showed that only the sigmoidal response curve of $Ag^+$ was found in the solution with 5 mM EDTA. On the other hand, only the sigmoidal response curve of $Hg^{2+}$ was found in the solution with 5 mM NaCl. For the $Hg^{2+}$ detection by elimination of $Ag^+$ with precipitation method, the precipitate of AgCl(s) may be occurred. However, the strip can be directly immersed into a turbid solution for $Hg^{2+}$ determination without further filtration. The use of EDTA and NaCl as a masking agents showed that the interference from $Hg^{2+}$ and $Ag^+$ could be eliminated up to the concentration of 50 μM (10 ppm) and 4 mM (431 ppm), respectively. The colors of the paper strip after immersing in various metal ions solutions in the presence of NaCl and EDTA as masking agents are shown in **Figure 4.9a** and **Figure 4.9b**, respectively.
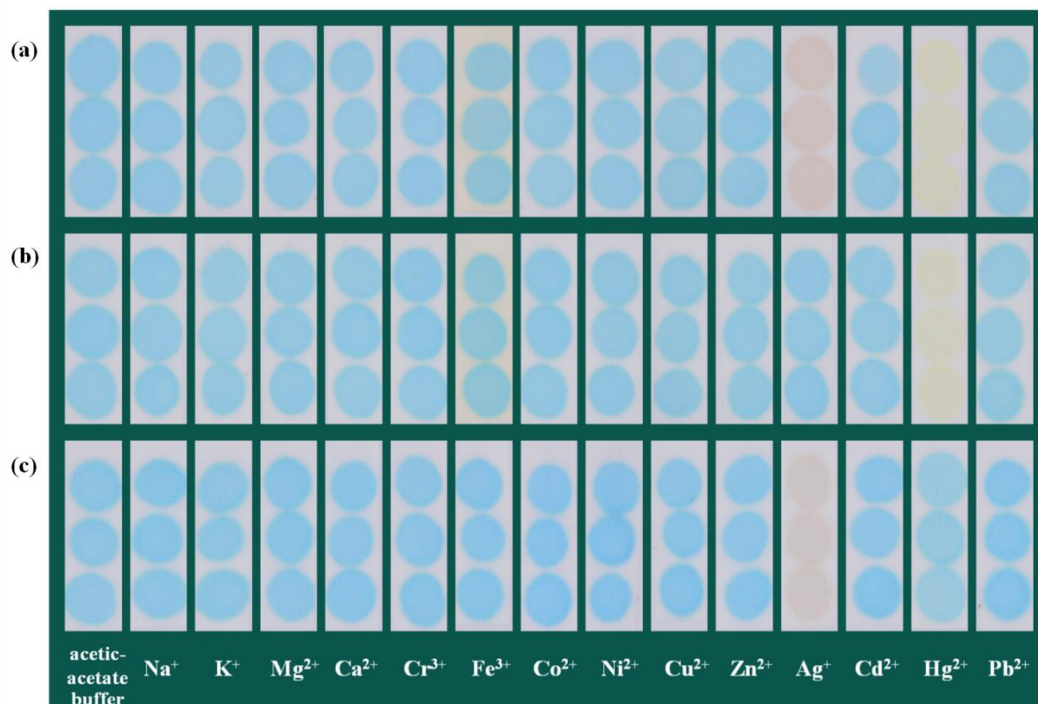
**Figure 4.9** Pictures of the paper-based optode device after immersing in the different solutions of 1 mM metal ions without masking agents (a), with 5 mM NaCl (b), and with 10 mM EDTA (c) as masking agents in 0.01 M acetic-acetate buffer at pH 5.0 with the immersing times of 10 min for (a), (c) and 15 min for (b).
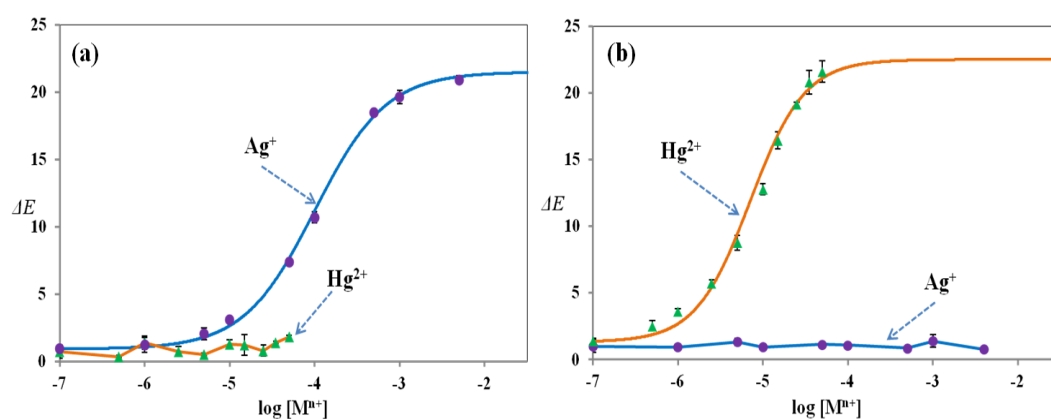


**Figure 4.10** Response curves of $Ag^+$ and $Hg^{2+}$ in the presence of 5 mM EDTA (a) and 5 mM NaCl (b) in 0.01 M acetic-acetate buffer at pH 5.0 with the immersion time of 10 and 15 min for $Ag^+$ and $Hg^{2+}$, respectively.

The dual detection of $Ag^+$ and $Hg^{2+}$ in mixing solutions using the proposed paper-based optode device was performed. In this experiment, two concentrations of $Ag^+$ including 20 and 100 µM were prepared by mixing with 2.5 or 8.0 µM of $Hg^{2+}$. The solutions were then divided into two detection procedures including $Ag^+$ and $Hg^{2+}$ detections. As mentioned above, one of mixing solution in the presence of 5 mM EDTA was prepared to detect only $Ag^+$. On the other hand, another mixing solution in the presence of 5 mM NaCl was prepared to detect only $Hg^{2+}$. After that, these solutions were determined $Ag^+$ or $Hg^{2+}$ concentrations using the proposed paper-based optode devices. The results in **Table 4.2** showed that the determination of $Ag^+$ and $Hg^{2+}$ in the mixing solutions using the proposed devices was achieved with %relative error within ±10%. It demonstrated that the proposed paper-based device was able to use for dual detection of $Ag^+$ and $Hg^{2+}$ in their mixing solution.

**Table 4.2** The dual determination of $Ag^+$ and $Hg^{2+}$ in the mixing solutions

| Solutions | Concentrations | | | | %Relative error | |
| | Prepared (µM) | | Observed (µM) | | | |
| | $Ag^+$ | $Hg^{2+}$ | $Ag^+$ | $Hg^{2+}$ | $Ag^+$ | $Hg^{2+}$ |
|---|---|---|---|---|---|---|
| 1 | 20 | 2.5 | 19.1 ± 0.4 | 2.3 ± 0.2 | − 4.5 | − 8.0 |
| 2 | 20 | 8.0 | 22.0 ± 0.9 | 8.1 ± 0.3 | + 10.0 | + 1.3 |
| 3 | 100 | 2.5 | 94.9 ± 7.6 | 2.5 ± 0.1 | − 5.1 | 0.0 |
| 4 | 100 | 8.0 | 90.3 ± 8.7 | 7.6 ± 0.5 | − 9.7 | − 5.0 |

### 4.3.8. Analytical Performance of the proposed paper-based analytical device

The standard solutions of $Ag^+$ and $Hg^+$ were prepared in the concentration ranges of 0.1 – 5000 µM for $Ag^+$ and 0.1 – 50 µM for $Hg^{2+}$, and the detection method was performed according to the procedure in **Section 3.3.2**. The pictures of the paper-

based device after immersing in various concentrations of $Ag^+$ and $Hg^{2+}$ are shown in **Figure 4.11a** and **Figure 4.11b**, respectively. The color changes ($\Delta E$) were plotted as a function of logarithm of $Ag^+$ or $Hg^+$ concentrations as shown in **Figure 4.12**. The experimental data was fitted to the sigmoidal relationship calculated from the Boltzman equation [59, 71] as shown in **Equation 3.2** where $A_1$, $A_2$, $x_0$, and dx in the Boltzman equation for $Ag^+$ and $Hg^+$ calibrations are the parameters given in **Table 4.3**. Moreover, the other analytical parameters obtained from the proposed paper-based device including correlation coefficients ($R^2$), limit of detections (LOD), dynamic ranges, and inter-device precision are also indicated in **Table 4.3.** The LODs were calculated with a criterion of the concentrations of $Ag^+$ or $Hg^+$ which gave the color changes signals ($\Delta E$) to a blank signal plus 3 times the standard deviation of blank [71, 75]. The LOD for $Ag^+$ detection using the proposed paper-based device was lower than the median effective concentration ($EC_{50}$) for silver nanoparticles to induce human cells death ($EC_{50} = 0.47$ mM, AgNPs diameter = 20 nm). The LOD for $Hg^{2+}$ detection was near to the LOD obtained from conventional planar film optode (0.2 $\mu$M) [25]. Additionally, the inter-device precisions of proposed device were also evaluated using 10 devices, and a good precision with %RSD less than 10% was obtained. All analytical parameters demonstrated that the proposed paper-based device had the capabilities for quantitative detection of $Ag^+$ and $Hg^{2+}$.
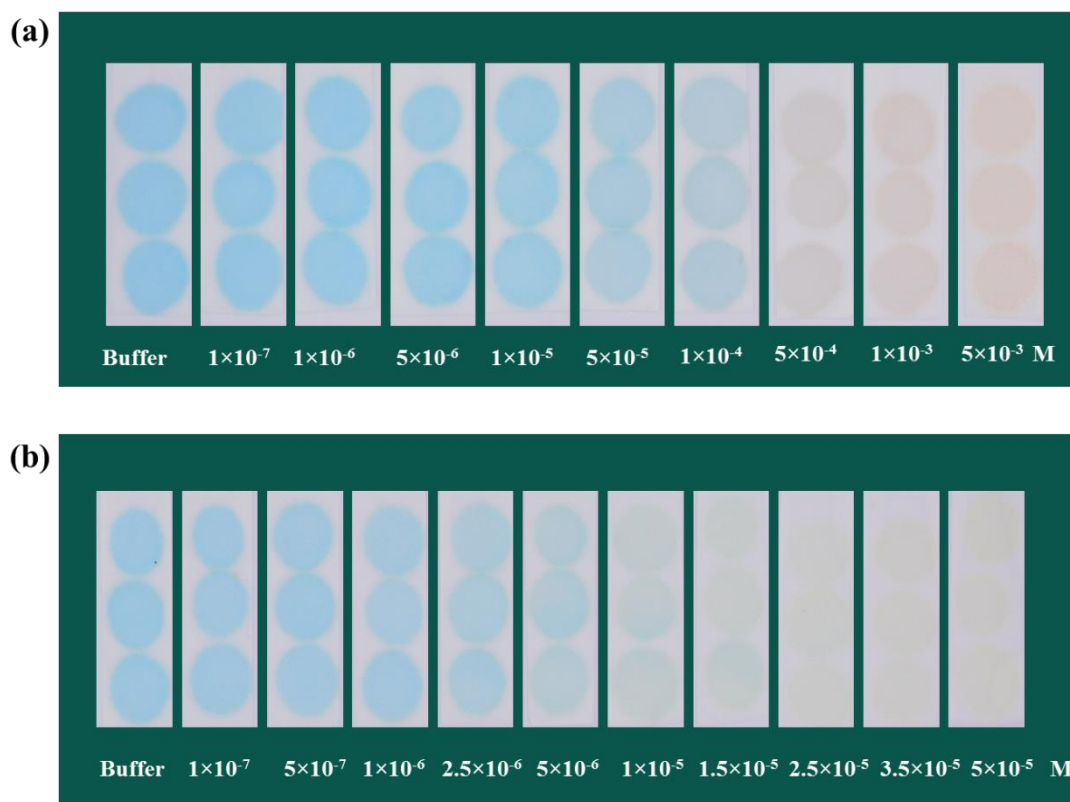
**Figure 4.11** Pictures of the paper-based optode devices after immersing in various concentrations of $Ag^+$ (a) and $Hg^{2+}$ (b) in 0.01 M acetic-acetate buffer at pH 5.0 with 5 mM EDTA for (a) and 5 mM NaCl for (b).
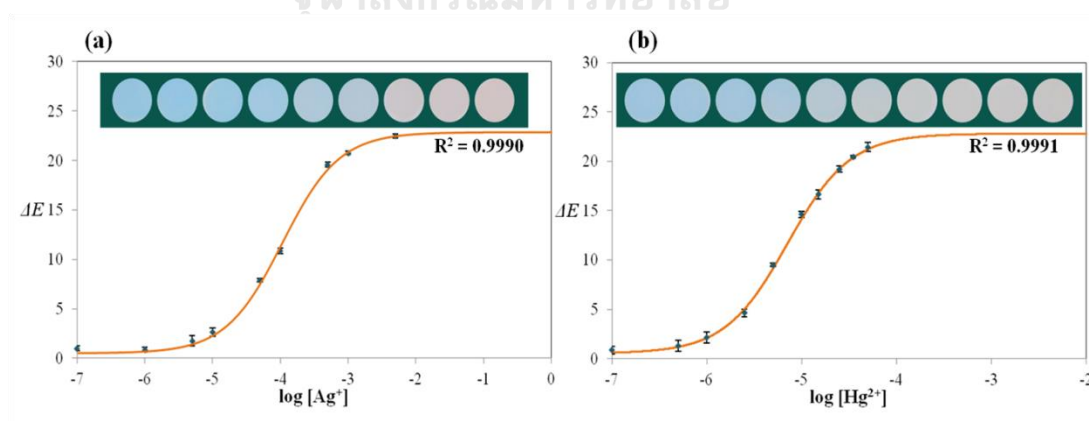


**Figure 4.12** Sigmoidal calibrations of $Ag^+$ (a) and $Hg^{2+}$ (b) in 0.01 M acetic-acetate buffer at pH 5.0 with 5 mM EDTA for (a) and 5 mM NaCl for (b)

**Table 4.3** Adjusting coefficients of Boltzmann equation and analytical parameters for the $Ag^+$ and $Hg^{2+}$ sensors.

| | Boltzmann and analytical parameters | |
|---|---|---|
| | $Ag^+$ detection | $Hg^{2+}$ detection |
| $A_1$ | $0.47 \pm 0.12$ | $0.53 \pm 0.26$ |
| $A_2$ | $22.83 \pm 0.55$ | $22.80 \pm 0.75$ |
| $x_0$ | $-3.97 \pm 0.03$ | $-5.15 \pm 0.03$ |
| dx | $0.42 \pm 0.02$ | $0.33 \pm 0.03$ |
| $R^2$ | 0.9990 | 0.9991 |
| LOD (n=10) | $1.92 \times 10^{-6}$ M (0.21 ppm) | $5.74 \times 10^{-7}$ M (0.12 ppm) |
| Dynamic range | $1.92 \times 10^{-6} - 5.00 \times 10^{-3}$ M | $5.74 \times 10^{-7} - 5.00 \times 10^{-5}$ M |
| Inter-device precision, %RSD (n=10) | 9.8% ($5.00 \times 10^{-5}$ M) <br> 5.7% ($3.00 \times 10^{-4}$ M) | 8.2% ($5.00 \times 10^{-6}$ M) <br> 8.5% ($1.50 \times 10^{-5}$ M) |

### 4.3.9 Real samples analysis

#### 4.3.9.1 Determination of $Ag^+$ and $Hg^{2+}$ in real water samples using paper-based optode device

The paper-based optode device was applied to determine the amount of $Ag^+$ and $Hg^{2+}$ in real water sample from various water sources including the water from commercial bottle, domestic tap, and pond water. To study the influence of various matrices in different water sources, the spiking method was performed. For $Ag^+$ detection, 20, 100, and 400 μM of $Ag^+$ were spiked into the sample solutions. From the results in **Table 4.4**, the percentage recoveries obtained from the paper-based device were less than 100% because the precipitation of AgCl(s) was occurred by the chloride ion in sample. Therefore, the determination of $Ag^+$ in real water sample cannot be performed when the chloride ion is found in the samples. For $Hg^{2+}$ detection, the

results are shown in **Table 4.5.** The percentage recoveries obtained from the paper-based devices were in the acceptable range of 87—120% with % RSD less than 10%. These results demonstrated that the matrices in various water sources did not interfere the $Hg^{2+}$ detection by this proposed method. In addition, the results were further compared with inductively coupled plasma optical emission spectrometry measurement (ICP-OES). According to results in **Table 4.5**, the results from the paper-based device provided a satisfactory agreement with ICP-OES ($t_{cri}$ = 4.30 > $t_{exp}$ = 0.59–3.76, n=3 at 95% confidence level).

**Table 4.4** Determination of $Ag^+$ in real water samples using the proposed paper-based device.

| Sample | Spiked (µM) | Paper strip | | |
|---|---|---|---|---|
| | | Found (µM) | %RSD | %Recovery |
| Bottled water | - | N.D. | | |
| | 20.0 | 4.5 ± 0.3 | 6.4 | 22 |
| | 100.0 | 34.5 ± 1.2 | 3.6 | 34 |
| | 400.0 | 388.2 ± 6.4 | 1.6 | 97 |
| Tap water | - | N.D. | | |
| | 20.0 | N.D. | - | 0 |
| | 100.0 | N.D. | - | 0 |
| | 400.0 | 39.1 ± 6.6 | 16.7 | 10 |
| Pond water | - | N.D. | | |
| | 20.0 | N.D. | - | 0 |
| | 100.0 | N.D. | - | 0 |
| | 400.0 | 6.4 ± 0.5 | 7.7 | 2 |

N.D. = not detectable

**Table 4.5** Determination of Hg$^{2+}$ in real water samples using the proposed paper-based device and ICP-OES.

| Sample | Spiked (µM) | Paper strip Found (µM) | % RSD | % Recovery | ICP-OES Found (µM) | % RSD | % Recovery |
|---|---|---|---|---|---|---|---|
| Bottled water | - | N.D. | | | N.D. | | |
| | 2.5 | 2.4 ± 0.1 | 5.6 | 96 | 2.5 ± 0.1 | 2.5 | 100 |
| | 8.0 | 7.6 ± 0.3 | 4.2 | 95 | 7.8 ± 0.1 | 0.7 | 98 |
| | 25.0 | 27.8 ± 2.0 | 7.1 | 111 | 25.8 ± 0.2 | 1.0 | 103 |
| Tap water | - | N.D. | | | N.D. | | |
| | 2.5 | 3.0 ± 0.2 | 7.9 | 120 | 2.7 ± 0.1 | 1.2 | 108 |
| | 8.0 | 8.4 ± 0.5 | 6.2 | 104 | 8.5 ± 0.2 | 2.0 | 106 |
| | 25.0 | 24.6 ± 0.6 | 2.6 | 99 | 25.5 ± 0.1 | 0.5 | 102 |
| Pond water | - | N.D. | | | N.D. | | |
| | 2.5 | 2.6 ± 0.1 | 5.2 | 104 | 2.8 ± 0.1 | 4.4 | 112 |
| | 8.0 | 7.0 ± 0.7 | 9.5 | 87 | 8.0 ± 0.1 | 1.5 | 100 |
| | 25.0 | 22.2 ± 0.7 | 3.2 | 89 | 23.8 ± 0.2 | 0.8 | 95 |

N.D. = not detectable

### 4.3.9.2 Determination of total silver in cleaning product sample using paper-based optode device

Normally, Ag$^+$ in AgNPs solutions could be found, and the speciation analysis of Ag$^+$ and Ag$^0$ was interesting. Hence, this proposed paper-based optode device was applied to determine the amount of Ag$^+$ in real sample containing AgNPs. The cleaning product sample labeled the amount of AgNPs as 100 ppm (0.93 mM) was diluted and spiked with 46.4, 92.7, and 139.1 µM of Ag$^+$. The amounts of Ag$^+$ in

sample solutions were determined with the paper-based device. In the detection method, AgNPs were adsorbed onto surface of cellulose paper, so the color of the paper strip changed to yellow. The color of AgNPs on the device provided the discrepancy of the colorimetric detection which affected to the repeatability of the device with high %RSD as shown in **Table 4.6**. Therefore, the determination of free $Ag^+$ in the sample containing AgNPs cannot be performed.

**Table 4.6** Determination of silver ion in a cleaning product sample containing AgNPs using the proposed sensor.

| Sample | Spiked (μM) | Paper strip | | |
| --- | --- | --- | --- | --- |
| | | Found (μM) | %RSD | %Recovery |
| | - | $56.8 \pm 7.2$ | 12.6 | |
| 30 folds | 46.4 | $101.4 \pm 7.5$ | 7.4 | 96 |
| Diluted | 92.7 | $138.9 \pm 29.6$ | 21.3 | 89 |
| | 139.1 | $244.7 \pm 28.5$ | 11.6 | 135 |

The determination of total silver concentration in real sample containing AgNPs was also performed by first oxidizing $Ag^0$ to $Ag^+$ via oxidation with $H_2O_2$. The sample was then diluted and spiked with 46.4, 92.7, and 139.1 μM of $Ag^+$. After that, the amounts of total $Ag^+$ in sample solutions were determined with the paper-based device. The results are shown in **Table 4.7.** The percentage recoveries obtained from the paper-based devices were in the acceptable range of 108－114% with % RSD less than 8%. These results demonstrated that the matrices in cleaning product sample did not interfere the total $Ag^+$ detection by this proposed method. In addition, the results were further compared with inductively coupled plasma optical emission spectrometry measurement (ICP-OES). According to results in **Table 4.7**, the results from the paper-

based device provided a satisfactory agreement with ICP-OES ($t_{cri}$ = 4.30 > $t_{exp}$ = 0.21–2.69, n=3 at 95% confidence level).

**Table 4.7** Determination of total silver concentration in a cleaning product sample containing AgNPs using the proposed paper-based device and ICP-OES.

| Sample | Spiked (µM) | Paper strip | | | ICP-OES | | |
|---|---|---|---|---|---|---|---|
| | | Found (µM) | % RSD | % Recovery | Found (µM) | % RSD | % Recovery |
| 30 folds diluted | - | 36.3 ± 2.8 | 7.6 | | 35.9 ± 0.8 | 2.3 | |
| | 46.4 | 89.2 ± 4.0 | 4.5 | 114 | 82.9 ± 0.4 | 0.5 | 101 |
| | 92.7 | 136.0 ± 10.8 | 8.0 | 108 | 130.4 ± 1.7 | 1.3 | 102 |
| | 139.1 | 186.4 ± 9.2 | 5.0 | 108 | 183.6 ± 2.4 | 1.3 | 106 |

## 4.4 Ion selective optode in a platform of thread-based analytical device

### 4.4.1 Response behavior of ISOs nanospheres

In this platform, the nanoparticle of sensing components (optode nanosphere) including **CU1** as an ion-selective ionophore, chromoionphore XIV as a proton-selective chromoionophore, KT*p*ClPB as an ion-exchanger, and DOS representing as a hydrophobic phase for the sensing process was prepared by solvent-displacement method [76]. The cocktail solution was first prepared by dissolving **CU1,** chromoionophore XIV, KT*p*ClPB, DOS, and pluronic P123 in THF. Then, the cocktail solution was slowly added into stirring aqueous phase, and blue clear solution was obtained. After evaporation of the organic solvent, the nanoparticles were formed. As mentioned in previous report [77], a neutral surfactant copolymer with hydrophobic chain and two hydrophilic ends can promote the formation of optode nanosphere by acting as a stabilizing agent. Pluronic P123 is one of neutral surfactants that has

hydrophobic poly(propylene glycol) chain and two ends of hydrophilic polyethylene glycol. The hydrophobic chains are able to insert and interact with the lipophilic sensing components in core while hydrophilic ends contact with water surrounding to help the particles suspension in water and prevent the nanoparticles aggregation [77]. The size of synthesized nanoparticles was analyzed by dynamic light scattering (DLS) and found to be around 110 nm in diameter (**Figure 4.13**). The optode nanosphere showed a relatively narrow size distribution with a polydispersity index (PDI) of 0.097. Since all of sensing reagents including **CU1**, chromoionophore XIV, and KT$p$ClPB were combined in the platform of nanoparticles suspension, the sensing process was supposed to be similar mechanism with conventional thin film optode. According to **Equation 2.1,** the ion-selective sensing behavior was based on the ion-exchange process of target ions ($Ag^+$ or $Hg^{2+}$) and hydrogen ion ($H^+$) between water surrounding and hydrophobic nanoparticles consisting of **CU1** (L), chromoionophore XIV (C), and KT$p$ClPB ($R^-$). **CU1** extracted $Ag^+$ or $Hg^{2+}$ from water to the optode nanosphere while $H^+$ from chromoionophore ($CH^+$) was released to water to maintain the electroneutrality. Hence, the color of optode nanosphere changed from blue ($CH^+$) to yellow (C).
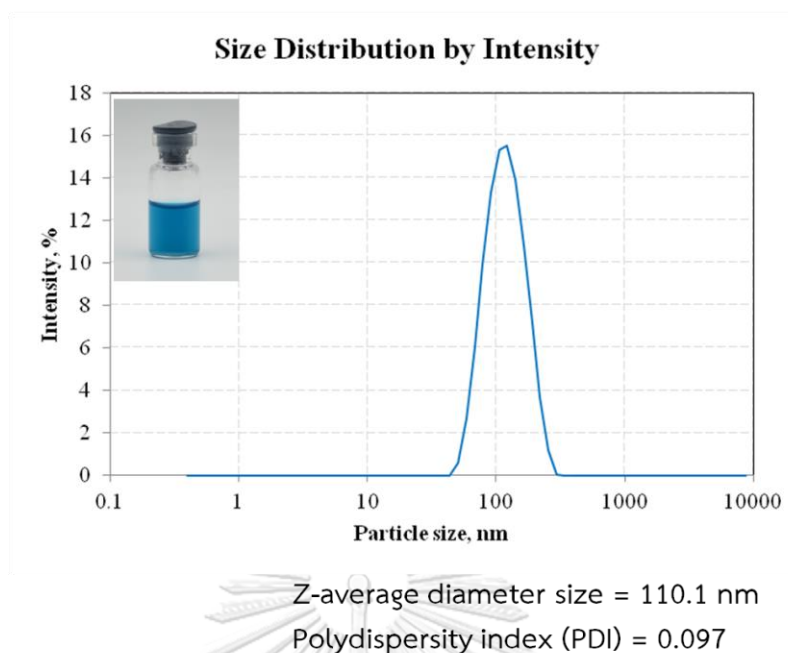
Figure 4.13 Dynamic light scattering analysis of the prepared optode nanospheres.

### 4.4.2 Property of ISOs nanosphere

To study the characteristic of the synthesized optode nanosphere, the optical properties of the optode nanosphere suspension were studied. Since the core of nanosphere was doped with the pH-dependent indicator (chromoionophore XIV), the pH responsive property should be observed. To investigate this, the absorption spectra of the optode nanosphere in the different pH buffer solutions from 3.0 to 10.0 were recorded. The pH responses of the optode are shown in **Figure 4.14**. From the results, the color of the optode nanosphere changed from blue to yellow when the pH increased from 3.0 to 10.0. This result indicated that chromoionophore XIV in the form of nanoparticles suspension can exchange the proton between particles surface and solution surrounding. In the acidic media, chromoionophore XIV was protonated with the maximum absorption wavelength ($\lambda_{max}$) at 634 nm. On the other hands, chromoionophore XIV became to the deprotonated form with the maximum absorption

wavelength at 432 nm in the basic media.



**Figure 4.14** Colors (a), absorption spectra in visible wavelength (b), and absorbance at 634 nm (c) of the optode nanosphere in different pH buffer solutions.

The sensing property of the optode nanosphere with $Ag^+$ and $Hg^{2+}$ was also investigated. The sensing process was assumed to be identical mechanism as the conventional planar film optode. To confirm this assumption, the absorption spectra of the optode nanosphere in acetic-acetate buffer solution at pH 5.0 (the optimum pH in proposed paper device) with various $Ag^+$ or $Hg^{2+}$ concentrations were measured as shown in **Figure 4.15** and **4.16,** respectively. The color of the optode changed from blue to yellow when the $Ag^+$ or $Hg^{2+}$ concentrations increased. The absorption spectra of the optode nanosphere showed that the chromoionophore XIV was a protonated form in the solution absent $Ag^+$ or $Hg^{2+}$. When the concentrations of $Ag^+$ or $Hg^{2+}$ increased, chromoionophore XIV became to the deprotonated form resulting in the color change.

**Figure 4.15** Colors (a), absorption spectra in visible wavelength (b), and absorbance at 634 nm (c) of the optode nanosphere in 0.01 M acetic-acetate buffer solution at pH 5.0 with various $Ag^+$ concentrations.
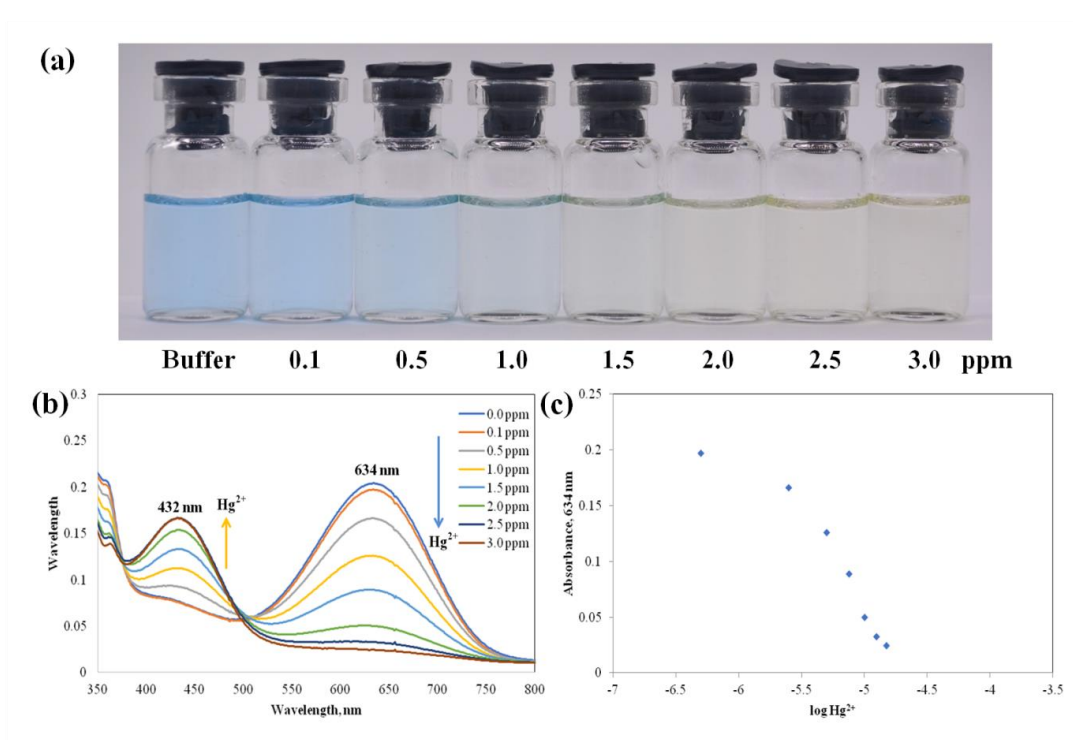
**Figure 4.16** Colors (a), absorption spectra in visible wavelength (b), and absorbance at 634 nm (c) of the optode nanosphere in 0.01 M acetic-acetate buffer solution at pH 5.0 with various $Hg^{2+}$ concentrations.

Moreover, the selectivity of the optode nanosphere response in the solution was also studied. The optode was prepared in the various metal ions including $Na^+$, $K^+$, $Ag^+$, $Mg^{2+}$, $Ca^{2+}$, $Co^{2+}$, $Ni^{2+}$, $Cu^{2+}$, $Zn^{2+}$, $Cd^{2+}$, $Hg^{2+}$, $Pb^{2+}$, and $Cr^{3+}$. The colors of the optode nanosphere in the different metal ions are shown in **Figure 4.17**. The results showed that the color of the optode nanosphere in the presence of $Ag^+$ and $Hg^{2+}$ changed from blue to yellow. Meanwhile, the absorption spectra showed the decrease in absorbance at 634 nm in the case of $Ag^+$ and $Hg^{2+}$. This indicated the high selectivity for $Ag^+$ and $Hg^{2+}$ over the other metal ions. From the characteristic of the synthesized optode nanosphere, it was possible to use this optode nanosphere platform as the sensing agent for determination of $Ag^+$ and $Hg^{2+}$.
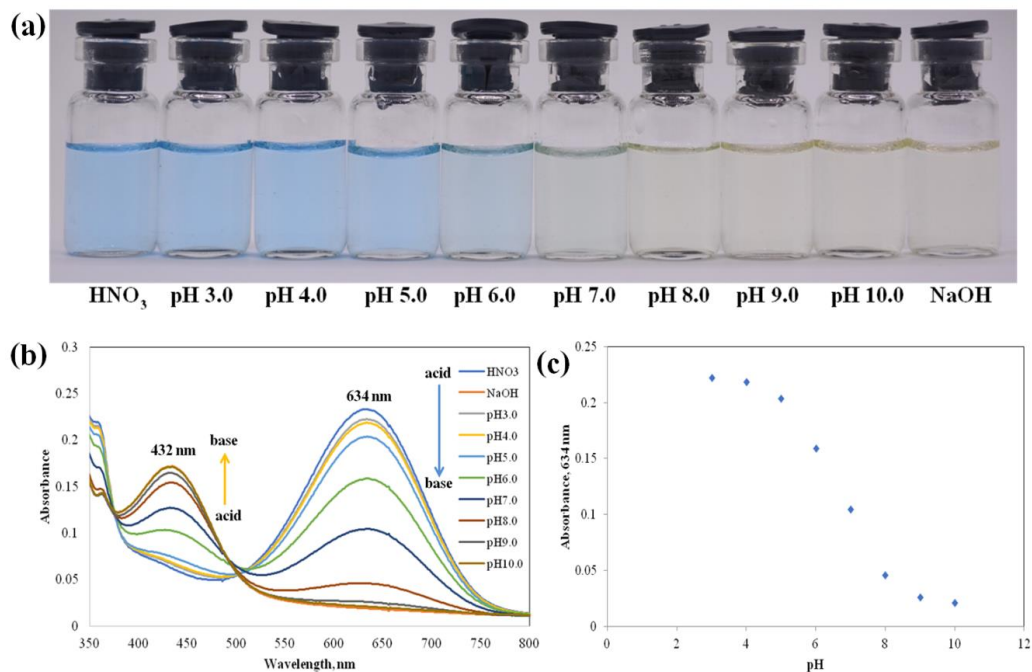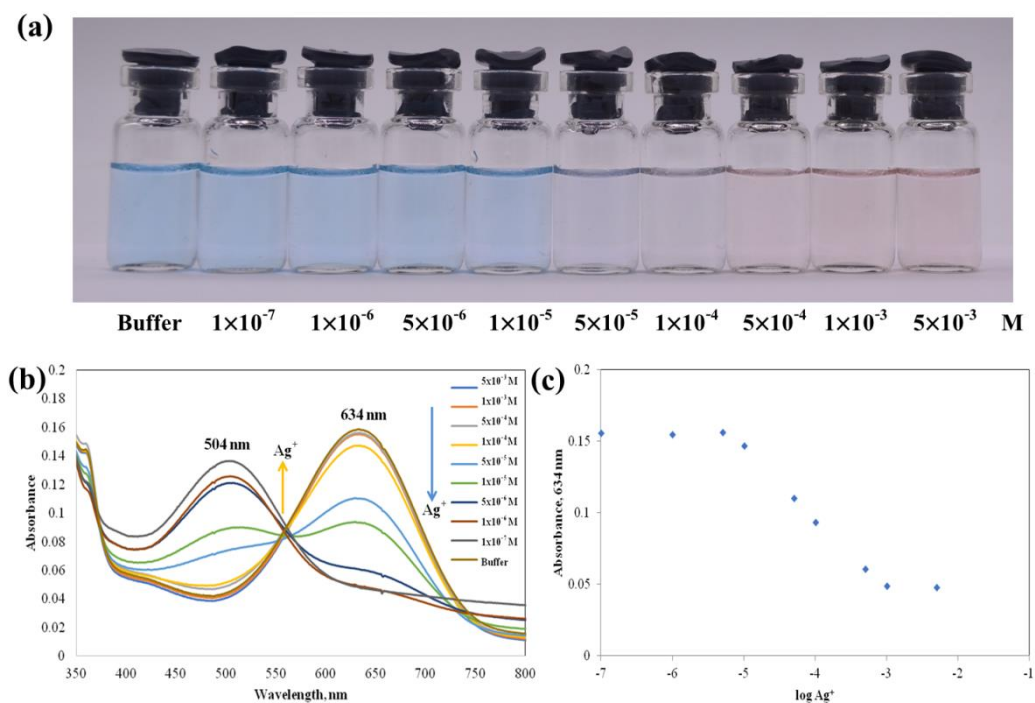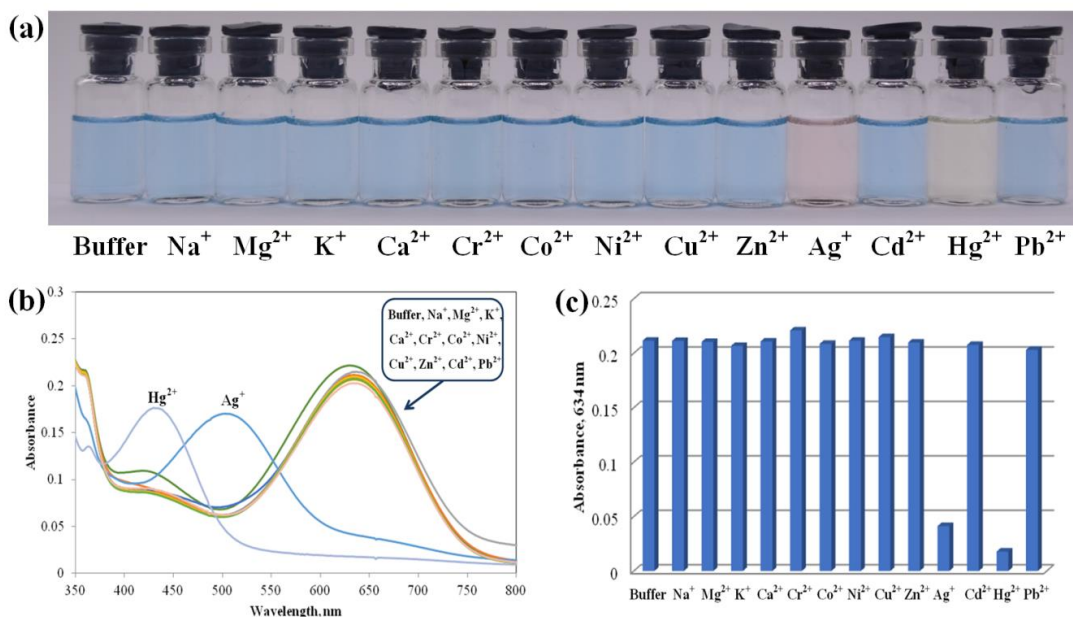
**Figure 4.17** Colors (a), absorption spectra in visible wavelength (b), and absorbance at 634 nm (c) of the optode nanosphere in 1 mM of different metal ions in 0.01 M acetic-acetate buffer solution at pH 5.0.

### 4.4.3 Detection of Ag$^+$ and Hg$^{2+}$ using optode nanosphere on thread-based analytical device

The determination of Ag$^+$ and Hg$^{2+}$ using ISO paper-based device by colorimetric detection still need a digital camera for data readout. To increase portability of the device by eliminating the need of external electronic equipments, the sensing agent was applied to thread for the distance-based detection. To study the response behavior of thread-based device for Ag$^+$ and Hg$^{2+}$ detections, the optode nonosphere suspension and one of target ion were applied to thread-based device. The experiment was performed by three repeats dropping of 3 µL of optode nanosphere suspensions onto a knot of thread. The optode nanosphere was then flowed through along the thread by the capillary force. The volatility of water caused the optode

nanosphere to deposit on polyester thread surface. After that, 3 μL of $Ag^+$ or $Hg^{2+}$ standard solutions was repeatedly dropped onto the same position onto a knot of thread. The reaction between $Ag^+$ or $Hg^{2+}$ in the aqueous sample and optode nanosphere on thread surface as described in **Section 4.4.1** produced the color change from blue to yellow. The picture of thread-based device after applying 15 × 3 μL of various concentrations of $Ag^+$ and $Hg^{2+}$ standard solutions are shown in **Figure 4.18a** and **Figure 4.18b**, respectively. For $Hg^{2+}$ detection, after applying 15 × 3 μL of $Hg^{2+}$ standard solutions, the color of thread changed from blue to yellow, and the difference of length of the color change on thread was observed. The response behavior of the distance-based detection using the optode nanosphere was found with the detection in "exhaustive sensing mode" where the target ion in solutions was completely extracted to the nanoparticles [66, 76, 78-80]. In the case of $Ag^+$ detection, after applying 15 × 3 μL of $Ag^+$ standard solutions, the color of thread also changed from blue to yellow when the concentration of $Ag^+$ increased. Unfortunately, the length of color change was not observed as shown in the colorimetric plot profile (**Figure A1**). The different behaviors between $Ag^+$ detection and $Hg^{2+}$ detection might be due to the extraction of $Ag^+$ was occurred more slowly than that of $Hg^{2+}$, and the extraction of $Ag^+$ was slowly occurred than the sample solution flowed along the thread. For this reason, the response of thread-based device for $Ag^+$ detection was a colorimetric-based same with a proposed paper-based device. Therefore, to demonstrate the distance-based detection of the proposed thread-based device, further experiments were performed only for the $Hg^{2+}$ detection.
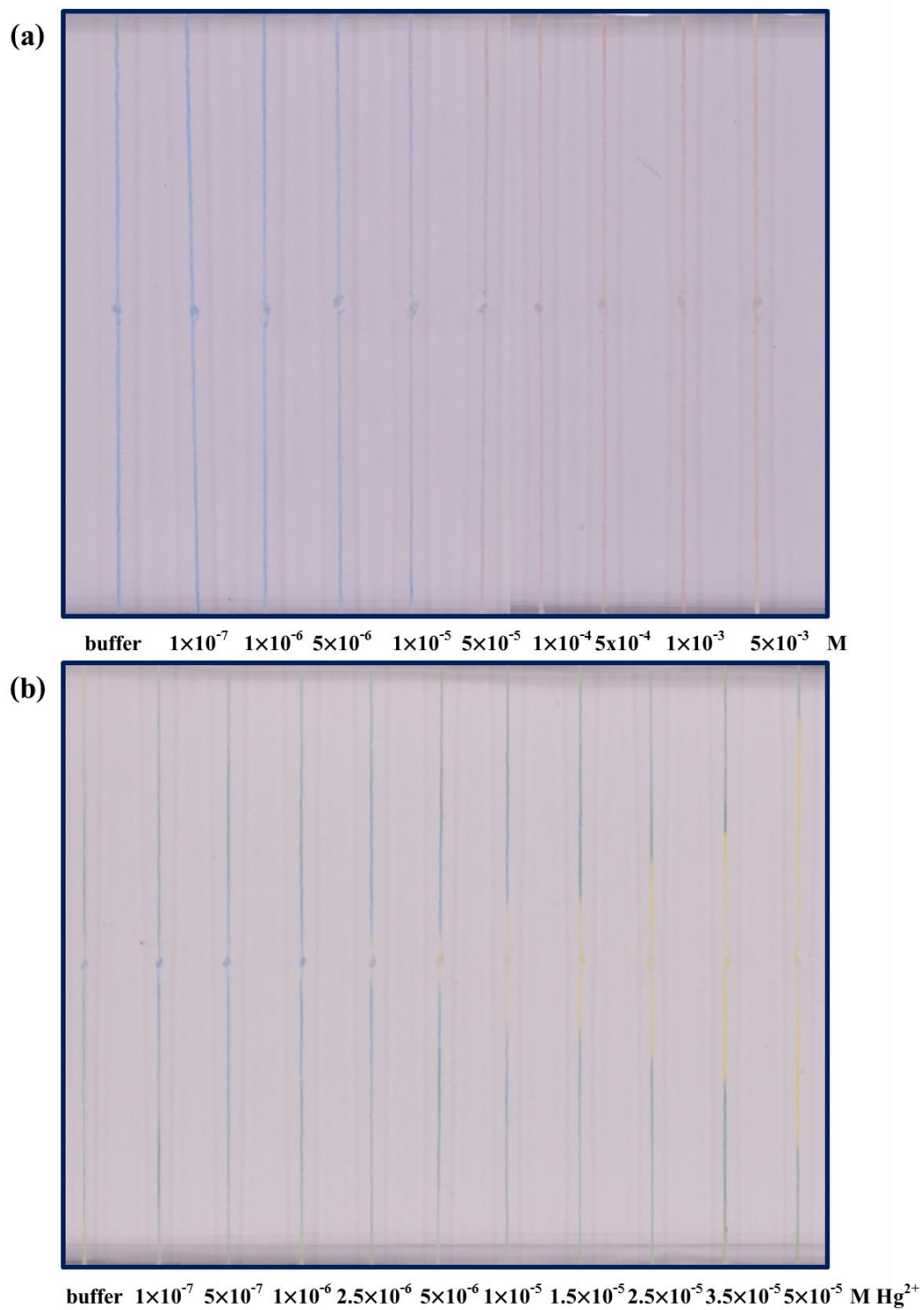
**Figure 4.18** Pictures of the thread-based device for $Ag^+$ (a) and $Hg^{2+}$ (b) detections.

**4.4.4 Distance-based detection of Hg$^{2+}$ using optode nansphere on thread**

**4.4.4.1 Modification of optode nanosphere on thread and in situ preconcentration of Hg$^{2+}$**

The amount of optode nanosphere deposited on thread surface can be increased by multiple additions of optode nanosphere suspension to the thread. The criteria to select number of repeats of optode nanosphere suspensions is the number of repeats provided long length of color change on thread and also given high color difference (Δ red value of blue and yellow) for easy readout. To investigate this, 3 μL of the optode nanosphere suspension with the number of repeats of 1-4 were applied to the knot of threads, and 3 μL of 10 ppm Hg$^{2+}$ standard solutions were then applied to the same position of threads with the number of repeats of 1, 3, 5, 7, 10, 13, and 15. The color change distances in function of number of repeats were measured for comparison the length of the developed color. The different red intensity values (Δ red value of blue and yellow) were measured for comparison the color difference. The large amount of sensing components located on thread surface required a large amount of Hg$^{2+}$ to develop an equal distance. Thus, the amount of optode nanosphere was inversely varied with the length of color change. According to this reason, a higher repeat number of the optode nanosphere suspension provided a shorter length of the color change as shown in **Figure 4.19a.** However, a higher repeat number of the optode nanosphere suspension provided a higher color difference as shown in **Figure 4.19b**. To obtain a high color difference and maintain a reasonable distance, 3 × 3 μL of the optode nanosphere suspension was selected for further experiment. In the same way, the number of repeats of sample solution was also studied as shown in **Figure 4.20**. The color change distance increased with the increased of the repeat number of 3 μL of Hg$^{2+}$ standard solutions. This result showed the possibility of in situ preconcentration of the target ions to obtain a lower limit of detection (LOD) by

multiple dropping sample solutions onto the devices. In this work, $15 \times 3$ µL of $Hg^{2+}$ standard solutions dropping onto the thread provided the working ranges of 1.0 to 10.0 ppm $Hg^{2+}$ and a limit of detection found to be 0.3 ppm which was closed to LOD calculated with the proposed paper-based ISO (0.12 ppm) and the conventional planar film optode (0.04 ppm) [25] for $Hg^{2+}$ detections.
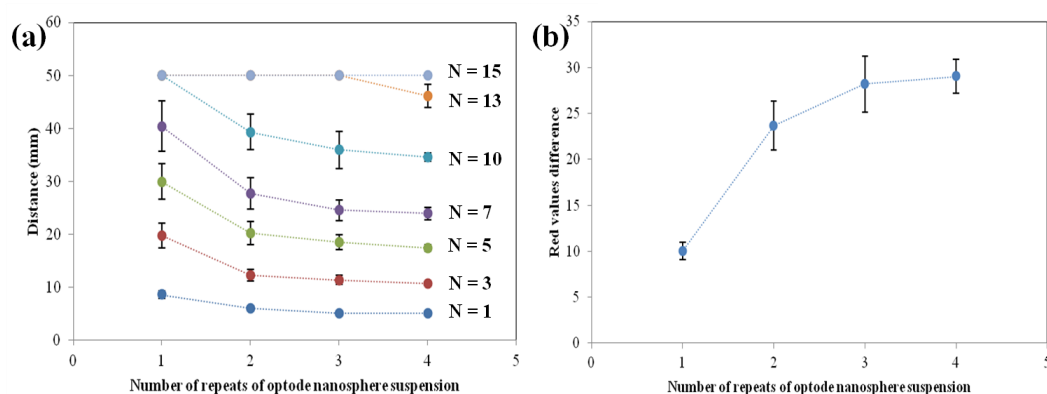


**Figure 4.19** Distances of the color change (a) and the color difference (b) of thread-based device. (N = repeat number of standard solutions).
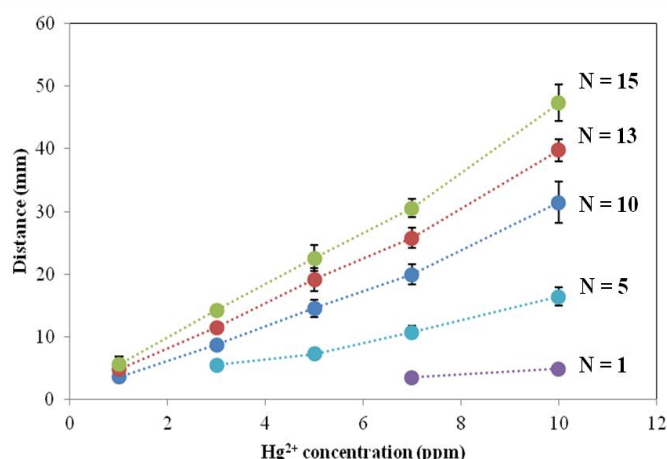
**Figure 4.20** Distances of the color change after repeatedly dropping 3 µL of $Hg^{2+}$ standard solutions (N = repeat number of standard solutions).

### 4.4.4.2 Effect of pH

To study the effect of pH toward the distance-based determination, the $Hg^{2+}$ standard solutions of 1.0 and 5.0 ppm were prepared in the buffer solutions at pH values of 3.0, 4.0, 5.0, 6.0 and 7.0. As presented in **Figure 4.21a**, the results showed no different distances when the pH of solution was in the range of 3.0 to 6.0 (P-value > 0.05 at 95% confidence level). The pH independence of sensor found in the thread-based device might be due to the "exhaustive sensing mode" where $Hg^{2+}$ in the solutions was completely extracted to the optode nanosphere. When the amount of optode nanosphere was excess to exhaustively extract all $Hg^{2+}$ in sample drops, the distance of the color change depended on only the total amount of $Hg^{2+}$ in the detection zone. This behavior was often found in the optode nanosphere sensor [66, 78-80]. However, the color of the optode nanosphere shown in term of red values difference in **Figure 4.21b** still depended on pH of solutions. The results showed that the red values difference tended to decrease when pH values increased. At pH 7.0, this pH was higher than pKa of chromoionophore XIV, so the optode nanosphere became yellow because of the deprotonated form of chromoionophore XIV. For this reason, the red value

difference was zero, and the distance of the color change could not be obtained. Therefore, the pH of solution used in the proposed device could be varied from 3.0 to 6.0. Nevertheless, to achieve the good selectivity as mentioned in the proposed paper-based device, pH 5.0 was used as experimental media for further experiments.
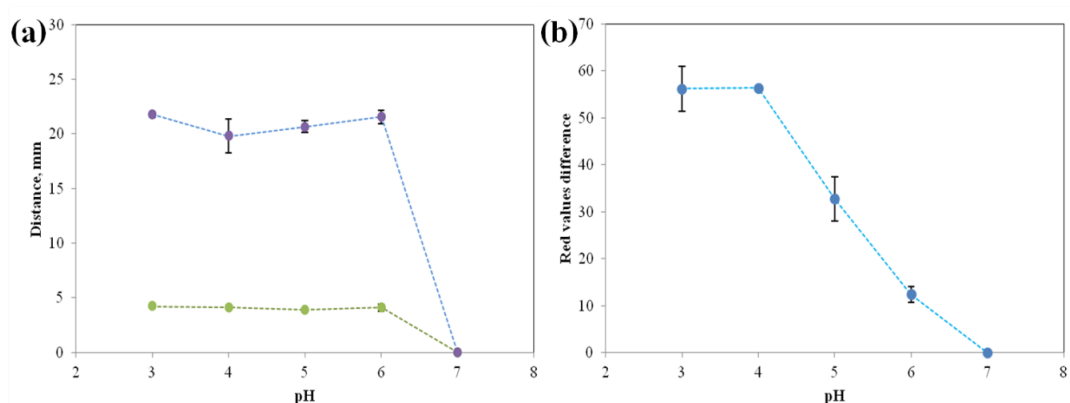


**Figure 4.21** Effect of pH on the color change distances (a) and the color difference of red values ($\Delta R$) after repeatedly dropping of $Hg^{2+}$ solutions 15 times.

### 4.4.4.3 Effect of interfering ions

To evaluate the selectivity of the thread-based optode device, the effect of others metal cations including $Na^+$, $K^+$, $Ag^+$, $Mg^{2+}$, $Ca^{2+}$, $Co^{2+}$, $Ni^{2+}$, $Cu^{2+}$, $Zn^{2+}$, $Cd^{2+}$, $Pb^{2+}$, and $Cr^{3+}$ was studied. Under the optimum conditions, each interfering ion was mixed with 5.0 ppm $Hg^{2+}$ with the concentrations of 1000 or 40 folds mole excess of interfering ions to $Hg^{2+}$ (1000 folds for $Na^+$, $Mg^{2+}$, $K^+$, $Ca^{2+}$ and 40 folds for $Cr^{3+}$, $Co^{2+}$, $Ni^{2+}$, $Cu^{2+}$, $Zn^{2+}$, $Ag^+$, $Cd^{2+}$, $Pb^{2+}$). All solutions were prepared in 0.01 M acetic-acetate buffer solution at pH 5.0. The mixing solutions were then dropped to the thread-based device according to the method in **Section 3.4.4**. The results in **Figure 4.22** showed no difference between the color change distances of pure $Hg^{2+}$ and theirs mixed solutions with relative error less than 5% ($t_{cri} = 2.78 > t_{exp} = 0.16 - 1.02$, n=3 at 95% confidence level). These results indicated that the thread-based device has capability to tolerate various interfering cations in aqueous sample solution.



\* in the presence of 5 mM NaCl
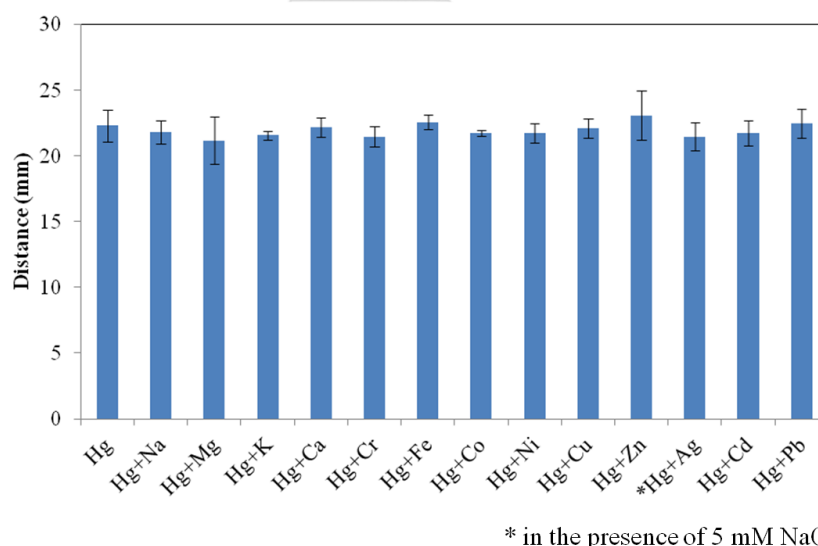
**Figure 4.22** Color change distances of the thread-based device after repeatedly droping $Hg^{2+}$ solutions mixing with various metal cations onto knot 15 times.

**4.4.4.4 Analytical performance for distance-based detection of Hg$^{2+}$**

As described above, the optimum conditions for Hg$^{2+}$ determination included 3×3 µL of optode nanosphere suspension, 15×3 µL of Hg$^{2+}$ standard solution, and pH 5.0. According to these optimum conditions, various concentrations of Hg$^{2+}$ standard solutions from 1.0 to 10.0 ppm were determined with the proposed thread-based device with three replicates (n=3). The picture of thread-based device upon addition of various concentration of Hg$^{2+}$ is shown in **Figure 4.23**. From the measurement of the color change distance as shown in **Figure 4.24**, the color change distance showed a good linear correlation with Hg$^{2+}$ concentrations (R$^2$ = 0.9943). To evaluate the inter-device precision, 3.0 and 7.0 ppm Hg$^{2+}$ were repeatedly dropped onto 10 thread devices (15×3 µL of standard solutions for each thread). The device showed good inter-devices precision with %RSD of 4.8 and 3.1 for 3.0 and 7.0 ppm Hg$^{2+}$, respectively. In addition, in order to confirm that the distances of color change were unprejudiced readout from users, imageJ software-assisted readout was used. In this readout technique, a picture of the device after developing the color change was taken a picture with camera. To measure the color change distance, acquired JPEG images were evaluated. The red values along the threads were analyzed with ImageJ software to obtain the colorimetric plot profile along the threads as shown in **Figure 4.25.** The distances of the color change were then obtained by measuring the length between the middle of two most slopes. The measurements of the color change distance by means of software-assisted readout were compared with the naked eyes readout (using a ruler). The Pearson's correlation analysis [68] according to the **Figure 4.26** showed no significant difference between ImageJ software-assisted readout and naked eyes readout by three volunteer users (r > 0.99). These results can be concluded that the proposed thread-based device can be used as an actual instrument-free device for Hg$^{2+}$ determination.
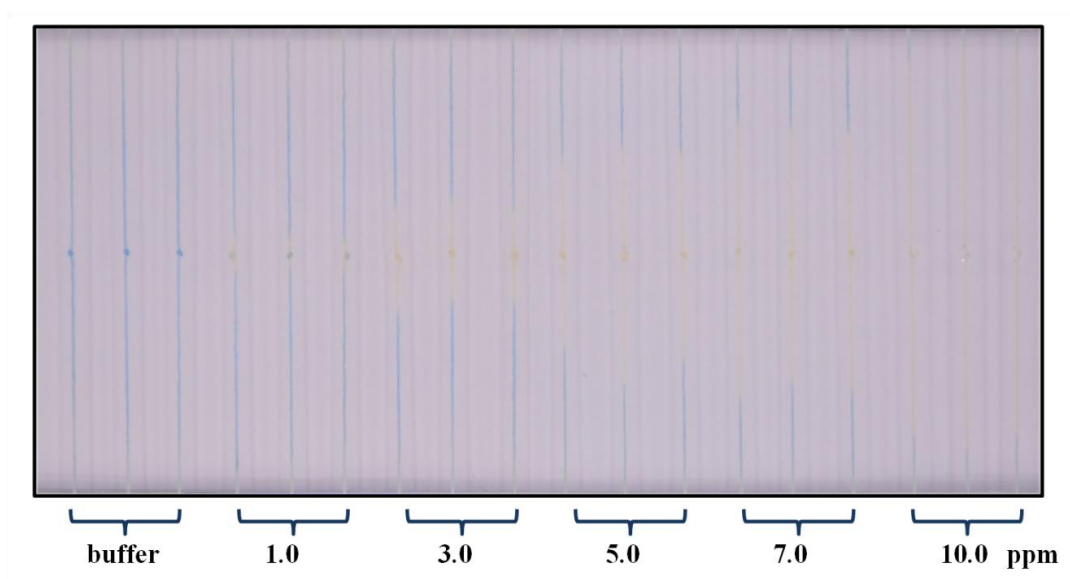
**Figure 4.23** Picture of the thread-based device for Hg$^{2+}$ detection.
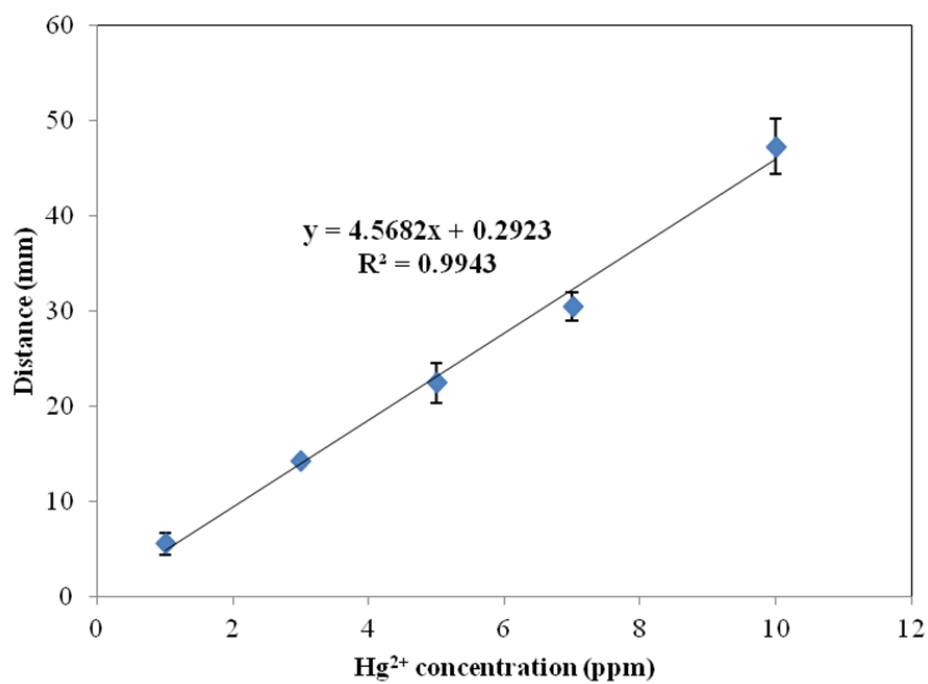


**Figure 4.24** Distance-based calibration of Hg$^{2+}$ using the proposed thread-based device.
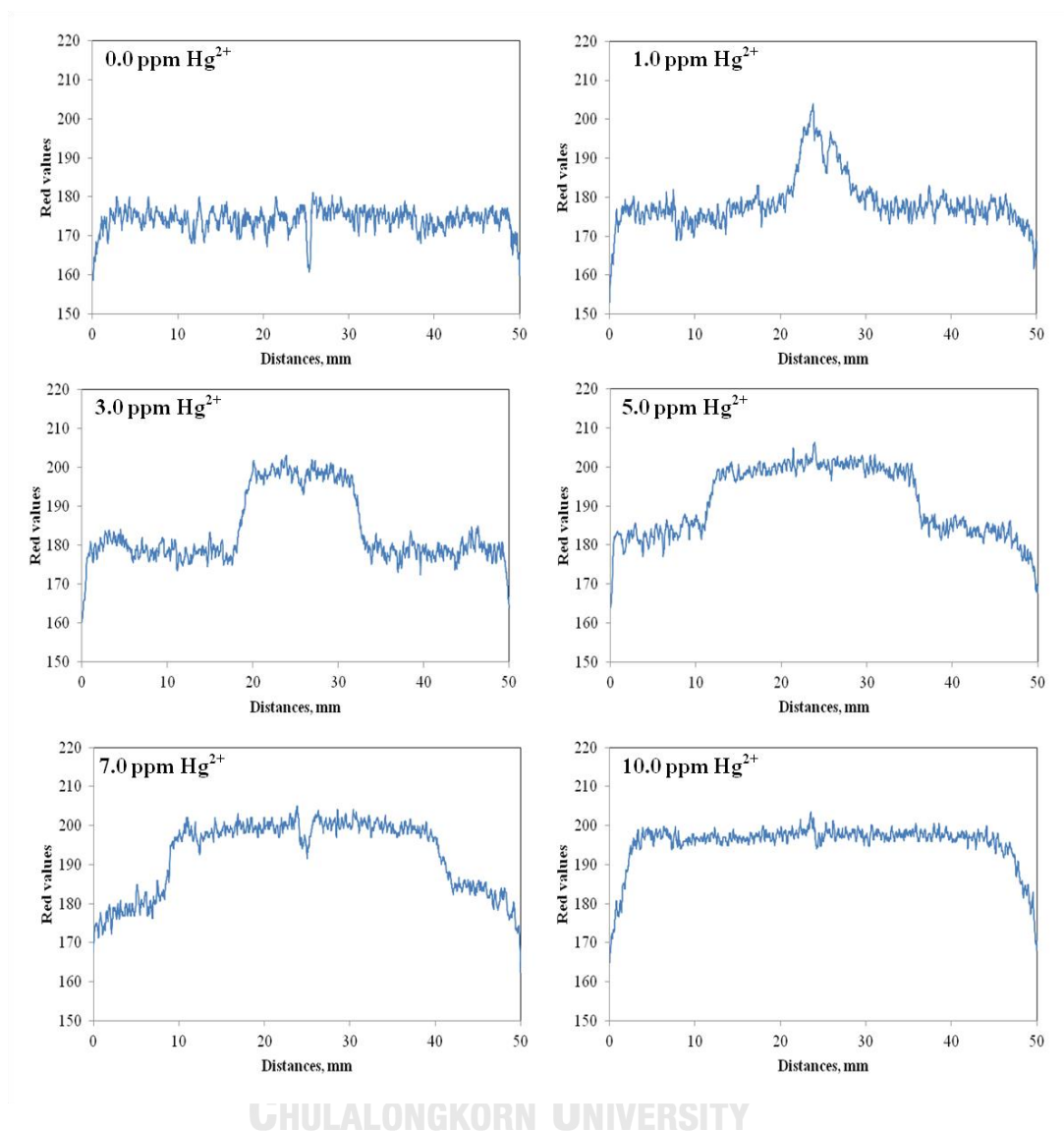
**Figure 4.25** Colorimetric plot profile of red values along the threads analyzed with ImageJ software.
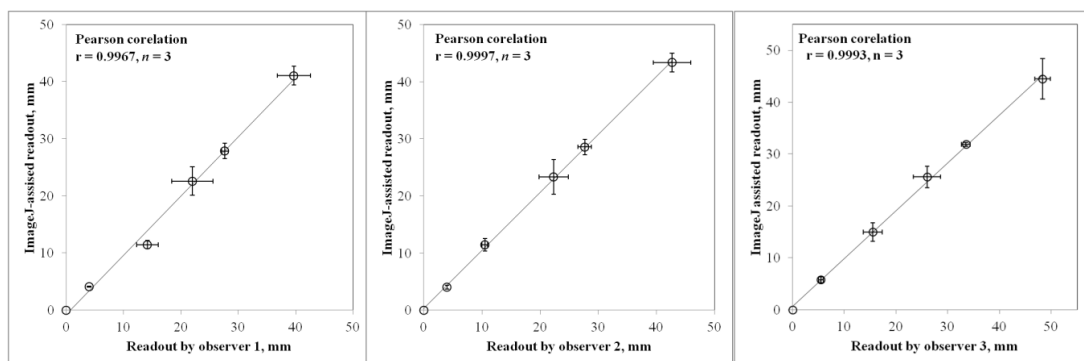
**Figure 4.26** Comparison of $Hg^{2+}$ distance-based determination using ImageJ-assisted readout and naked eye readout using a ruler by three users.

### 4.4.4.5 Real samples analysis

The thread-based optode device was applied to determine the amount of $Hg^{2+}$ in real water samples from various water sources including the water from commercial bottle, domestic tap, pond, and agricultural wastewater. To study the influence of various matrices in different water sources, the samples were spiked with 3.0, 5.0, and 7.0 ppm $Hg^{2+}$. From the results in **Table 4.8**, the percentages recoveries obtained from the thread-based devices were in the acceptable range of 97–108% with % RSD less than 10. These finding demonstrated that the matrices in various water sources did not interfere the $Hg^{2+}$ detection by the proposed methods. In addition, the results were further compared with inductively coupled plasma optical emission spectrometry measurement (ICP-OES). According to results in **Table 4.8**, the results from thread-based device provided a satisfactory agreement with ICP-OES ($t_{cri}$ = 4.30 > $t_{exp}$ = 0.22 – 3.01, n=3 at 95% confidence level).

**Table 4.8** Determination of $Hg^{2+}$ in real water samples using thread-based device and ICP-OES.

| Sample | Added (ppm) | Thread-based device | | | ICP-OES | | |
|---|---|---|---|---|---|---|---|
| | | Found (ppm) | % RSD | % Recovery | Found (ppm) | % RSD | % Recovery |
| Bottled | 0.0 | N.D. | | | N.D. | | |
| water | 3.0 | 2.9 ± 0.2 | 6.1 | 97 | 3.0 ± 0.1 | 0.4 | 100 |
| | 5.0 | 5.0 ± 0.4 | 7.0 | 100 | 5.0 ± 0.1 | 0.4 | 100 |
| | 7.0 | 6.9 ± 0.1 | 1.1 | 99 | 6.9 ± 0.1 | 0.2 | 99 |
| Tap | 0.0 | N.D. | | | N.D. | | |
| water | 3.0 | 3.1 ± 0.3 | 9.3 | 103 | 3.1 ± 0.1 | 3.1 | 103 |
| | 5.0 | 5.4 ± 0.3 | 6.1 | 108 | 5.0 ± 0.1 | 0.6 | 100 |
| | 7.0 | 7.3 ± 0.2 | 2.8 | 104 | 6.9 ± 0.1 | 0.4 | 99 |
| Pond water | 0.0 | N.D. | | | N.D. | | |
| | 3.0 | 3.0 ± 0.1 | 3.4 | 100 | 3.1 ± 0.1 | 0.6 | 103 |
| | 5.0 | 5.1 ± 0.1 | 2.6 | 102 | 5.1 ± 0.1 | 0.5 | 102 |
| | 7.0 | 7.2 ± 0.1 | 1.5 | 103 | 7.0 ± 0.1 | 0.5 | 100 |
| Agriculture | 0.0 | N.D. | | | N.D. | | |
| wastewater | 3.0 | 3.0 ± 0.1 | 3.0 | 100 | 3.1 ± 0.1 | 3.4 | 103 |
| | 5.0 | 5.0 ± 0.3 | 6.2 | 100 | 5.1 ± 0.1 | 1.1 | 102 |
| | 7.0 | 7.2 ± 0.4 | 5.3 | 103 | 7.0 ± 0.1 | 0.4 | 100 |

N.D. = non detectable

## 4.5 Comparison of the proposed devices with previous methods

A comparison of the performance of paper-based and thread-based analytical devices was considered. Because the proposed devices did not require any sophisticated scientific instruments, they were dramatically simpler than the conventional planar film optodes (see in **Table 2.5, Section 2.4.1**). From the $Ag^+$ and $Hg^{2+}$ detection methods in the previous works as shown in **Table 2.2** (**Section 2.2.2**), our proposed devices does not needed the hydrophobic barrier fabrications which make them easier than other works. The proposed paper-based device showed a high selectivity for $Ag^+$ and $Hg^{2+}$, and the dual quantitative detection of $Ag^+$ and $Hg^{2+}$ in mixed solutions was achieved. Moreover, the comparison between a proposed paper-based device and a proposed thread-based device was also considered. The proposed thread-based device was simpler than the paper-based device because the distance readout by naked-eye in the proposed thread-based device did not require any electronic equipment. Additionally, the proposed thread-based device used a smaller sample volume than the proposed paper-based device. Hence, it was appropriate for $Hg^{2+}$ detection in the case of limited sample volume.

# CHAPTER V

# CONCLUSION

We have successfully developed the sensing platforms based on ISOs for $Ag^+$ and $Hg^{2+}$ detection. The optode containing **CU1** as an ion-selective ionophore, chromoionphore XIV as a lipophilic pH indicator, and KT$p$ClPB as an ion-exchanger was prepared and used as a sensing agent in the proposed devices. Firstly, the fabrication of the paper-based analytical device incorporating with ISOs for dual colorimetric detection of $Ag^+$ and $Hg^{2+}$ was achieved. A simple fabrication method was performed by simply dropping the cocktail solution onto the filter paper. The detection method was easily performed by immersing the paper strip into the sample solutions. The proposed paper-based device showed high selectivity toward $Ag^+$ and $Hg^{2+}$ over other 12 cations by changing the color from blue to yellow. In this platform, the dual $Ag^+$ and $Hg^{2+}$ detection in their mixed solution using EDTA and NaCl as masking agents for $Ag^+$ and $Hg^{2+}$ assay, respectively was accomplished. 75% (5.6 mmol kg$^{-1}$) of chromoionophore XIV, pH 5.0, immersion time of 10 and 15 min (for $Ag^+$ and $Hg^{2+}$ detections, respectively) were selected for the optimum conditions in this platform. It also provided a calibration response fitted with Boltzman equation ($R^2 >$ 0.99) over a concentration range of $1.92 \times 10^{-6}$ to $5.00 \times 10^{-3}$ M for $Ag^+$ and $5.74 \times 10^{-7}$ to $5.00 \times 10^{-5}$ M for $Hg^{2+}$ with LOD of $1.92 \times 10^{-6}$ M (0.21 ppm) for $Ag^+$ and $5.74 \times 10^{-7}$ M (0.12 ppm) for $Hg^{2+}$. The proposed paper-based device showed good inter-devices precision with %RSD less than 10%. The proposed paper-based device was successfully applied for $Hg^{2+}$ detection in real water sample with the percentage recoveries of 87–119 % and %RSD less than 10% and applied for detection of total silver in cleaning product samples containing AgNPs with the percentage recoveries of

108–114 % and %RSD less than 8%. The results from the paper-based device were in agreement with the values obtained from ICP-OES.

However, the colorimetric detection by a proposed paper-based device still required a digital camera for detection step. To increase portability of the method, a truly instruments-free device without the need of any external electronic equipment was developed. The distance-based detection using a proposed thread-based device was successfully prepared for $Hg^{2+}$ detection. The optode nanosphere with 110 nm in diameters was successfully prepared and incorporated onto the surface of polyester thread by a simple manual pipetting. The detection method was easily performed by repeatedly dropped 3 μL of sample solutions onto the thread, and then the distances of the color change correlated with the $Hg^{2+}$ concentrations were observed. The numbers of repeatedly dropping of 4 times for optode nanosphere suspension and 15 times of sample solutions were selected for the optimum conditions in this platform. The distance of color change showed a good linear correlation with $Hg^{2+}$ concentrations ($R^2$ > 0.99) over a concentration range of 1 to 10 ppm with LOD of 0.3 ppm. The proposed thread-based device showed good inter-devices precision with %RSD less than 5%. The Pearson's correlation analysis showed no significant difference between the software-assisted readout and the naked eyes readout ($r > 0.99$). Finally, the proposed thread-based device was successfully applied for $Hg^{2+}$ detection in real water sample with the percentage recoveries of 97–108% and %RSD less than 10%. The results from thread-based device were in agreement with the values obtained from ICP–OES.

**Suggestion for future works:**

In this research, the limit of detection was still higher than the maximum residue limits recommended by World Health Organization (0.050 ppm for $Ag^+$ and 0.002 ppm for $Hg^{2+}$ in drinking water). Therefore, the proposed methods could not be performed for determination of very low $Ag^+$ and $Hg^{2+}$ concentration in the samples.

To solve this restriction, pre-concentration step before the use of proposed devices should be performed.

# REFERENCES

1.    Pons-Branchu, E.; Ayrault, S.; Roy-Barman, M.; Bordier, L.; Borst, W.; Branchu, P.; Douville, E.; Dumont, E., Three centuries of heavy metal pollution in Paris (France) recorded by urban speleothems. *Science of the Total Environment* **2015,** *518-519*, 86-96.

2.    Yu, R.; He, L.; Cai, R.; Li, B.; Li, Z.; Yang, K., Heavy metal pollution and health risk in China. *Global Health Journal* **2017,** *1* (1), 47-55.

3.    Qadeer, A.; Saqib, Z. A.; Ajmal, Z.; Xing, C.; Khan Khalil, S.; Usman, M.; Huang, Y.; Bashir, S.; Ahmad, Z.; Ahmed, S.; Thebo, K. H.; Liu, M., Concentrations, pollution indices and health risk assessment of heavy metals in road dust from two urbanized cities of Pakistan: Comparing two sampling methods for heavy metals concentration. *Sustainable Cities and Society* **2020,** *53*, 101959.

4.    Eisler, R., Mercury hazards from gold mining to humans, plants, and animals. In *Reviews of Environmental Contamination and Toxicology*, Springer New York: New York, NY, 2004; pp 139-198.

5.    Wang, J.; Feng, X.; Anderson, C. W.; Xing, Y.; Shang, L., Remediation of mercury contaminated sites - A review. *Journal of Hazardous Materials* **2012,** *221-222*, 1-18.

6.    Boening, D. W., Ecological effects, transport, and fate of mercury: a general review. *Chemosphere* **2000,** *40* (12), 1335-1351.

7.    Doudoroff, P.; Katz, M., Critical review of literature on the toxicity of industrial wastes and their components to fish, II: the metals, as salts. *Sewage and Industrial Waste* **1953,** *25*, 802-812.

8.    Ratte, H. T., Bioaccumulation and toxicity of silver compounds: a review. *Environmental Toxicology and Chemistry* **1999,** *18*, 89-108.

9.    Maramba, N. P.; Reyes, J. P.; Francisco-Rivera, A. T.; Panganiban, L. C.; Dioquino, C.; Dando, N.; Timbang, R.; Akagi, H.; Castillo, M. T.; Quitoriano, C.; Afuang, M.; Matsuyama, A.; Eguchi, T.; Fuchigami, Y., Environmental and human exposure assessment monitoring of communities near an abandoned mercury mine in the Philippines: a toxic legacy. *Journal of Environmental Management* **2006,** *81* (2), 135-145.

10.   Luo, Y.; Duan, L.; Wang, L.; Xu, G.; Wang, S.; Hao, J., Mercury concentrations in forest soils and stream waters in northeast and south China. *Science of the Total Environment* **2014,** *496*, 714-720.

11.   Zhang, Z.; Wu, D.; Guo, X.; Qian, X.; Lu, Z.; Xu, Q.; Yang, Y.; Duan, L.; He, Y.; Feng, Z., Visible study of mercuric ion and its conjugate in living cells of mammals and plants. *Chemical Research in Toxicology* **2005,** *18* (12), 1814-1820.

12.   Li, W. C.; Tse, H., Health risk and significance of mercury in the environment. *Environmental science and pollution research international* **2015,** *22*, 192–201.

13.   Sim, W.; Barnard, R. T.; Blaskovich, M. A. T.; Ziora, Z. M., Antimicrobial silver in medicinal and consumer applications: a patent review of the past decade (2007-2017). *Antibiotics (Basel)* **2018,** *7* (4), 93.

14.   Ma, X.; Huang, B.; Cheng, M., Analysis of trace mercury in water by solid phase extraction using dithizone modified nanometer titanium dioxide and cold vapor atomic absorption spectrometry. *Rare Metals* **2007,** *26* (6), 541-546.

15.   Mullapudi, V. B. K.; Garg, N.; Karunasagar, D., Development of a novel and robust microprecipitation approach using cetyltrimethyl ammonium bromide (CTAB) for preconcentration and speciation of mercury in waters prior to CVAAS determination. *International Journal of Environmental Analytical Chemistry* **2018,** *98* (9), 811-829.

16.  Lin, M. L.; Jiang, S. J., Determination of As, Cd, Hg and Pb in herbs using slurry sampling electrothermal vaporisation inductively coupled plasma mass spectrometry. *Food Chemistry* **2013,** *141* (3), 2158-2162.

17.  Chew, L. T.; Bradley, D. A.; Mohd, A. Y.; Jamil, M. M., Zinc, lead and copper in human teeth measured by induced coupled argon plasma atomic emission spectroscopy (ICP-AES). *Applied Radiation and Isotopes* **2000,** *53* (4), 633-638.

18.  Roy, S.; Prasad, A.; Tevatia, R.; Saraf, R. F., Heavy metal ion detection on a microspot electrode using an optical electrochemical probe. *Electrochemistry Communications* **2018,** *86*, 94-98.

19.  Pereira, L.; Maranhão, T. d. A.; Frescura, V. L. A.; Borges, D. L. G., Multivariate assessment of extraction conditions for the fractionation analysis of mercury in oily sludge samples using cold vapor atomic fluorescence spectrometry. *Journal of Analytical Atomic Spectrometry* **2019,** *34* (9), 1932-1941.

20.  Seiler, K.; Simon, W., Theoretical aspects of bulk optode membranes. *Analytica Chimica Acta* **1992,** *266*, 73-87.

21.  Bualom, C.; Ngeontae, W.; Nitiyanontakit, S.; Ngamukot, P.; Imyim, A.; Tuntulani, T.; Aeungmaitrepirom, W., Bulk optode sensors for batch and flow-through determinations of lead ion in water samples. *Talanta* **2010,** *82* (2), 660-667.

22.  Lerchi, M.; Bakker, E.; Rusterholz, B.; Simon, W., Lead-selective bulk optodes based on neutral ionophores with subnanomolar detection limits. *Analytica Chimica Acta* **1992,** *64*, 1534-1540.

23.  Ensafi, A. A.; Fouladgar, M., Development a simple PVC membrane bulk optode for determination of lead ions in water samples. *Sensor Letters* **2009,** *7*

(2), 177-184.

24.  Wu, J.; Qin, Y., Polymeric optodes based on upconverting nanorods for fluorescence measurements of Pb$^{2+}$ in complex samples. *Sensors and Actuators B: Chemical* **2014,** *192*, 51-55.

25.  Ensafi, A. A.; Fouladgar, M., A sensitive and selective bulk optode for determination of Hg(II) based on hexathiacyclooctadecane and chromoionophore V. *Sensors and Actuators B: Chemical* **2009,** *136* (2), 326-331.

26.  Sanchez-Pedreño, C.; Ortuño, J. A.; Albero, M. I.; Garcia, M. S.; Valero, M. V., Development of a new bulk optode membrane for the determination of mercury(II). *Analytica Chimica Acta* **2000,** *414* (1), 195-203.

27.  Albero, M. I.; Ortuño, J. A.; García, M. S.; Cuartero, M.; Alcaraz, M. C., Novel flow-through bulk optode for spectrophotometric determination of lithium in pharmaceuticals and saliva. *Sensors and Actuators B: Chemical* **2010,** *145* (1), 133-138.

28.  Ngeontae, W.; Janrungroatsakul, W.; Morakot, N.; Aeungmaitrepirom, W.; Tuntulani, T., New silver selective electrode fabricated from benzothiazole calix[4]arene: Speciation analysis of silver nanoparticles. *Sensors and Actuators B: Chemical* **2008,** *134* (2), 377-385.

29.  Wattanayon, R. Development of a selective bulk optode membrane containing benzothiazole calix[4]arene for determination of silver ion. Chulalongkorn University, Thailand, 2013.

30.  Bakker, E.; Buhlmann, P.; Pretsch, E., Carrier-based ion-selective electrodes and bulk optodes. 1. general characteristics. *Chemical Reviews* **1997,** *97*, 3083-3132.

31.  Martinez, A. W.; Phillips, S. T.; Butte, M. J.; Whitesides, G. M., Patterned paper as a platform for inexpensive, low-volume, portable bioassays.

*Angewandte Chemie International Edition* **2007,** *46* (8), 1318-1320.

32.     Cate, D. M.;   Adkins, J. A.;   Mettakoonpitak, J.; Henry, C. S., Recent developments in paper-based microfluidic devices. *Analytical Chemistry* **2015,** *87* (1), 19-41.

33.     Mentele, M. M.;   Cunningham, J.;   Koehler, K.;   Volckens, J.; Henry, C. S., Microfluidic paper-based analytical device for particulate metals. *Analytical Chemistry* **2012,** *84* (10), 4474-4480.

34.     Hossain, S. M.; Brennan, J. D., beta-Galactosidase-based colorimetric paper sensor for determination of heavy metals. *Analytical Chemistry* **2011,** *83* (22), 8772-8778.

35.     e Silva, R. F.;   Longo Cesar Paixão, T. R.;   Der Torossian Torres, M.; de Araujo, W. R., Simple and inexpensive electrochemical paper-based analytical device for sensitive detection of Pseudomonas aeruginosa. *Sensors and Actuators B: Chemical* **2020,** *308*, 127669.

36.     Fiedoruk-Pogrebniak, M.; Koncki, R., LED&Paper-based analytical device for phosphatemia/calcemia diagnostics. *Journal of Pharmaceutical and Biomedical Analysis* **2020,** *186*, 113321.

37.     Primpray, V.;   Chailapakul, O.;   Tokeshi, M.;   Rojanarata, T.; Laiwattanapaisal, W., A paper-based analytical device coupled with electrochemical detection for the determination of dexamethasone and prednisolone in adulterated traditional medicines. *Analytica Chimica Acta* **2019,** *1078*, 16-23.

38.     Peters, J. J.;   Almeida, M.;   O'Connor Sraj, L.;   McKelvie, I. D.; Kolev, S. D., Development of a micro-distillation microfluidic paper-based analytical device as a screening tool for total ammonia monitoring in freshwaters. *Analytica Chimica Acta* **2019,** *1079*, 120-128.

39.     Shishov, A.;   Trufanov, I.;   Nechaeva, D.; Bulatov, A., A reversed-phase air-

assisted dispersive liquid-liquid microextraction coupled with colorimetric paper-based analytical device for the determination of glycerol, calcium and magnesium in biodiesel samples. *Microchemical Journal* **2019,** *150*, 104134.

40. Pourreza, N.; Golmohammadi, H.; Rastegarzadeh, S., Highly selective and portable chemosensor for mercury determination in water samples using curcumin nanoparticles in a paper based analytical device. *RSC Advances* **2016,** *6* (73), 69060-69066.

41. Apilux, A.; Siangproh, W.; Praphairaksit, N.; Chailapakul, O., Simple and rapid colorimetric detection of Hg(II) by a paper-based device using silver nanoplates. *Talanta* **2012,** *97*, 388-394.

42. Meelapsom, R.; Jarujamrus, P.; Amatatongchai, M.; Chairam, S.; Kulsing, C.; Shen, W., Chromatic analysis by monitoring unmodified silver nanoparticles reduction on double layer microfluidic paper-based analytical devices for selective and sensitive determination of mercury(II). *Talanta* **2016,** *155*, 193-201.

43. Chen, G. H.; Chen, W. Y.; Yen, Y. C.; Wang, C. W.; Chang, H. T.; Chen, C. F., Detection of mercury(II) ions using colorimetric gold nanoparticles on paper-based analytical devices. *Analytical Chemistry* **2014,** *86* (14), 6843-6849.

44. Chen, W.; Fang, X.; Li, H.; Cao, H.; Kong, J., A simple paper-based colorimetric device for rapid mercury(II) assay. *Scientific Reports* **2016,** *6*, 31948.

45. Yang, X.; Wang, E., A nanoparticle autocatalytic sensor for $Ag^+$ and $Cu^{2+}$ ions in aqueous solution with high sensitivity and selectivity and its application in test paper. *Analytical Chemistry* **2011,** *83* (12), 5005-5011.

46. Liu, L.; Lin, H., Paper-based colorimetric array test strip for selective and semiquantitative multi-ion analysis: simultaneous detection of $Hg^{2+}$, $Ag^+$, and

$Cu^{2+}$. *Analytical Chemistry* **2014,** *86* (17), 8829-8834.

47. Dhavamani, J.; Mujawar, L. H.; El-Shahawi, M. S., Hand drawn paper-based optical assay plate for rapid and trace level determination of $Ag^+$ in water. *Sensors and Actuators B: Chemical* **2018,** *258*, 321-330.

48. Li, C.-r.; Hai, J.; Fan, L.; Li, S.-l.; Wang, B.-d.; Yang, Z.-y., Amplified colorimetric detection of $Ag^+$ based on $Ag^+$-triggered peroxidase-like catalytic activity of ZIF-8/GO nanosheets. *Sensors and Actuators B: Chemical* **2019,** *284*, 213-219.

49. Li, X.; Tian, J.; Shen, W., Thread as a versatile material for low-cost microfluidic diagnostics. *ACS Applied Materials & Interfaces* **2010,** *2* (1), 1-6.

50. Sateanchok, S.; Wangkarn, S.; Saenjum, C.; Grudpan, K., A cost-effective assay for antioxidant using simple cotton thread combining paper based device with mobile phone detection. *Talanta* **2018,** *177*, 171-175.

51. Dossi, N.; Toniolo, R.; Terzi, F.; Sdrigotti, N.; Tubaro, F.; Bontempelli, G., A cotton thread fluidic device with a wall-jet pencil-drawn paper based dual electrode detector. *Analytica Chimica Acta* **2018,** *1040*, 74-80.

52. Mao, X.; Du, T. E.; Wang, Y.; Meng, L., Disposable dry-reagent cotton thread-based point-of-care diagnosis devices for protein and nucleic acid test. *Biosensors and Bioelectronics* **2015,** *65*, 390-396.

53. Song, T.-T.; Wang, W.; Meng, L.-L.; Liu, Y.; Jia, X.-B.; Mao, X., Electrochemical detection of human ferritin based on gold nanorod reporter probe and cotton thread immunoassay device. *Chinese Chemical Letters* **2017,** *28* (2), 226-230.

54. Caetano, F. R.; Carneiro, E. A.; Agustini, D.; Figueiredo-Filho, L. C. S.; Banks, C. E.; Bergamini, M. F.; Marcolino-Junior, L. H., Combination of electrochemical biosensor and textile threads: A microfluidic device for phenol

determination in tap water. *Biosensors and Bioelectronics* **2018,** *99*, 382-388.

55.    Li, Y. D.;  Chai, H. H.;  Zhang, S. J.;  Lu, Z. S.;  Li, C. M.; Yu, L., Sensitive and portable colorimetric detection of copper in water by cotton thread based pre-concentration. *Microchemical Journal* **2019,** *148*, 735-742.

56.    Xu, C.;  Huang, W.;  Zhu, S.;  Li, Z.;  Cai, L.; Zhong, M., Distance readout of Al content with naked eyes on a cotton thread. *AIP Advances* **2018,** *8*, 105016.

57.    Yan, Y.;  Kou, B.; Yan, L., Thread-based microfluidic three channel device in combination with thermal lens detection for the determination of copper and zinc. *Analytical Methods* **2015,** *7* (20), 8757-8762.

58.    Nilghaz, A.;  Ballerini, D. R.;  Fang, X.-Y.; Shen, W., Semiquantitative analysis on microfluidic thread-based analytical devices by ruler. *Sensors and Actuators B: Chemical* **2014,** *191*, 586-594.

59.    Erenas, M. M.;  de Orbe-Paya, I.; Capitan-Vallvey, L. F., Surface modified thread-based microfluidic analytical device for selective potassium analysis. *Analytical Chemistry* **2016,** *88* (10), 5331-5337.

60.    Jarujamrus, P.;  Malahom, N.;  Puchum, S.;  Meelapsom, R.;  Amatatongchai, M.;  Siripinyanond, A.;  Chairam, S.; Kulsing, C., Complexometric and argentometric titrations using thread-based analytical devices. *Talanta* **2018,** *183*, 228-236.

61.    Mousavi, M. P. S.;  Ainla, A.;  Tan, E. K. W.;  M, K. A. E.-R.;  Yoshida, Y.;  Yuan, L.;  Sigurslid, H. H.;  Arkan, N.;  Yip, M. C.;  Abrahamsson, C. K.;  Homer-Vanniasinkam, S.; Whitesides, G. M., Ion sensing with thread-based potentiometric electrodes. *Lab on a Chip* **2018,** *18* (15), 2279-2290.

62.    Xie, X.;  Crespo, G. A.;  Zhai, J.;  Szilagyi, I.; Bakker, E., Potassium-selective optical microsensors based on surface modified polystyrene microspheres. *Chemical Communications* **2014,** *50* (35), 4592-4595.

63.     Shakhsher, Z. M.;  Odeh, I.;  Jabr, S.; Rudolf Seitz, W., An optical chemical sensor based on swellable dicarboxylate functionalized polymer microspheres for pH copper and calcium determination. *Microchimica Acta* **2004,** *144* (1-3), 147-153.

64.     Zhai, J.;  Xie, X.; Bakker, E., Ionophore-based ion-exchange emulsions as novel class of complexometric titration reagents. *Chemical Communications* **2014,** *50* (84), 12659-12661.

65.     Wang, X.;  Qin, Y.; Meyerhoff, M. E., Paper-based plasticizer-free sodium ion-selective sensor with camera phone as a detector. *Chemical Communications* **2015,** *51* (82), 15176-15179.

66.     Gerold, C. T.;  Bakker, E.; Henry, C. S., Selective distance-based $K^+$ quantification on paper-based microfluidics. *Analytical Chemistry* **2018,** *90* (7), 4894-4900.

67.     Shibata, H.;  Henares, T. G.;  Yamada, K.;  Suzuki, K.; Citterio, D., Implementation of a plasticized PVC-based cation-selective optode system into a paper-based analytical device for colorimetric sodium detection. *Analyst* **2018,** *143* (3), 678-686.

68.     Shibata, H.;  Hiruta, Y.; Citterio, D., Fully inkjet-printed distance-based paper microfluidic devices for colorimetric calcium determination using ion-selective optodes. *Analyst* **2019,** *144* (4), 1178-1186.

69.     Hirayama, E.;  Sugiyama, T.;  Hisamoto, H.; Suzuki, K., Visual and colorimetric lithium ion sensing based on digital color analysis. *Analytical Chemistry* **2000,** *72*, 465-474.

70.     Suzuki, K.;  Hirayama, E.;  Sugiyama, T.;  Yasuda, K.;  Okable, H.; Citterio, D., Ionophore-based lithium ion film optode realizing multiple color variations utilizing digital color analysis. *Analytical Chemistry* **2002,** *74*, 5766-5773.

71.    Cantrell, K.;  Erenas, M. M.;  de Orbe-Paya, I.; Capitan-Vallvey, L. F., Use of the hue parameter of the hue, saturation, value color space as a quantitative analytical parameter for bitonal optical sensors. *Analytical Chemistry* **2010,** *82*, 531-542.

72.    Bakker, E.; Simon, W., Selectivity of ion-sensitive bulk optodes. *Analytical Chemistry* **1992,** *64*, 1805-1812.

73.    Morf, W. E.;  Kahr, G.; Simon, W., Theoretical treatment of the selectivity and detection limit of silver compound membrane electrodes. *Analytical Chemistry* **1974,** *46*, 1538-1543.

74.    Shamsipur, M.; Mashhadizadeh, M. H., Highly efficient and selective membrane transport of silver(I) using hexathia-18-crown-6 as a specific ion carrier. *Separation and Purification Technology* **2000,** *20*, 147-153.

75.    Long, G. L.; Winefordner, J. D., Limit of detection. A closer look at the IUPAC definition. *Analytical Chemistry* **1983,** *55*, 712A-724A.

76.    Soda, Y.;  Shibata, H.;  Yamada, K.;  Suzuki, K.; Citterio, D., Selective detection of $K^+$ by ion-selective optode nanoparticles on cellulosic filter paper substrates. *ACS Applied Nano Materials* **2018,** *1* (4), 1792-1800.

77.    Xie, X.;  Mistlberger, G.; Bakker, E., Ultrasmall fluorescent ion-exchanging nanospheres containing selective ionophores. *Analytical Chemistry* **2013,** *85* (20), 9932-9938.

78.    Xie, X.; Bakker, E., Ion selective optodes: from the bulk to the nanoscale. *Analytical and bioanalytical chemistry* **2015,** *407*, 3899-3910.

79.    Xie, X.;  Zhai, J.; Bakker, E., pH independent nano-optode sensors based on exhaustive ion-selective nanospheres. *Analytical Chemistry* **2014,** *86* (6), 2853-2856.

80.    Xie, X.;  Zhai, J.;  Crespo, G. A.; Bakker, E., Ionophore-based ion-selective

optical nanosensors operating in exhaustive sensing mode. *Analytical Chemistry* **2014,** *86* (17), 8770-8775.
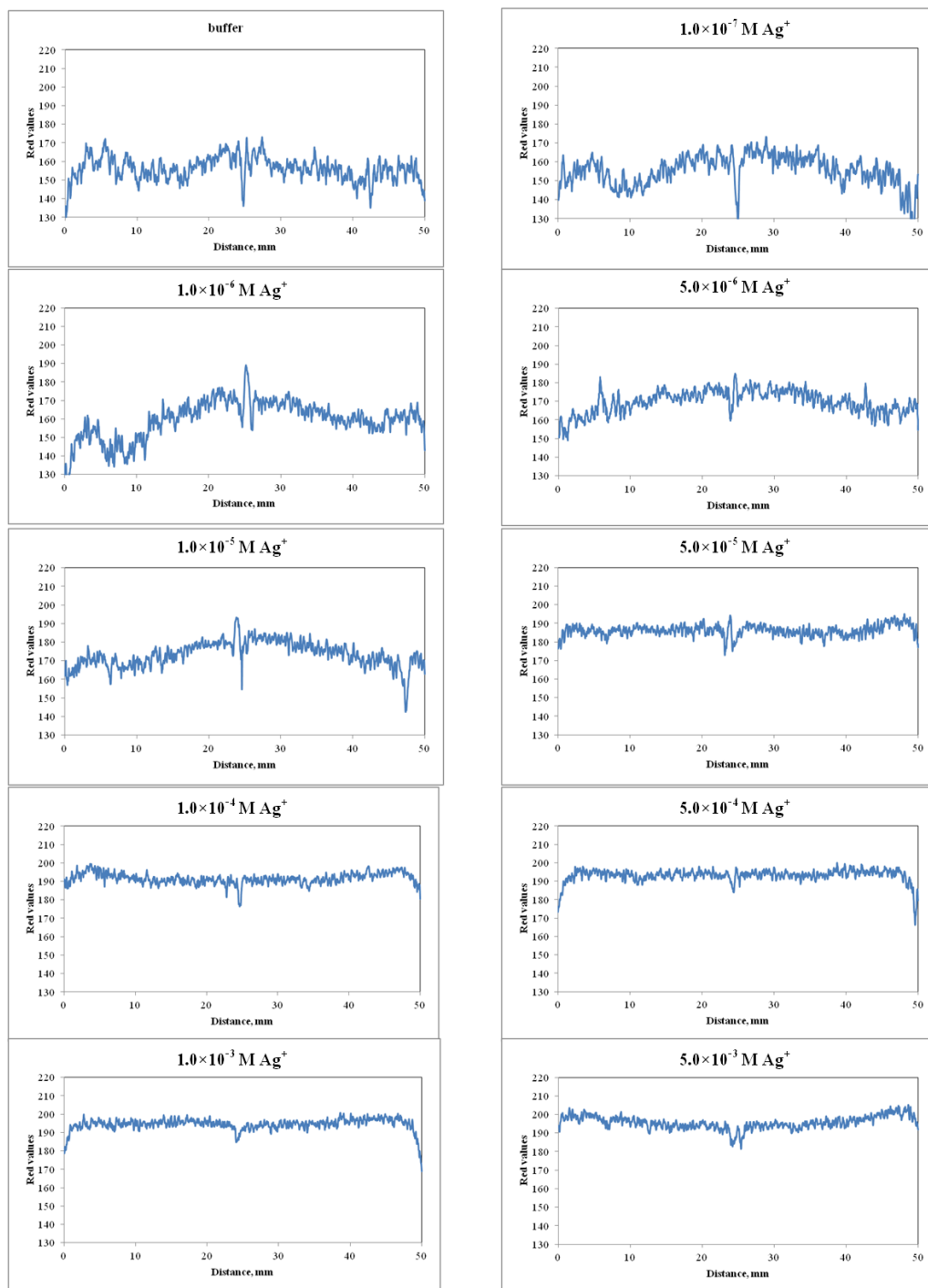
# APPENDIX A



**Figure A1** Colorimetric plot profile of red values along the threads in **Figure 4.18**a. These values were acquired using ImageJ software.

# VITA

**NAME**                    Manoon Phichi

**DATE OF BIRTH**           10 July 1991

**PLACE OF BIRTH**          Suphanburi

**HOME ADDRESS**            71/3 Village No.2, Salee Sub-district, Bangplama District,

Suphanburi, 72150